Title
Elucidation of the Regulatory Role of Osteopontin on the Pathology of Duchenne Muscular Dystrophy

Author
Capote Zulueta, Joana Carolina

Publication Date
2017

Peer reviewed|Thesis/dissertation

UNIVERSITY OF CALIFORNIA

Los Angeles

Elucidation of the Regulatory Role of Osteopontin on the Pathology of Duchenne Muscular Dystrophy

A dissertation submitted in partial satisfaction of the requirements for the degree Doctor of Philosophy in Molecular, Cellular, and Integrative Physiology

by

Joana Carolina Capote Zulueta

2017

ABSTRACT OF THE DISSERTATION

Elucidation of the Regulatory Role of Osteopontin
on the Pathology of Duchenne Muscular Dystrophy

by

Joana Carolina Capote Zulueta

Doctor of Philosophy in Molecular, Cellular, and Integrative Physiology

University of California, Los Angeles, 2017

Professor Melissa J. Spencer, Chair

Osteopontin (OPN) is one of the most highly up-regulated genes in Duchenne Muscular Dystrophy (DMD) patients and also in the *mdx* mouse. Single nucleotide polymorphisms in the *SPP1* gene (OPN gene) are associated with changes in muscle strength and age of loss of ambulation in DMD patients. Previous work in the lab has shown that ablation of OPN in mdx mice significantly ameliorates their dystrophic phenotype by decreasing muscle fibrosis and increasing muscle regeneration and strength in young mice. These changes in the pathology of mdx mice were associated with a decrease in NKT and Gr-1+ cell populations, and decreased intramuscular TGF-β.

In this project, we expanded on these previous observations and further explored the ways in which OPN exerts its regulatory role in the dystrophic pathology. Our current study shows that OPN ablation in mdx mice induces long term benefits on dystrophic muscles. OPN-/-mdx (up to more than one year old) display increased muscle mass and myofiber size, which translates to an improved performance in wire, grip and pulmonary function tests in dystrophic mice.

We show here that OPN expression in dystrophic muscle impairs muscle regeneration indirectly, by skewing the macrophage population toward a pro-inflammatory/pro-fibrotic phenotype. OPN ablation in mdx mice leads to reductions in M1 and M2a macrophages and increases in M2c. These changes were also associated with increased macrophage expression of pro-regenerative factors, without significantly changing pro-fibrotic factor expression. Moreover, OPN may impact regeneration directly by impairing terminal differentiation of myoblasts. In addition, we showed that OPN may promote muscle fibrosis in dystrophic muscle by directly interacting with fibroblasts and increasing collagen expression. This effect of OPN in fibroblast cultures is likely dependent in cell-type specific post-translational modifications.

This study validates OPN as a therapeutic target in DMD and lays a foundation for therapies involving pharmacological targeting of OPN, by providing a mechanistic understanding of OPN's relationship to the processes of immune response, regeneration and fibrosis in dystrophic muscle.

The dissertation of Joana Carolina Capote Zulueta is approved.

M. Carrie Miceli

Rachelle Hope Crosbie-Watson

Alan D. Grinnell

Melissa J. Spencer, Committee Chair

University of California, Los Angeles

2017

Dedication

This work is dedicated to my parents who, having nothing, gave me everything in my life; to my brothers and family in general who have understood that my work has taken a big part of my life for a long time; to my husband who is the best partner, friend and supporter that I could have ever asked for; to my friends Joanna, Meyerling and now Erin who, more than friends, are now like sisters; to my parents-in-law who have been very supportive during this time; and finally to Venezuela and all that people that are today fighting on the streets there for freedom and democracy, because I hope one day all their current sacrifices help us rebuild a new and prosperous nation.

Table of Contents

List of Figures

List of Tables

List of Acronyms

ACK	Ammonium-Chloride-Potassium
Arg	Arginase
BSA	Bovine Serum Albumin
CCL17	Chemokine Ligand 17
CK	Creatine Kinase
CTGF	Conective Tissue Growth Factor
DMD	Duchenne Muscular Dystrophy
dMHC	Developmental Myosin Heavy Chain
ECL	Entactin-Collagen IV-Laminin
ECM	Extracellular Matrix
EDL	*Extensor Digitorum Longus*
FACS	Fluorescence-Activated Cell Sorting
FBS	Fetal Bovine Serum
FDB	*Flexor Ditorum Brevis*
IFN-γ	Interferon gamma
IGF-1	Insulin-like Growth Factor 1
IL-4	Interleukin 4
IL-10	Interleukin 10
iNOS	Inducible Nitric Oxide Synthase
ITS	Insulin-Transferrin-Selenium
LIF	Leukemia Inhibitory Factor
MACS	Magnetic-Activated Cell Sorting
NK	Natural Killer cells

NKT	Natural Killer T-cells
OPN	Osteopontin
PBS	Phosphate-Buffered saline
P/S	Penicillin/Streptomycin
SE	Standard Error of the mean
SNP	Single Nucleotide Polymorphism
TGF-β	Transforming Growth Factor beta
uPA	Urokinase Plasminogen-Activator

Acknowledgments

I would like to thank Dr. Melissa J. Spencer and all the members of the Center for Duchenne Muscular Dystrophy (CDMD) at UCLA for their valuable contribution in my formation as a professional. I would also like to thank all the members of the Spencer lab for their help and support, especially to Natalia Ermolova, Diana Becerra and Jian Liu because you always made my days in the lab special. I am also thankful to all my previous mentors: Dr. Freddy Gonzalez-Mujica, Dr. Norma Motta, Dr. Marino DiFranco, Marbella Quiñonez, Dr. Carlo Caputo, Pura Bolaños and Dr. Julio Vergara, because all of you one way or another have defined and molded me into the professional I am today.

Chapter 2 specific acknowledgments: Chapter 2 is a version of the publication "Capote, Joana; Kramerova, Irina; Martinez, Leonel; Vetrone, Sylvia; Barton, Elisabeth R.; Sweeney, H. Lee; Miceli, M. Carrie; Spencer, Melissa J. Osteopontin ablation ameliorates muscular dystrophy by shifting macrophages to a pro-regenerative phenotype. Journal of Cell Biology. 2016. vol. 213 (2): 275-288." The authors' participation was as follows: J.C. participated in the conception and design of the project, collection and/or assembly of data, data analysis and interpretation, manuscript writing and final approval of manuscript. I.K. participated in the conception and design of the project, data analysis and interpretation, manuscript writing and final approval of manuscript. L.M. participated in collection and/or assembly of data. S.V. participated in collection and/or assembly of data and data analysis. E.R.B. participated in collection and/or assembly of data, data analysis and final approval of manuscript. H.L.S.

participated in the design of the project, funding and final approval of manuscript. M.C.M. participated in the design of the project, data interpretation and final approval of manuscript. M.J.S. participated in the conception and design of the project, collection and/or assembly of data, data analysis and interpretation, manuscript writing, funding and final approval of manuscript.

Chapter 3 specific acknowledgements: Chapter 3 is a version of a manuscript in preparation describing the direct effect of OPN in the regulation of fibrosis and regeneration in dystrophic muscle. This work was supported by funding from the National Institute of Arthritis, Musculoskeletal and Skin Diseases for a Wellstone Cooperative Muscular Dystrophy Center (U54AR052646-Sweeney) and partially by supported by grant number 1T32AR065972-01A1 (MPI) from NIH and a Dissertation Year Fellowship 2016 from the University of California, Los Angeles.

Biographical Sketch

EDUCATION

1996 – 2004 Biology, Licenciado.
School of Biology, Faculty of Science.
Central University of Venezuela.
Caracas, Venezuela.

RESEARCH EXPERIENCE

2007- 2009 Staff Research Associate II.
Laboratory of electro-optical cellular physiology.
(Dr. Julio Vergara, PI).
Department of Physiology.
David Geffen Medical School. University of California, Los Angeles.
California, United States.

2004- 2007 Staff Research Associate I.
Laboratory of electro-optical cellular physiology.
(Dr. Julio Vergara, Ph.D., Head).
Department of Physiology.
David Geffen Medical School. University of California, Los Angeles.
California, United States.

2003 – 2004 "Characterization of calcium release inactivation during postnatal development in mouse skeletal muscle fibers".
Undergraduate Thesis
Dr. Pura Bolaños, Mentor (Dr. Carlo Caputo, Ph.D., Head).
Laboratory of Muscle Biophysics.
Biophysics and Biochemistry Center.
Venezuelan Institute of Scientific Research (IVIC).
Altos de Pipe, Venezuela.

2003 "Amperometric study of exocitotic events from single mast cells".
Undergraduate Fellow.
Laboratory of Neurochemistry (Dr. Erica H. Jaffe, Ph.D., Head)
Biophysics and Biochemistry Center.
Venezuelan Institute of Scientific Research (IVIC).
Altos de Pipe, Venezuela.

2002 "Photometric recording of action potential evoked calcium release in amphibian muscle fibers mounted in an inverted grease gap chamber".
Undergraduate Fellow.
Laboratory of Muscle Biophysics and Physiology
(Dr. Marino DiFranco, Ph.D., Head).
Institute of Experimental Biology.
Faculty of Sciences. Central University of Venezuela.
Caracas, Venezuela.

2001 – 2003 "Effects of plant extracts on intestinal glucose absorption and Glut-4 activity".
Undergraduate Fellow.
Laboratory of Medical Biochemistry.
(Dr. Freddy Gonzalez Mujica, Ph.D., Head).
Institute of Experimental Medicine.
Faculty of Medicine. Central University of Venezuela.
Caracas, Venezuela.

SELECTED PUBLICATIONS

- Peter, Angela K.; Miller, Gaynor; Capote, Joana; DiFranco, Marino; Solares-Perez, Alhondra; Wang, Emily; Coral-Vazquez, Ramon M.; Heighway, Jim; Vergara, Julio; Crosbie-Watson, Rachelle H. 2017. "*Nanospan, an alternatively spliced isoform of sarcospan, localizes to the sarcoplasmic reticulum in skeletal muscle and is absent in limb girdle muscular dystrophy 2F"*. Skeletal Muscle. Accepted.
- Capote, Joana; Kramerova, Irina; Martinez, Leonel; Vetrone, Sylvia; Barton, Elisabeth R.; Sweeney, H. Lee; Miceli, M. Carrie; Spencer, Melissa J. 2016. "*Osteopontin ablation ameliorates muscular dystrophy by shifting macrophages to a pro-regenerative phenotype"*. Journal of Cell Biology. vol. 213 (2): 275-288.
- Capote, Joana; DiFranco, Marino; Vergara, Julio. 2010. *"Excitation-contraction coupling alterations in mdx and utrophin/dystrophin double knockout mice: a comparative study"*. American Journal of Physiology - Cell Physiology; 298: C1077-C1086.
- DiFranco, Marino; Quinonez, Marbella; Capote, Joana; Vergara, Julio. 2009. *"DNA transfection of mammalian skeletal muscles using in vivo electroporation"***.** Journal of visualized experiments : JoVE 2009;(32).
- DiFranco, Marino; Woods, Christopher E; Capote, Joana; Vergara, Julio L. 2008**.** *"Dystrophic skeletal muscle fibers display alterations at the level of calcium microdomains"* Proceedings of the National Academy of Sciences of the United States of America ;105(38):14698-703.
- DiFranco, Marino; Capote, Joana and Vergara, Julio L.. 2007. *"Voltage-dependent dynamic FRET signals from the transverse tubules in mammalian skeletal muscle fibers ."* The Journal of general physiology 2007;130(6):581-600.
- DiFranco, Marino; Ñeco, Patricia; Capote, Joana; Pratap, Meera and Vergara, Julio L. 2006. *"Quantitative evaluation of mammalian skeletal muscle as a heterologous protein expression system ."* Protein Expression & Purification 47, 281-288.
- Capote, Joana; Bolaños, Pura and Caputo, Carlo. Spring 2006*. "Calcium signalizing in developing mouse skeletal muscle fibres*." Physiology News 62,33-34 .
- DiFranco, Marino; Capote, Joana and Vergara, Julio L. 2005. *"Optical Imaging and Functional Characterization of the Transverse Tubular System of Mammalian Muscle Fibers using the Potentiometric Indicator di-8-ANEPPS ."* Journal of membrane biology 208, 141-153.
- Capote, Joana; Bolaños, Pura; Schumeir, Ralph Peter; Melzer, Werner and Caputo, Carlo. 2005. *"Calcium transients in developing mouse skeletal muscle fibres."* Journal of Physiology 564 (2), 451-464.

Chapter 1

Background

1.1 Significance

DMD was first described almost two centuries ago (1836) and, since that time, we have gained insights about its cause, features and consequences. However, there is still no cure for DMD and the most employed treatment at present is still the use of steroid drugs. Even though steroids have been shown to benefit DMD patients, these drugs have multiple undesired side effects. Therefore, development of targeted therapies is essential. In order to design specifically targeted approaches for DMD treatment, it is crucial to understand the mechanisms involved in the modulation of DMD pathology.

Our lab has previously shown that ablation of osteopontin (OPN) alters inflammation, fibrosis and muscle regeneration in dystrophic muscle, making OPN an attractive therapeutic target for the treatment of DMD patients [1]. However, the mechanisms by which OPN ablation ameliorates dystrophic pathology are not completely understood. Therefore, the main goal of this project was to investigate how OPN exerts its role as a modifier of the dystrophic pathology in mdx mice. Defining the sources of OPN expression and the mechanisms by which it is able to regulate inflammation, fibrosis and muscle mass will lay a foundation for development of targeted OPN inhibiting agents for the treatment of DMD.

1.2 Duchenne Muscular Dystrophy

Duchenne Muscular dystrophy (DMD) is an X-linked muscle disorder that affects approximately one of every 5,000 male births. DMD is caused by mutations in the largest known human gene, *DMD*, which generate non-functional or total absence of dystrophin expression [2]. Dystrophin is located at the sarcolemma of muscle fibers, where it provides a structural link between the cytoskeleton and the extracellular matrix [3]. In DMD, lack or non-functional expression of dystrophin renders the muscle fibers susceptible to contraction-induced muscle damage [3-6]. This continuous muscle damage causes an imbalance between muscle degeneration and regeneration that is further exacerbated by the elicited chronic inflammation [4, 5, 7]. The net loss of specific muscle mass, together with excessive extracellular matrix deposition caused by these ongoing processes, finally drives a decline in muscle function. This progressive decline in muscle function is what leads DMD patients to become wheelchair dependent in the teenage years and prompts the early death of patients by cardiac or respiratory complications [2, 4, 5].

Most of the current knowledge about this muscle disorder comes from the study of animal models. The most common animal model of DMD is the mdx mouse, discovered more than 30 years ago (1984) [8]. This mouse model harbors a spontaneous point mutation in exon 23 of the murine dystrophin gene that introduces a stop codon and causes a total loss of dystrophin expression [9]. The mdx mouse is a good genocopy of the human disease and reproduces some of the pathological features observed in DMD patients; however it has a much milder phenotype than human DMD patients [8, 9].

1.3 Role of the immune system in DMD pathology

Although there is no argument that the lack of functional dystrophin expression is the cause of DMD, the mechanical role of dystrophin in muscle is not enough to explain many aspects of the dystrophic pathophysiology such as the extensive fibrosis, inflammation and failure of muscle regeneration [10-13]. Temporal gene expression profiles from mdx mice and DMD patients have shown that there is an elevated expression of pro-inflammatory genes even before the muscles exhibit signs of pathological symptoms, establishing the immune system response as a key contributor to the pathogenesis of DMD [10, 12-14]. Support for an important contribution of immune mediators in disease progression comes from experiments demonstrating improvement in disease features following inhibition of NF-κB pathway or inflammatory mediators such as TNF-α and inducible nitric oxide synthase (iNOs) [15-19]. One of the proteins associated to the immune response and shown to be systematically overexpressed in dystrophic muscle from DMD patients and mdx mice even before any sign of muscle pathology is osteopontin [10, 12-14].

1.4 Osteopontin

Osteopontin (OPN) is a small, multifunctional and ubiquitously expressed protein [20-23]. The OPN gene (secreted phosphoprotein-1, *SPP1*) has seven exons, and spans 5 kilobases of the long arm of chromosome 4 in humans (chromosome 5 in mice) [24, 25]. The polypeptide backbone of OPN has an estimated molecular weight of ~33 KDa. However, multiple forms of the protein have been found in different tissues with apparent molecular weights ranging from ~15 KDa to ~85 KDa [22, 23, 26-29]. The

diversity of OPN forms is the result of both pre- and post-translational modifications. OPN was first described as a secreted protein (sOPN), but later studies identified an intracellular form (iOPN), which is the consequence of an alternative translation start site in the mRNA sequence of the protein [21-23, 30]. However, little is known about this intracellular form. OPN can be highly post-translationally modified, having multiple sites of phosphorylation, glycosylation, sulfation, transglutamination and proteolytic cleavage [20, 22, 27, 31] that increase the assortment of possible forms of OPN. Also, contributing to this diversity is the fact that the OPN gene is a target of alternative splicing. It has been described, at least in humans, that alternative splicing of SPP1 can generate three different splice variants of the protein: OPN-a (full length), OPN-b (lack exon 5) and OPN-c (lack exon 4) [20, 22, 32, 33].

OPN has been reported to be synthesized by a variety of cells including fibroblasts, osteoblasts, osteocytes, dendritic cells, macrophages, T and B cells, neutrophils, smooth muscle cells, myoblasts, endothelial cells, and others [30, 34, 35].

1.5 Osteopontin Function

OPN has been shown to be involved in a plethora of physiological and pathological processes including angiogenesis, inflammation, fibrosis, aging, wound healing and tumor metastasis [20, 30, 35-43]. OPN's assorted functions are supported by the diversity of OPN forms created by pre- and post-translational modifications of the peptide backbone and by the different ways it can interact with different cell types [22, 23, 30, 31]. sOPN and iOPN have different biological functions [21-23, 31]. sOPN can act as a mediator of cell adhesion when conjugated with the extracellular matrix or as an autocrine or paracrine factor that binds cell surface receptors, such as integrins or

CD44, to regulate different cell functions [21, 22]. OPN contains two different integrin-binding domains, an RGD motif that binds integrins αvβ3, αvβ1, αvβ5, αvβ6, α5β1 and α8β1 [32, 44, 45] and a SVVYGLR (SLAYGLR motif in mice) that is exposed upon cleavage by thrombin and binds integrins α4β1, α9β1 and α4β7 [21, 22, 29, 45-47]. OPN also binds to CD44, CD147 and αxβ2 receptors through RGD-independent motifs [21, 22, 45, 47]. On the other hand, perimembrane and cytosolic iOPN have been shown to be involved in the regulation of signal transduction pathways downstream of innate immune receptors, such as toll-like receptors (TLRs), and in cytoskeletal rearrangement [21, 48, 49]. In addition, iOPN has been also found in the nucleus and is suggested to play a role in mitosis by physical association with polo-like kinase 1 [21, 50].

1.6 Osteopontin and DMD

Our lab was the first to demonstrate that OPN can modulate disease severity in DMD using the mdx mouse model. This study showed that ablation of OPN in mdx mice correlated with a decrease in muscle fibrosis, an increase in muscle regeneration, and an improvement in muscle strength in young mice [1]. These effects in the dystrophic pathology were associated with changes in the composition of the immune cell population infiltrating mdx muscles, where $OPN^{-/-}$mdx mice had significantly reduced neutrophil and NKT-like populations, and increased T-cell populations, compared to muscles from $OPN^{+/+}$mdx mice [1]. In addition, muscles of $OPN^{-/-}$mdx mice had significantly less TGF-β expression [1]. OPN was subsequently shown to be highly expressed in muscle from patients with dystrophinopathies and related to the degree of severity of the pathology (higher in DMD than Becker patients) [51]. Moreover, single

nucleotide polymorphisms (SNP) of the human SPP1 gene were shown to modify DMD progression [52, 53]. These studies found that patients carrying the less common G allele have reduced muscle strength and lose ambulation at an earlier age than patients with the T allele. Although previous in vitro studies reported that haplotypes with the G allele were associated with lower transcriptional activity in culture cells [54], the human study demonstrated a 2.7 fold increase in the patients that lost ambulation sooner [52, 53]. While not all studies have demonstrated a correlation between the G allele and worsened disease, [55], two recent studies have confirmed this OPN's SNP as a modifier of DMD [56, 57]. These mouse and human studies validate the initial hypothesis that OPN promotes DMD disease. In this project, we aimed to investigate the OPN-mediated mechanisms involve in the regulation of DMD's disease process.

Chapter 2

OPN's role in the regulation of the immune response in dystrophic muscle

2.1 Abstract

In the degenerative muscle disease Duchenne muscular dystrophy, inflammatory cells enter the muscle in response to repetitive muscle damage. Immune cell factors are required for proper muscle regeneration, but the chronic inflammatory environment creates a pro-fibrotic milieu that exacerbates disease progression. We previously identified osteopontin (OPN) as an immunomodulator, which is highly expressed in dystrophic muscles. Ablation of OPN correlates with reduced fibrosis and improved muscle strength in short term assessments. Moreover, OPN ablation reduces NKT and Gr-1+ cells and TGF-β levels. Here we demonstrate that the improved dystrophic phenotype observed with OPN ablation is not a result of reductions in NKT cells: instead we found that OPN ablation skews macrophage polarization towards a pro-regenerative phenotype. OPN ablation leads to reductions in M1 and M2a macrophages and increases in M2c. These changes are also associated with increased expression of pro-regenerative factors IGF-1, LIF and uPA. Furthermore, altered macrophage polarization correlated with increases in muscle weight and muscle fiber diameter resulting in long-term improvements in muscle strength and function in mdx

mice, up to seventy weeks of age. These findings suggest that OPN ablation promotes muscle repair via macrophage secretion of pro-myogenic growth factors.

2.2 Introduction

Patients with mutations in the *DMD* gene have Duchenne muscular dystrophy (DMD), which is a progressive muscle degenerative disease that leads to loss of skeletal, and cardiac muscle and eventual death [58]. In DMD, defective dystrophin protein causes muscle membrane fragility, leading to contraction-induced injury, due to high forces on the cell membrane and leading to cycles of muscle fiber degeneration and regeneration [1, 59]. Inflammatory cells invade in response to the repeated waves of damage and repair and release cytokines, which promote pathological fibrosis [60]. Fibrosis leads to loss of mobility and function and has the potential to interfere with gene and stem cell therapies. Inflammatory cells also secrete pro-myogenic factors that enable proper myogenic differentiation and are absolutely necessary for successful muscle repair [61-63]. Thus, modulating the inflammatory cell infiltrate in dystrophic muscle has the potential to target both fibrosis and regeneration and represents a therapeutic target for DMD. Such treatment may attenuate disease and improve the efficacy of other therapies if used in combination.

Macrophages are the predominant immune cell type found in the inflammatory infiltrate of human DMD and mdx muscles [64, 65]. Macrophages that infiltrate dystrophic muscles are a heterogeneous mix of classically (M1) and alternatively (M2) activated types [66, 67]. M1 macrophages are classified as pro-inflammatory, since they

express known pro-inflammatory mediators (TNF-α, IL-1β, IL-6), reactive nitrogen and oxygen intermediates [68-72]. M1 macrophages have also been shown to promote myoblast proliferation and collagen production in fibroblasts *in vitro* [61, 73]. The alternatively activated M2 macrophages on the other hand a more heterogeneous group; M2 macrophages can be subdivided in M2a, M2b and M2c macrophages [68-72]. M2a macrophages are believed to be fibrosis-promoting [61, 73], whereas M2c macrophages are thought to be deactivating for M1 macrophages and pro-regenerative. While the markers for M1 macrophages are fairly well defined, the markers to distinguish different subpopulations of M2 macrophages are less so, particularly M2c.

Osteopontin (OPN), encoded by the *SPP1* gene, is the most highly upregulated transcript in dystrophic muscles [14, 74]. OPN is a multi-functional protein that binds to a vast array of cell surface receptors, (primarily integrins) [75, 76], to activate diverse signaling pathways including NFκB and AKT. Osteopontin activity has been shown to affect diverse cellular processes such as bone remodeling, cell motility, cell adhesion and cell survival [77-79]. Our prior work identified OPN as a potential immunomodulator that regulates fibrosis in the mouse model of DMD [1]. In those studies, OPN ablation correlated with reduced muscle fibrosis, reduced TGF-β and increased regeneration. Moreover, we found that OPN ablation altered the inflammatory milieu leading to reductions in several immune cell populations such as NKT cells and Gr-1+ cells, as well as an increase in FoxP3 mRNA levels (a marker of regulatory T cells). However, the net effect of these changes in immune cell populations and the specific manner in which OPN ablation alters dystrophic disease is not completely understood.

Here we elucidate how changes induced by OPN ablation impact the pathogenesis of dystrophinopathies. The data show that OPN ablation skews dystrophic macrophages towards a pro-regenerative phenotype, leading to improved and sustained muscle mass and strength on long term functional testing. This investigation provides insight into the role of OPN in dystrophic muscle and further substantiates its value as a therapeutic target for DMD.

2.3 Materials and Methods

2.3.1 Animals

C57BL/6J, *mdx* (C57BL/10ScSn-Dmd^{mdx}/J) and OPN-Knockout mice (OPN-KO, B6.Cg-Spp1^{tm1Blh}/J) were obtained from The Jackson Laboratory. The *mdx* mice have a point mutation on exon 23 that generate a premature stop codon, leading to loss of expression of the full length form of the dystrophin protein [80]. On the other hand, OPN ablation in the OPN-KO mice was attained by replacing exons 4-7 of the *SPP1* gene with the phosphoglycerokinase neomycin resistance gene [38]. OPN$^{-/-}$mdx and OPN$^{+/+}$mdx mice came from colonies previously established in the lab [1] by breeding male OPN-KO mice with homozygous mdx females, which later resulted OPN$^{+/-}$mdx mice that were crossed between them to obtain OPN$^{-/-}$mdx and OPN$^{+/+}$mdx mice. These colonies have been maintained in the UCLA vivarium by homozygous crosses. OPN$^{-/-}$ mdx and OPN$^{+/+}$mdx colonies, are in a mixed C57BL10/C57BL6 background with a predominance of the C57BL10 background (~60% as determined by congenic analysis). All mice used in these experiments were genotyped using the previously published

protocols [38, 81] for the OPN and dystrophin mutations respectively. All animals were handled and bred according to the guidelines stipulated by the Animal Research Committee at the University of California, Los Angeles.

2.3.2 Intramuscular cardiotoxin injection

Quadriceps muscles from 3 month old C57BL/6J and OPN-KO mice were injected once with 100 µl of a 10 µM Cardiotoxin solution (CTX, Cardiotoxin from Naja mossambica mossambica, Sigma-Aldrich) using a glass syringe (Hamilton company) with a 32 gauge needle (Hamilton company). CTX-injected muscles were dissected at 12, 24, 48 and 72 hours after injection to be used for leukocyte isolation.

2.3.3 GM1 treatment of animals

Mdx mice were treated with an intra-peritoneal injection of 30µl (1.1mg)/injection polyclonal anti-asialo GM1 (CL8955, Cedarlane Laboratories, USA) or polyclonal rabbit sera (as a control, Invitrogen, Carlsbad, CA) twice a week. For all studies, injections began at 6 days of age and continued until mice reached 4 wks or 24 wks (6 months) of age.

2.3.4 Wire test

Mice were tested by wire test as previously described [1]. Briefly, mice were placed on a wire secured 2 feet above a safety net and allowed to use forelimbs and hindlimbs (but not their tail) to hang. Each mouse was subjected to 5 trials, with one minute of rest between trials. Hang time was recorded from the moment the experimenter placed the mouse onto the wire until the mouse fell onto the safety net. The five data points were averaged and data expressed in seconds.

2.3.5 Grip strength

Forelimb grip strength was measured using a digital force gauge (DFIS 2, Chatillon CE). Five trials were performed with 30-seconds of rest in between. In each trial, the mouse was allowed to grasp a metal rod and the technician slowly pulled the mouse by the tail until the digital gauge recorded the peak tension produced (in Newtons (N)). Data is reported as an average of the peak tension recorded in the 5 trials.

2.3.6 Wire Mesh Test

To assess overall muscle strength *in vivo*, mice were tested by wire mesh (custom built in the Spencer Lab). Briefly, mice were placed in the center of a wire mesh pulled over a square wooden frame on a swivel. The apparatus was placed ~1.5 ft over a cushioned floor. Once the mouse was in position, the wire mesh was rotated 180°, resulting in the mouse hanging upside down from the mesh. Because of the structure of the mesh, mice were only able to hang on to the mesh using their hindlimb and forelimb paws. Hang time was recorded from the moment the experimenter began to rotate the mesh until the mouse fell off the mesh. Each mouse was subjected to five trials, with one minute of rest between trials. The average hang time across five trials was calculated for each mouse.

2.3.7 Isolated Muscle Mechanics

Muscle specific force measurements from isolated Extensor Digitorum Longus (EDL), soleus and diaphragm muscles of 7 months old OPN+/+ mdx and OPN-/- mdx mice, were performed as previously described [82, 83]. Briefly, mice were anesthetized

with ketamine/xylazine and then executed; muscles were consequently removed and placed in a bath of Ringers solution gas-equilibrated with 95% O2 / 5% CO2. Sutures were attached to the distal and proximal tendons of the EDL and soleus muscles, and to the central tendon and rib of the diaphragm preparations. Muscles were subjected to isolated mechanical measurements using a previously described device (Aurora Scientific, Ontario, Canada) [84] and bathed in Ringers solution gas-equilibrated with 95% O2 / 5% CO2. After determining optimum length (Lo) by supramaximal twitch stimulation, maximum isometric tetanus was measured in the muscles during a 500 msec stimulation. Upon completion of these measurements, samples were rinsed in PBS, blotted, weighed. Muscle cross-sectional areas (CSA) were determined using the following formula: CSA = m / (Lo x L/Lo x 1.06 g/cm3). Where m is muscle mass (m), Lo is muscle length, L/Lo is the ratio of fiber length to muscle length, and 1.06 is the density of muscle.

2.3.8 Whole body plethysmography

Respiratory function was measured in conscious, unrestrained mice using a whole body plethysmograph from Buxco (Buxco, Data Sciences international (DSI)). In this system, mice are placed in a chamber that allows them to breathe naturally, unrestrained and untethered. The system measures the small changes in the air that is exchanged in and out of the entire chamber due to the animal's respiration (box flow). Each Chamber was calibrated before every experiment selecting the most appropriate response observed in the FinePoint Software (Buxco, Data Sciences international (DSI)) to the injection of 1ml of air into the chambers. Once all chambers were calibrated, mice were placed into their respective chamber and allowed to acclimate for

55 minutes. A Bias Flow Regulator (Buxco, Data Sciences international (DSI)) was used to prevent a rise in CO2 concentration during the acclimation and room air breathing periods. After acclimation, baseline respiratory function was measured for 5 minutes. Subsequently, mice were subjected to two hypercapnic challenges in which a flow of 1ml/min of 8% CO_2/21% O_2/balance N_2 (Praxair) was injected for 5 min into the chamber. In between the two hypercapnic challenges, mice were allowed to return to room air breathing for 10 min to evaluate their capability to recover. All data was collected and analyzed using the FinePoint Software. The FinePoint software, uses complicated algorithms that include variables affecting the respiratory function, such as humidity and temperature, to calculate from the measured box flow, the physiological values of the respiratory parameters from the animal. Mice were weighed prior to the beginning of the experiment. Minute ventilation and peak flows values were normalized to body weight.

2.3.9 Serum Creatine Kinase

Blood samples were collected by retro-orbital puncture using heparinized capillary tubes and transfered to serum separating tubes. Samples were kept at room temperature for 15 min to allow the blood to clot and then centrifuged at 3400g for 10 minutes to separate the serum. Once separated, serum was collected and store at -80 ^{o}C. Creatine kinase (CK) activity in blood was estimated using the Creatine Kinase-SL Kit from Sekisui Diagnostics. Assay was performed according to manufacturer's instructions. Briefly, serum samples were diluted 1:50 (V/V) with sterile Ca^{2+}, Mg^{2+}-free PBS. Controls for this test were established using the commercial control serums DC-TROL level-1 and level-2 (Sekisui Diagnostics). Samples and controls were set on

triplicates in a 96 wells plate, and mixed with the reaction buffers provided in the kit. Absorbance of the samples was measured at 340nm using a Synergy HT multi-detection microplate reader (Biotek Instruments). CK concentracion was reported in units per liter (U/L) and calculated using the following equation:

$$CK\left(U/L\right) = \frac{\Delta Abs/_{min} \times TV \times 1000}{d \times \varepsilon \times SV}$$

Where:

ΔAbs = Average absorbance change per minute

ε = milimolar absorptivity of NADH (6.22)

TV = Total reaction volume (ml)

SV = sample volume (ml)

d = light path in centimeter (cm)

1000 = conversion of U/ml to U/L

2.3.10 Muscle infiltrating leukocyte isolation

Mice were sacrificed and all muscles (hindlimb muscles, pectoralis, diaphragm and abdominal muscles) from each mouse were collected and pooled together into a petri dish containing sterile Ca^{2+}, Mg^{2+}-free PBS. Tissues were washed twice with sterile Ca^{2+}, Mg^{2+}-free PBS and then minced and digested into collagenase type 2 (Worthington Biochemical corporation) solution (1700 U/ml) at 37 ^{o}C with slow agitation. Once the tissue was digested, the sample volume was raised with sterile Ca^{2+}, Mg^{2+}-free PBS, to stop the digestion, and passed through a 70µm cell strainer. Cells were

then pelleted by centrifugation of the filtered mix at 900g for 5 min. Supernatant was discarded and pellet resuspended in ammonium-chloride-potassium (ACK) lysing buffer for 5 min to lyse the red blood cells. The lysing process was then stopped by raising the volume of the sample with sterile Ca^{2+}, Mg^{2+}-free PBS and centrifuged at 900g for 5 min to collect the cells. Cell pellet was resuspended again in sterile Ca^{2+}, Mg^{2+}-free PBS and passed through a 40µm cell strainer. Filtered cell suspension was then centrifuged at 900g for 5 min, supernatant discarded and cell pellet resuspended in a small volume of sterile Ca^{2+}, Mg^{2+}-free PBS. At this point, a small fraction of the sample was mixed 1:1 with a 0.4% trypan blue solution and the number of unstained cells in the sample counted using a hemocytometer. Concentration of viable cells in the sample and total number of viable cells was then assessed using the following formulas:

Viable cells/ml = unstained number of cells X dilution factor X 10^4

Total viable cells = viable cells/ml X Final volume of the sample

2.3.11 Magnetic-Activated cell sorting (MACS) of isolated macrophages

Macrophage isolation from the total leukocyte population was carried out using Miltenyi Biotec Magnetic-Activated Cell Sorting (MACS) technology. Isolated intramuscular leukocyte samples were first blocked with an antibody against CD16/CD32 (clone 93/Biolegend) to decrease non-specific labeling and then stained with fluorescently labeled anti-F4/80 (clone BM8, either PE or APC labeled, eBioscience). We used the company protocol for cell labeling and separation with magnetic nanoparticles coated with antibodies against the fluorescent label used for the primary antibody (either anti-PE or anti-APC coated microbeads, Miltenyi Biotec).

2.3.12 Fluorescence-Activated cell sorting (FACS) of isolated macrophages

MACS sorted F4/80^{+} samples were labeled with fluorescently tagged antibodies against Ly6C (Clone HK1.4 Biolegend), Siglec-F (clone E50-2440, BD Biosciences) or their respective isotypes controls (Rat IgG2c,K and Rat IgG2a,k, respectively). Fluorescently labeled samples were sorted using a FACScalibur (Becton-Dickinson) flow cytometer. Acquisition parameters (voltage, gain, etc.) were adjusted with aliquots of the same samples, to obtain the maximum dynamic range of side scatter height (SSC-H), forward scatter height (FSC-H) and fluorescence (at the different channels). FACS acquisition files were analyzed using FlowJo analysis software.

2.3.13 Macrophages sub-types isolation using FACS

Six OPN+/+mdx mice 4 weeks old and six 8 weeks old were used to isolated the individual macrophage sub-type populations. Muscles (hindlimb muscles, pectoralis, diaphragm and abdominal muscles) from all six mice were pooled together and intramuscular leukocyte isolation carried out as previously described. Isolated intramuscular leukocyte samples were first blocked with an antibody against CD16/CD32 (clone 93/Biolegend) to decrease non-specific labeling and then dually stained with anti-F4/80-APC (clone BM8, eBioscience) and anti-Ly6C-FITC (Clone HK1.4/ Biolegend). Fluorescently labeled samples were sorted using a FACSARIA III (Becton-Dickinson) cell sorter. Unlabeled samples were used as control. Acquisition parameters (voltage, gain, etc.) were adjusted with aliquots of the same samples, to obtain the maximum dynamic range of side scatter height (SSC-H), forward scatter height (FSC-H) and fluorescence (at the different channels). Macrophage populations limits were stablished using gates resembling those of the analytical experiments.

2.3.14 Macrophage culture and polarization treatments

The murine monocyte/macrophage cell line J774A.1 (ATCC) was used as the in vitro macrophage model. Macrophages were grown and maintained in macrophage growth medium (DMEM, 1% penicillin/streptomycin, 10% FBS) and subculture was prepared by scrapping. Macrophage polarization was attained by incubation of the macrophages cultures with growth medium supplemented with 100ng/ml of murine IFN-γ, IL-4 or IL-10 (BD Pharmingen) to polarize the cultures to M1, M2a or M2c macrophages respectively.

2.3.15 Isolation of liver NKT cells

Livers were removed and dissociated using the end of a 5cc syringe plunger and a 70µM cell strainer. Cell suspensions were centrifuged at 900 g for 6 min at room temperature. Cell pellets were resuspended in 0.85% ammonium chloride, and then incubated at room temperature for 10 min to lyse red blood cells. Following incubation, suspensions were diluted with DPBS without Ca^{+} and Mg^{+} (Invitrogen, Carlsbad, CA) to stop the lysing process and centrifuged for 6 min at 900 g. Pellets were resuspended in 40% Percoll and loaded to the top of a Percoll gradient (70% percoll at bottom and 40% Percoll at the top). Tubes were then centrifuged at room temperature for 20 min at 2,000 rpm. The cells at the interface were collected, washed and resulting pellets were resuspended in PBS and counted.

2.3.16 Antibody staining for flow cytometry of NKT cells

Muscle leukocyte suspensions were incubated with anti-CD16/CD32 (clone 2.4G2, BD Pharmingen, San Diego, CA) to block binding to Fc receptors, prior to

staining. The following mouse mAbs antibodies used for staining were all obtained from BD Bioscience/Pharmingen: CD3e (clone 145-2C11), Vβ8.1/8.2 (clone MR5-2), NK1.1 (clone PK136), pan NK (clone DX5). Antibodies were conjugated to FITC, PE, and/or Cy5. The following antibodies were biotinylated and revealed with Tricolor-conjugated streptavidin (ebioscience): anti-asialo GM1 (CL8955, Cedarlane Laboratories, USA) or rabbit sera (control, Invitrogen, Carlsbad, CA). Optimal working dilutions were determined for each antibody prior to use. All incubations were performed in Ca^{+}, Mg^{+} free DPBS (Invitrogen) at 4ºC for 30 min. Following the last wash, 10^3 live cells per sample were acquired on a FACS Calibur (Becton Dickinson, San Jose, CA) and analyzed with CELL Quest Pro software (Becton Dickinson). CD1d tetramers were obtained from the NIH Tetramer Core Facility.

2.3.17 Immunohistochemistry

Muscles were dissected, placed on balsa wood, coated with Tissue Tek ® O.C.T. (optimal cutting temperature, Sakura Finetek, Torrance, CA, USA) mounting media and frozen in isopentane cooled by liquid nitrogen. Diaphragm muscles were cut in half down the midline and rolled before freezing. Sections were cut on a Micron HM 505E cryostat (10 µm thick, Micron Instruments Inc., San Marcos, CA, USA) and stored at -20ºC until use. Immunohistochemistry was performed as previously described [85]. Briefly, sections were thawed at room temperature for 30 min, then treated with 0.3% H_2O_2 for 5 min and blocked in phosphate-buffered saline (PBS) with 0.2% gelatin, 0.5% Tween-20 and 3% bovine serum albumin (BSA) for 30 min. When necessary, binding to endogenous mouse IgG was blocked with a mouse on mouse kit (MOM Kit, Vector Laboratories). Sections were later incubated with antibodies against T-cell receptor

(TCR) Vα24 (eBioscience) to identify NKT cells in human biopsies, CD11b (clone M1/70, BD Biosciences) to emphasize areas of inflammation, or stained with neural cell adhesion molecule (NCAM, clone H28.123, Chemicon International) or developmental myosin heavy chain (dev. MHC, clone RNMy2/9D2, Novacastra) to emphasize regenerating fibers. Biotin-conjugated antibodies were used as secondary antibodies; follow by incubation with avidin-conjugated horseradish peroxidase and then stained using AEC substrate kit (Vector Laboratories). Muscle sections were later imaged using an Axio Imager M1 microscope (Zeiss) equipped with an AxioCam HRc camera (Zeiss). Mosaic images of the muscle sections were taken using a 10X EC Plan-NEOFLUAR objective (numerical aperture (NA): 0.3, Zeiss) and zoom in images were acquired using a 20X EC Plan-NEOFLUAR objective (NA:0.5, Zeiss). Images were acquired, processed and analyzed using the proprietary software Axiovision 4.8.1 (Zeiss).

2.3.18 Histopathology Index

Muscle necrosis was quantified from the muscle sections labeled with anti-CD11b antibody as the sum of the labeled (CD11b positive) areas in a section, normalized by the total cross-sectional area of the muscle section. Similarly, muscle regeneration was evaluated from the muscle sections labeled with anti-NCAM or anti-dev. MHC antibodies by counting the number of both, small diameter myotubes and large diameter regenerating myofibers positively labeled with NCAM or dev. MHC, and normalizing this by the total muscle cross-sectional area of the muscle. Cross-sectional areas were measured using the proprietary software Axiovision 4.8.1 (Zeiss). All analyses were performed blindly.

2.3.19 Western Blots

Cell culture samples were lysed in reducing sample buffer (RSB, 50 mM Tris-HCl pH 6.8, 10% Glycerol, 2% SDS, 100 mM β-mercaptoethanol) supplemented with protease and phosphatase inhibitors. Bromophenol blue (0.1%) was later added and samples boiled at 100 ^{o}C for 5 min for protein denaturation. SDS-PAGE and Western blotting were carried out as previously described [85]. BenchMark™ protein ladder was used as molecular weight marker in every gel. Proteins were separated by gel electrophoresis and then transferred into a nitrocellulose membrane. Membranes were blocked with 5% milk in TBS-T (Tris-Buffered saline, 0.1% Tween) and then incubated with 1/500 anti-mouse OPN antibody (# AF808/R&D systems) solution in 5% milk TBS-T overnight at 4 ^{o}C. Membranes were then washed and incubated with the Horseradish peroxidase (HRP) conjugated secondary antibody in 5% milk TBS-T. The chemiluminescence substrate kit, ChemiGlow West (Protein simple) was used to detect the protein bands. Chemilumiscence signals were detected and densitometry analyzed using the FluorChem FC2 system (Alpha Innotech).

2.3.20 Quantitative RT PCR

RNA was isolated and qRT PCR carried out as previously described [16]. Briefly, total RNA was isolated from cell cultures and isolated cells using Trizol reagent (Invitrogen) according to the manufacturer's protocol. Genomic DNA contamination was removed by DNase I treatment (Invitrogen). To synthesize cDNA, 1.5 µg of DNA-free RNA was used for first-strand cDNA synthesis with random hexamer primers and Superscript III reverse transcriptase (Invitrogen) following the company's protocol. The resulting cDNAs were used for PCR amplification using the primers sequences detailed

in Table 2.1. Quantitative PCR reaction was set using the iTaq™ universal SYBR® green supermix (Bio-Rad) following the manufacturer's protocol. PCR product formation was evaluated using the CFX- Connect Real Time System (Bio-Rad).

2.3.21 Statistical Analysis

Means were compared by genotype and age using a factorial analysis of variance model where variances were allowed to be heterogeneous since variance homogeneity did not hold. For pulmonary outcomes where the same animal was exposed to CO2 and room air conditions, means were compared by genotype and condition using a repeated measure analysis of variance model (mixed model). Post hoc (under the model) p values were computed using the Fisher LSD criterion. Residual error normal quartile plots were examined to confirm that the residual errors followed a normal distribution, allowing the use of a parametric model. Student's t-test and/or a Mann-Whitney U test were used for experiments using only 2 groups. Values were considered significantly different if $p \leq 0.05$.

2.3.22 Acknowledgements

This work was supported by funding from the National Institute of Arthritis, Musculoskeletal and Skin Diseases for a Wellstone Cooperative Muscular Dystrophy Center (U54AR052646-Sweeney), a P30 Muscular Dystrophy Core Center (NIAMS-P30AR057230-01-Spencer) and an RO1 (AR046911). Funding was also provided by Parent Project Muscular Dystrophy (Spencer) and the Muscular Dystrophy Association (Spencer). All functional assessments were carried out in the Center for Duchenne Muscular Dystrophy Mouse Phenotyping and Imaging Core (supported by P30 AR057230). CD1d tetramers were obtained from the NIH Tetramer Core Facility

(contract HHSN272201300006C). Some of the flow cytometry was performed in the UCLA Johnsson Comprehensive Cancer Center (JCCC) and Center for AIDS Research Flow Cytometry Core Facility that is supported by National Institutes of Health awards P30 CA016042 and 5P30 AI028697, and by the JCCC, the UCLA AIDS Institute, and the David Geffen School of Medicine at UCLA. The authors are grateful to Dr. Enca Montecino-Rodriguez for her help in the design and conduct of the NKT related experiments and to Julia Overman, Jane Wen and Diana Becerra for technical assistance. The authors also thank Yasmine Pichvai for her valuable help in the staining and analysis of the muscle sections in the evaluation of the muscle cross sectional areas.

2.3.23 Supplemental material

Figure 2.5 shows the effect of OPN ablation on macrophage polarization in acute injury experiments (Ctx-injection experiments). Table 2.3 provides the total cell number in the different macrophage sub-types per muscle mass, from the experiments shown in Figure 2.4 for 8-week-old mice. Figure 2.12 provides information about the degree of improvement caused by OPN ablation in mdx mice by comparing the performance of C57BL/6J and OPN-/-mdx mice in different muscle strength tests. Finally, Table 2.1 summarizes the sequences of the primers used in this paper.

2.4 Results

2.4.1 Role of NKT cells in the mdx phenotype

Our previous investigations demonstrated modulation of the mdx immune infiltrate following OPN ablation [1]. In those studies, OPN-ablation led to a significant decrease in the frequencies of intramuscular NKT and Gr-1+ cells invading mdx muscles [1]. NKT cells are T cells that also express NK cell markers (e.g. NK1.1 or DX5) (see [86] for review). These cells are activated by glycolipids, which are presented in the context of membrane bound CD1d molecules, akin to the manner in which T cells recognize peptides in the context of MHC class I and II. To determine whether these cells are relevant to the human disease, ten biopsies from DMD boys ranging from 3 to 9 years of age were examined for evidence of NKT cells presence within the muscle tissue, by using an antibody against the invariant alpha chain (Vα24) expressed by human NKT cells. This analysis confirmed that scattered Vα24+ cells were present within the biopsies (Figure 2.1A).

To understand whether changes in NKT populations (such as those observed with OPN ablation) might underlie amelioration of the dystrophic phenotype, we conducted *in vivo* depletion of NKT cells using an antibody against asialo-GM1, which was injected to mdx mice. Asialo-GM1 is a well-established cell surface ganglioside of NK and NKT cells, which is necessary for their complete activation. Treatment with anti-asialo-GM1 has been previously shown to result in a reduction of both cell types [87-90]. mdx mice were treated from one week of age until they were assessed for functional and phenotypic features of muscular dystrophy at 4 and 24 weeks of age. To verify that treatments were effective in depleting NKT cells, we evaluated intramuscular

NKT cells in treated mice, using tetramers of CD1d in conjunction with markers of NK and T cells (Figure 2.1B). Liver NKT cells were examined in parallel as a positive control. This analysis showed that GM1 treatment reduced intramuscular NKT cells (i.e. cells co-expressing CD3+, NK1.1 and CD1d+ tetramer) by 85% (Figure 2.1B). Tetramer negative NKT cells (i.e. cells expressing CD3+, NK1.1+, CD1d-) were also depleted by GM1 treatment by 83% (Figure 2.1B). In spite of reductions in NK and NKT cells, attenuation of intramuscular fibrosis or other features of the mdx phenotype was not observed at either the 4 or 24-week time points (Table 2.2). Thus, the studies eliminate NKT cells as effectors of the dystrophic phenotype and suggest that the previously observed phenotypic improvements on OPN ablation were not a result of reductions in NKT cells.

2.4.2 Macrophage polarization is altered in the absence of OPN

Our prior studies demonstrated that the frequency of Gr-1+ cells (previously used as a Ly6G marker) was significantly reduced in OPN-/-mdx muscles [1]. Because the Gr-1 antibody recognizes both Ly6G (a neutrophil specific marker) and Ly6C (a pan granulocyte and macrophage marker) we sought to further explore the Gr-1+ cell types affected by OPN ablation. Double staining of isolated mdx leukocytes with Gr-1 and F4/80 antibodies revealed that neutrophils make up approximately 7% of the total CD45+ leukocytes at 4 weeks and 5 months of age (Figure 2.2A), which is a smaller percent of the leukocyte infiltrate than we had previously estimated [1]. However, consistent with our prior results, the frequency of neutrophils was slightly decreased in OPN-/-mdx muscles (Figure 2.2A). Also consistent with our prior results, there was no change in the frequency of F4/80+ cells upon OPN ablation. To determine the frequency

of eosinophils vs macrophages within the F4/80+ population, we stained for Siglec F, which is a marker of eosinophils. Eosinophils comprised about 15% of all F4/80+ cells (Figure 2.2B) and their frequency was not altered in the absence of OPN (Figure 2.2B).

Examination of the Ly6C marker on isolated leukocytes revealed a striking shift in its distribution (between $Ly6C_{low}$ vs. $Ly6C_{high}$) in OPN-/- mdx mice (Figure 2.3A). Since Ly6C levels change from high to low as macrophages undergo polarization [91-93]; we reasoned that the altered Ly6C levels might reflect changes in macrophage subtypes. To determine whether the observed shift in Ly6C was due to a change in macrophage polarization, we examined sorted F4/80+ cells from 4 and 8 week old mdx mice for expression of Ly6C. To obtain reproducible data, it was necessary to sort the F4/80+ cells and then exclude the eosinophils, based on SSC-H and FSC-H gating (Figure 2.3B). The macrophages were subsequently analyzed for Ly6C expression, which revealed the presence of three distinct populations; 1) F4/80-low Ly6C-high; 2) F4/80-medium Ly6C-medium; and 3) F4/80-high Ly6C-low (Figure 2.3C). Quantitative evaluation of these macrophage populations showed that the Ly6C-high and the Ly6C-medium populations were significantly decreased in the OPN-/- mdx mice while a significant increase was observed in the Ly6C-low population in both 4 and 8 week old OPN-/- mdx mice (Figure 2.4). A similar tendency in skewing of macrophage polarization was also observed in an acute injury model with OPN ablation (Figure 2.5). Thus, a consistent skewing of Ly6C was observed on isolated macrophages from OPN-/-mdx mice.

2.4.3 Levels of F4/80 and Ly6C correlate with M1, M2a and M2c macrophage sub-types.

To further characterize the phenotype of the macrophage populations that we observed, we FACS sorted, based on their Ly6C and F4/80 surface expression. After sorting, leukocytes from 4 and 8 week old mdx mice were examined for gene expression profiles commonly associated with macrophage sub-types (Figure 2.6). The F4/80-low Ly6C-high macrophages displayed high levels of iNOS expression, with very little or no Arg-1, CD206 or CD163 expression, thus resembling M1 macrophages. The other two groups of macrophages, F4/80-medium Ly6C-medium and F4/80-high Ly6C-low, were both Arg-1+, CD206+ and CD163+, with little to no iNOS expression. However, the F4/80-medium Ly6C-medium group had the highest Arg-1 expression, suggesting that they resembled the M2a subtype, while the F4/80-high Ly6C-low showed higher CD206 and CD163 expression and low Arg-1, suggesting that these cells align with the profile of M2c macrophages. Thus, based on these expression profiles, we have defined F4/80-low Ly6C-high macrophages as M1, F4/80-medium Ly6C-medium as M2a and F4/80-high Ly6C-low as M2c. These data reveal that OPN-ablation in mdx mice alters macrophage polarization towards decreased M1 and M2a subtypes and increased M2c type macrophages. Overall, the ratios of M1 to M2 are decreased at both 4 and 8 weeks of age (Figure 2.6C and Table 2.3).

2.4.4 OPN is a novel marker of M2c macrophages.

We next examined if OPN is differentially expressed in the three macrophage subtypes. Analysis of OPN expression in the sorted populations demonstrated that M2c macrophages express the highest levels of OPN compared to M1 and M2a subtypes

suggesting that OPN may be a novel and suitable marker for identification of M2c macrophages (Figure 2.7). To further characterize the expression of OPN in macrophage populations, we evaluated OPN expression in a macrophage cell line that was induced to polarize to defined macrophage phenotypes by exposure to specific cytokines. J774A.1 macrophages were exposed to either interferon gamma (IFNγ, interleukin 4 (IL-4) or interleukin 10 (IL-10) and their expression of traditional macrophage polarization markers was assessed: iNOS for M1, Arg-1 for M2a and IL-10 for M2c macrophages (Figure 2.8A). We observed that expression of iNOS, Arg-1 and IL-10 were induced by IFNγ, IL-4 and IL-10 treatments (respectively), suggesting that the macrophages polarized as expected; however, we observed that IL-10 expression was also induced in cells treated with IFNγ suggesting that IL-10 is not a specific M2c marker (Figure 2.8A). Additionally, we observed that OPN expression was specifically induced in M2c in macrophages treated with IL-10, both at the RNA (Figure 2.8C) and protein (Figure 2.8D) levels, suggesting that OPN is most highly expressed in this subtype of macrophage. The data show that OPN is a marker that distinguishes M2c macrophages from M1 and M2a types. To our knowledge, this finding suggests that OPN may represent the first specific M2c macrophage marker.

2.4.5 OPN-ablation promotes the expression of pro-regenerative factors from mdx macrophages

Since the phenotype of tissue macrophages dictates the manner in which they influence a disease process, we sought to identify the functional outcome of the observed shift in macrophage polarization in the setting of OPN ablation in mdx mice. To this end, we assessed the expression of pro-fibrotic and pro-regenerative factors by

RT-PCR on sorted F4/80+ cells, isolated from OPN-/-mdx and OPN+/+mdx muscles. Based on the previous observations of reduced fibrosis in OPN-/-mdx muscles [1], we expected to detect a decrease in pro-fibrotic cytokines such as TGF-β. However, no significant differences were observed in the expression of different pro-fibrotic factors such as: fibronectin [94], chemokine ligand 17 (CCL17) [95] and transforming growth factor beta (TGF-β) [94] (Figure 2.9A). On the contrary, OPN-/-mdx macrophages showed significantly increased expression of pro-regenerative factors, such as insulin-like growth-1 (*IGF-1)* [96], leukemia inhibitory factor (*LIF)* [97] and urokinase plasminogen activator (*uPA)* [98] (Figure 2.9B). Thus, OPN ablation appears to skew macrophages towards a pro-regenerative macrophage phenotype in dystrophic muscles.

2.4.6 OPN-ablation correlates with increased muscle mass and fiber diameter.

The observed increase in pro-regenerative growth factors is consistent with our prior report of increased regenerating fibers in OPN-/-mdx muscles [1]. To determine if the observed shift toward a pro-regenerative macrophage phenotype on OPN ablation leads to overall increases in muscle mass, we examined muscle weight and fiber diameter in the two genotypes of mice. Quadriceps muscles were carefully dissected and weighed and the muscle weight was normalized by tibial length. This analysis showed a significant increase in quad muscle mass at 3 months, 6 months and 1 year of age (Figure 2.10). Extensor digitorum longus (EDL) muscle mass was also significantly increased at 6 months of age (Figure 2.10). Because the EDL is a small muscle with parallel fiber architecture, we also assessed the number of fibers and fiber diameter in this muscle. While the number of fibers per cross sectional area did not

differ between genotypes, we observed an overall increase in the fiber cross sectional area in OPN-/-mdx EDL. Examination of the distribution of the fiber diameters revealed that the differences were in the smallest and largest fibers, suggesting that two processes were being affected in the OPN-/-mdx: muscle regeneration as well as muscle growth.

2.4.7 OPN-ablation induces long-term amelioration of the dystrophic phenotype in mdx mice.

To determine if the improvements in muscle mass that we observed lead to long-term consequences on the health and function of dystrophic muscles, we carried out non-invasive functional muscle testing and physiological muscle strength tests on OPN-/- mdx and OPN+/+ mdx mice over a long time course. These studies revealed that OPN ablation led to a sustained improvement in muscle strength in dystrophic mice (Figure 2.11). OPN-/-mdx mice performed better on wire hanging (Figure 2.11A), grip strength (Figure 2.11B) and wire mesh tests (Figure 2.11C), without large changes in body weight (Figure 2.11D). Additionally, physiological testing of single isolated extensor digitorum longus (EDL), soleus and diaphragm muscles from OPN-/- mdx mice showed a significant increase in specific force (Figure 2.11E). Moreover, we observed significantly reduced serum creatine kinase (Figure 2.11F) and improved pulmonary function (based on improved minute ventilation and peak expiratory flow shown in Figure 2.11G, H, I). Thus, these studies reveal that the pro-regenerative phenotype observed in OPN-/-mdx macrophages correlates with long-term improvements in muscle strength and function.

2.5 Discussion

In this investigation, we sought to understand the manner in which OPN ablation attenuates the severity of muscular dystrophy using the mdx mouse model. Several leukocyte populations were evaluated, in follow up to our prior investigation in which we observed changes in NKT and Gr-1+ cells in OPN-/-mdx mice [1]. Here we demonstrate that the reduced frequency of NKT cells on OPN ablation [1] does not contribute to the amelioration of dystrophic pathology: as depletion of greater than 80% of NKT cells in mdx muscles did not improve phenotypic features of the disease (Table 2.2). Thus, our results confirm that these cells are not disease promoting in dystrophinopathies and that reductions in NKT cells do not play a causal role in the improvements that occur in OPN-/- mdx mice.

An important finding of this investigation is the role that we revealed for OPN in macrophage polarization in the setting of dystrophinopathy. Shifts in macrophage phenotypes have been previously proposed to influence the course of mdx dystrophy [67, 99, 100]; whereby reductions in IFN-γ, iNOS or CCR2, reduce the M1/M2 ratio and attenuate disease [99, 101], while IL-10 ablation, increases the M1/M2 ratio, and exacerbates disease [100]. In agreement with the prior findings, we show here that the OPN ablation-induced decrease in the M1/M2 ratio of mdx macrophages improves the dystrophic phenotype and increases muscle mass and strength. In addition, we identify OPN as a potential new marker of M2c macrophages. Our studies show that OPN is more specific than CD163 and IL-10 in identifying the M2c macrophage sub-type, both *in vivo* and *in vitro*.

The increased muscle strength observed in this investigation is highly likely to be related to the significant increase in macrophage expression of pro-regenerative factors, IGF-1 [96], LIF [96, 97] and uPA [98, 102]. At the same time, no significant difference was observed in the expression of pro-fibrotic factors such as: fibronectin [94, 103], CCL17 [95, 104] and TGF-β (Figure 2.9). The increase in pro-regenerative factors agrees with the relative shift towards M2c macrophages that we observed with OPN-ablation, since M2c macrophages have been traditionally classified as the "pro-regenerative" macrophage sub-type.

The effect of OPN ablation on macrophage polarization may be direct or indirect. OPN has been previously shown to suppress iNOS and IL-10 expression and to induce IL-12, IL-6, TNF and IL-1β expression in a variety of *in vitro* macrophage models [105-111]. Future studies are needed to gain insight into the specific relationship between OPN and macrophage polarization in the context of dystrophic muscles.

We previously observed reductions in TGF-β in muscles of OPN-/- mdx mice, but the results here revealed that alterations in TGF-β levels are not due to the observed shift in macrophage polarization. MACS sorting allowed us to more specifically evaluate the cytokine contribution of macrophages to the dystrophic milieu, and eliminate macrophages as the source of reduced TGF-β on OPN ablation. This result leaves us without an explanation for why OPN ablation reduces TGF-β levels in dystrophic muscles. OPN biology is complex and thus, intensive studies on isolated cell types will be required to fully elucidate all of the pathways it regulates in dystrophic muscle. OPN binds to a large number of different integrins, as well as to the glycoprotein CD44, and may affect different cell types including fibroblasts [112]. OPN can also be retained

intracellularly or post-translationally modified by cleavage, phosphorylation and glycosylation; thus, adding complexity to understanding its role in dystrophy. More studies are necessary to fully understand which of its targets and signaling pathways are involved in DMD.

The changes induced in the macrophage population by OPN-ablation, correlated with improved muscle strength and function: OPN-/- mdx mice were stronger than OPN+/+mdx mice. Mdx mice lacking OPN were able to hang from 1.2 to 8 times longer than mdx mice when tested in the wire and mesh tests, at most ages tested. They also had less muscle damage as shown by a significant decrease in the serum creatine kinase levels. Additionally, we showed that OPN-ablation in mdx mice improved the respiratory function of these mice, suggesting that the diaphragm muscle pathology is reduced. Although there was a significant improvement in the dystrophic phenotype, OPN ablation does not restore mdx mice muscle strength back to normal (Figure 2.12). We anticipate that OPN inhibitors would be beneficial and could be used in combination therapy with other agents to slow disease progression and improve muscle function.

The complex biology of OPN and its multifaceted impact on signaling pathways in different cells types may provide an explanation for conflicting reports about OPN as a disease modifier of DMD. Pegararo and colleagues identified a single nucleotide polymorphism (SNP) in the promoter of the OPN gene (*SPP1*) that correlated with a more severe disease course, compared to the more common haplotype [53]. The SNP is found in the AP1 binding site, very close to the translational start site of the protein. In that initial study, patients with the “GG/TG” SNP lost ambulation sooner than patients with the “TT” SNPs and expressed 2.7 fold higher levels of OPN. While a few

subsequent studies on this modifier were inconclusive, follow-up study confirmed the modifier effect, but interestingly, the effect was only observed in steroid treated patients [56]. Studies in the dog model of DMD have demonstrated that levels of osteopontin correlate with degree of disability in different muscles [113]. Therefore, modulation of OPN has been demonstrated in mice, dogs and humans to impact disease progression.

This study suggests that modulating immune cell infiltrates toward a more pro-regenerative phenotype may slow down disease progression and improve muscle function in the dystrophinopathies. Furthermore, it provides insights into OPN-mediated mechanisms of mdx dystrophy and supports the development of OPN inhibitors to treat DMD.

Table 2.1 qPCR primers used.

	Forward	Reverse
GAPDH	TCCACCACCCTGTTGCTGTA	GACTTCAACAGCAACTCCCAC
iNOS	ATCGACCCGTCCACAGTATG	GATGGACCCCAAGCAAGACT
Arg-1	GCACTGAGGAAAGCTGGTCT	GACCGTGGGTTCTTCACAAT
IL-10	CCAAGCCTTATCGGAAATGA	TTTTCACAGGGGAGAAATCG
CD206	CAGGTGTGGGCTCAGGTAGT	TGTGGTGAGCTGAAAGGTGA
CD163	TCTCCACACGTCCAGAACAG	CCTCGTCACCTTGGAAACAG
IGF-1	GCAACACTCATCCACAATGC	TGGATGCTCTTCAGTTCGTG
LIF	TACAGGGGTGATGGGAAGAG	GAAAACGGCCTGCATCTAAG
uPA	GGGCTTGTTTTTCTCTGCAC	GGACCCAGAGTGGAAAACAG
Fibronectin	CTGGGGGTCTCCGTGATAAT	GGGAGAAGTTTGTGCATGGT
CCL17	ATCCCTGGAACACTCCACTG	TGCTTCTGGGGACTTTTCTG
TGF-β	AAGTTGGCATGGTAGCCCTT	GGAGAGCCCTGGATACCAAC

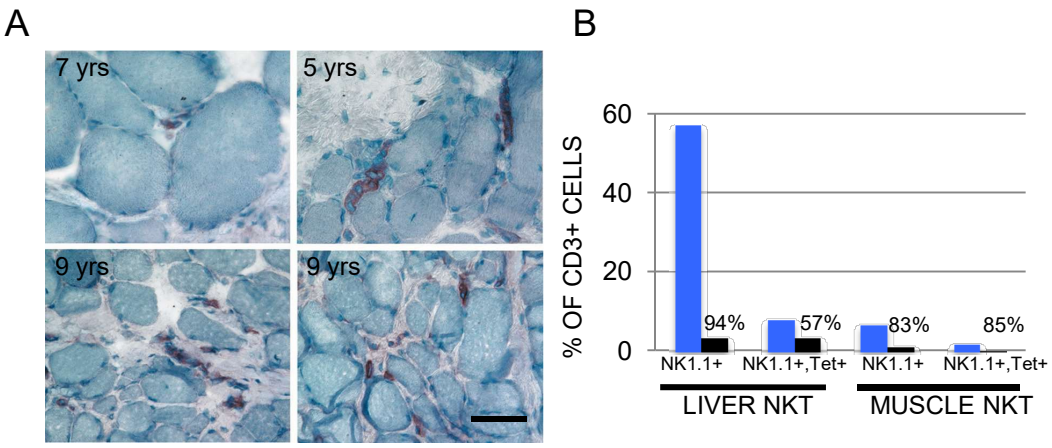

Figure 2.1 NKT cells are observed in muscles from patients with Duchenne muscular dystrophy, and are depleted from mdx muscle and liver by GM1 treatment.

A) Cross sections from DMD biopsies were immunostained with an antibody against Vα24, the invariant chain of human NKT cells. Positive staining appears red and counterstain with hematoxylin labels the nuclei, dark blue and the muscle tissue light blue. All micrographs were taken at the same magnification. Bar, 100μm. B) Quantification of liver and muscle NKT cells from GM1 or PBS treated animals. The graph shows a representative experiment with three animals for each bar, demonstrating the frequency of CD3+ cells that co-express either [NK1.1] or [NK1.1+ CD1d-tetramer]. Blue bars represent cells isolated from PBS injected mice and black bars represent cells isolated from GM1-treated mice. Numbers shown represent the amount of depletion attained by GM1 treatment compared to PBS controls.

Table 2.2. Functional and histological features of dystrophic mice treated with GM1.

	4 weeks		6 months	
	mdx-R.sera	**mdx-GM1**	**mdx-R.sera**	**mdx-GM1**
Body weight (g)	11.08 ± 2.2, n=30	11.61 ± 1.79, n=29	28.94 ± 4.46, n=11	29.93 ± 3.9, n=11
Wire Test (seconds on wire)	31.83 ± 10.6, n=23	33.46 ± 13.27, n=28	18.93 ± 10.76, n=11	15.6 ± 11.34, n=11
Creatine Kinase (IU/L)	25039 ± 11620, n=6	26851 ± 8997, n=6	10745 ± 4959, n=6	11086 ± 3789, n=6
Histopathology- quadriceps (% necrotic area)	8.04 ± 4.35, n=6	11.08 ± 5.39, n=8	3.71 ± 1.27, n=9	4.82 ± 2.66, n=9
Histopathology- diaphragms (% necrotic area)	n/a	n/a	6.69 ± 2.05, n=6	6.15 ± 2.22, n=6
Histopathology- NCAM (% positive fibers)	5.11 ± 2.3, n=13	5.91 ± 3.03, n=12	n/a	n/a
Histopathology- dev. MHC (% positive fibers)	5.06 ± 1.61, n=9	6.79 ± 2.93, n=10	n/a	n/a

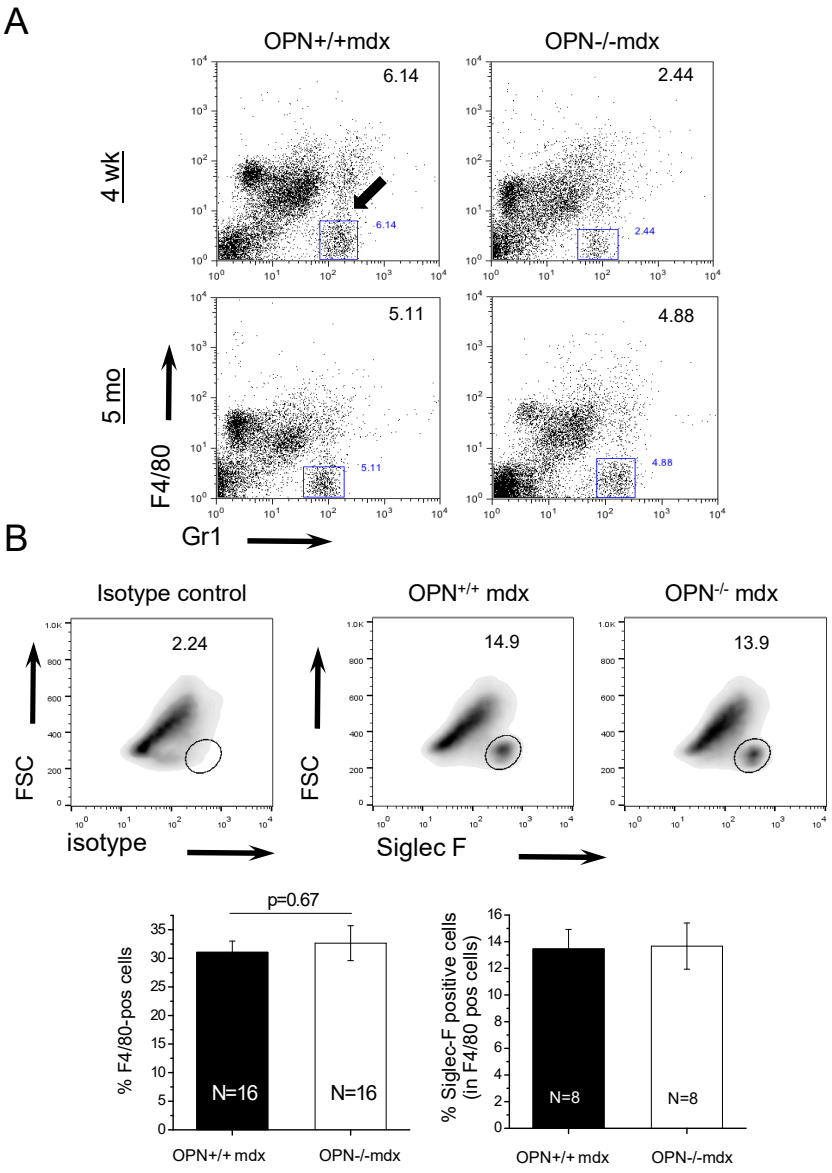

Figure 2.2 Analysis of Ly6C+ cells in OPN-/-mdx infiltrates

A) Muscle leukocytes were isolated from OPN-/-mdx and OPN+/+mdx muscles, stained for Gr1 and F4/80 and assessed by flow cytometry. FACS-plots above show F4/80 plotted against Gr1. Cells enclosed by the blue square represent neutrophils. The frequency of neutrophils is indicated in the top right of each quadrant. B) Analysis of eosinophils was carried out by Siglec F staining on sorted F4/80+ cells from OPN+/+ mdx and OPN-/- mdx muscles. Circled region in the FACS-plots represent the eosinophil population and numbers indicate eosinophil frequencies (upper panel). Lower graphs show the quantification of F4/80+ cell frequency in the total intramuscular leukocyte population (lower left) and eosinophils in the intramuscular F4/80+ cell population (lower right panel). Black bars represent OPN+/+mdx, white bars represent OPN-/-mdx. Animal numbers are indicated on graphs. P values were generated by Student's T-test. Vertical lines represent standard error of the mean.

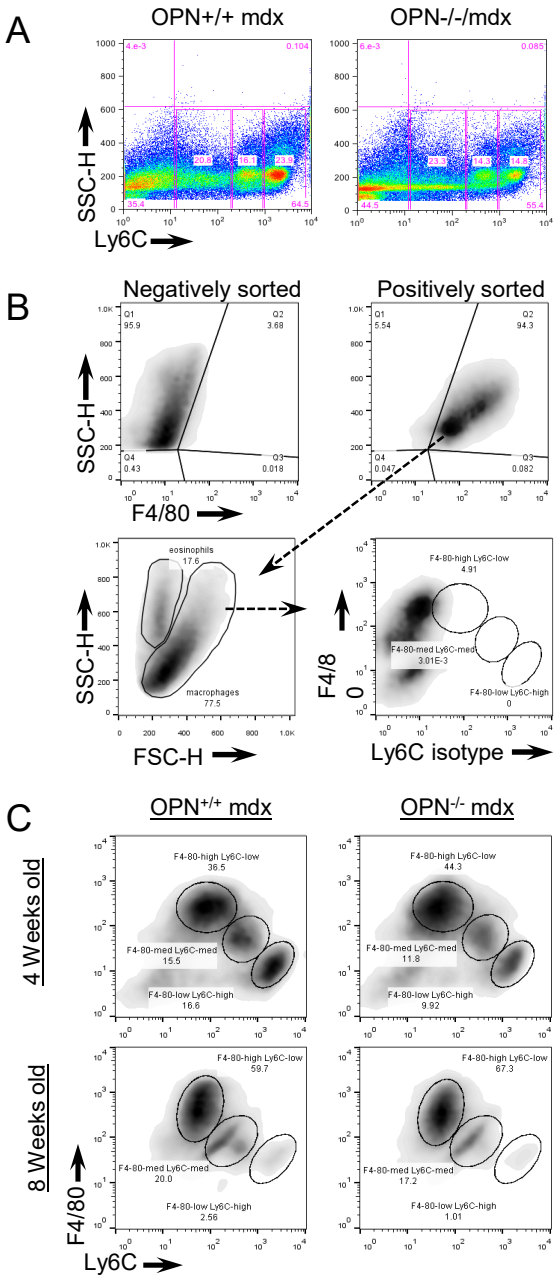

Figure 2.3 Evaluation of macrophage polarization by cell sorting and FACS analysis

A) Shown are representative FACS plots of muscle infiltrating leukocytes stained for Ly6C and plotted against FSC for OPN+/+mdx and OPN-/-mdx; B) Demonstration of the purity of the MACS sorting. Top left FACS plot shows F4/80 staining of the negatively sorted population and the right FACS plot shows F4/80 staining of the positively sorted population. Positively sorted cells (arrow) were examined by SSC and FSC to isolate macrophages (larger population on the right) from eosinophils (left population). Bottom right FACS-plot shows Ly6C-isotype control staining on the macrophage population used in these studies; C) Representative FACS-plots of MACS sorted F4/80+ macrophages, stained for F4/80 and Ly6C. Circled regions represent distinct macrophage populations. Experiments were done at 4 weeks and 8 weeks of age. Quantification of these experiments is shown in Figure 3.4.

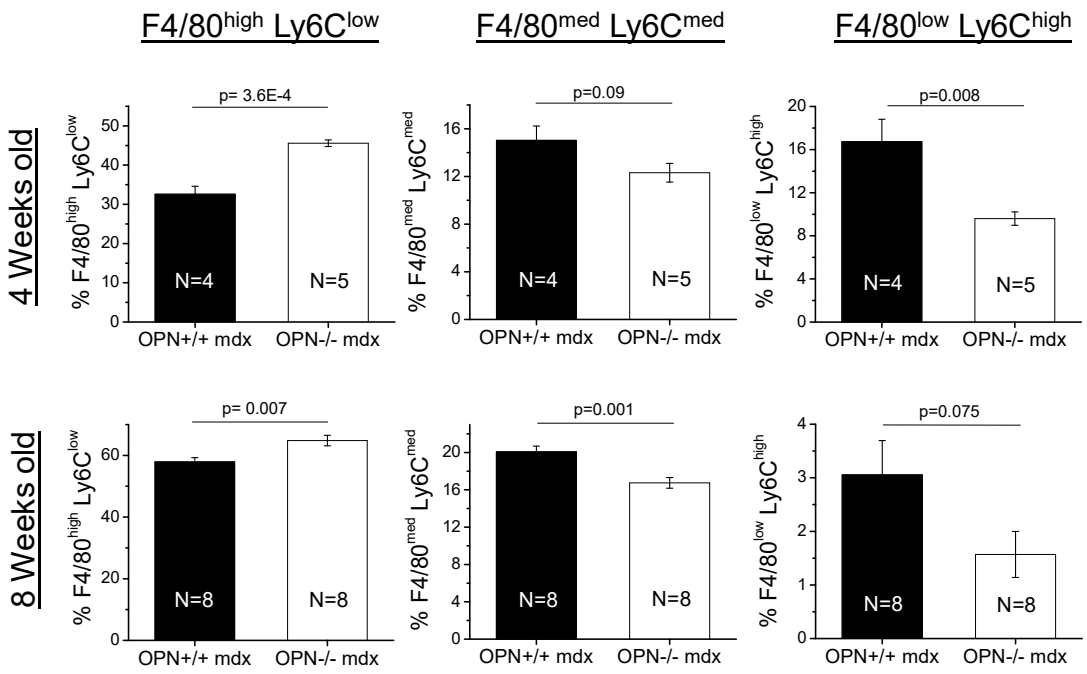

Figure 2.4 Macrophage polarization is skewed in OPN-/-mdx muscles.

Quantification of macrophage subpopulations from MACS sorted F4/80+ macrophages, isolated from OPN+/+mdx and OPN-/-mdx muscles. Plots depict mean values of pooled data from 4 week (upper panel) and 8 week (lower panel) old mice, assessed as described in Figure 3.3. Vertical lines represent standard errors. Animal numbers are indicated on each bar of the graph. Statistical significance determined by Student's T test. P values are indicated.

Table 2.3. Total number of cells in the different macrophage sub-types per muscle mass.

	M1 macrophages/ gram of muscle	M2a macrophages/ gram of muscle	M2c macrophages/ gram of muscle	M1/M2 (cells/ gram of muscle)
OPN+/+ mdx	5,114.46 ± 904.57	51,224.95 ± 17,766.53	150,805.14 ± 54,867.11	0.040 ± 0.0086
OPN-/- mdx	3,470.12 ± 622.14	46,037.68 ± 8,489.52	185,280.27 ± 10,551.16	0.020 ± 0.0057

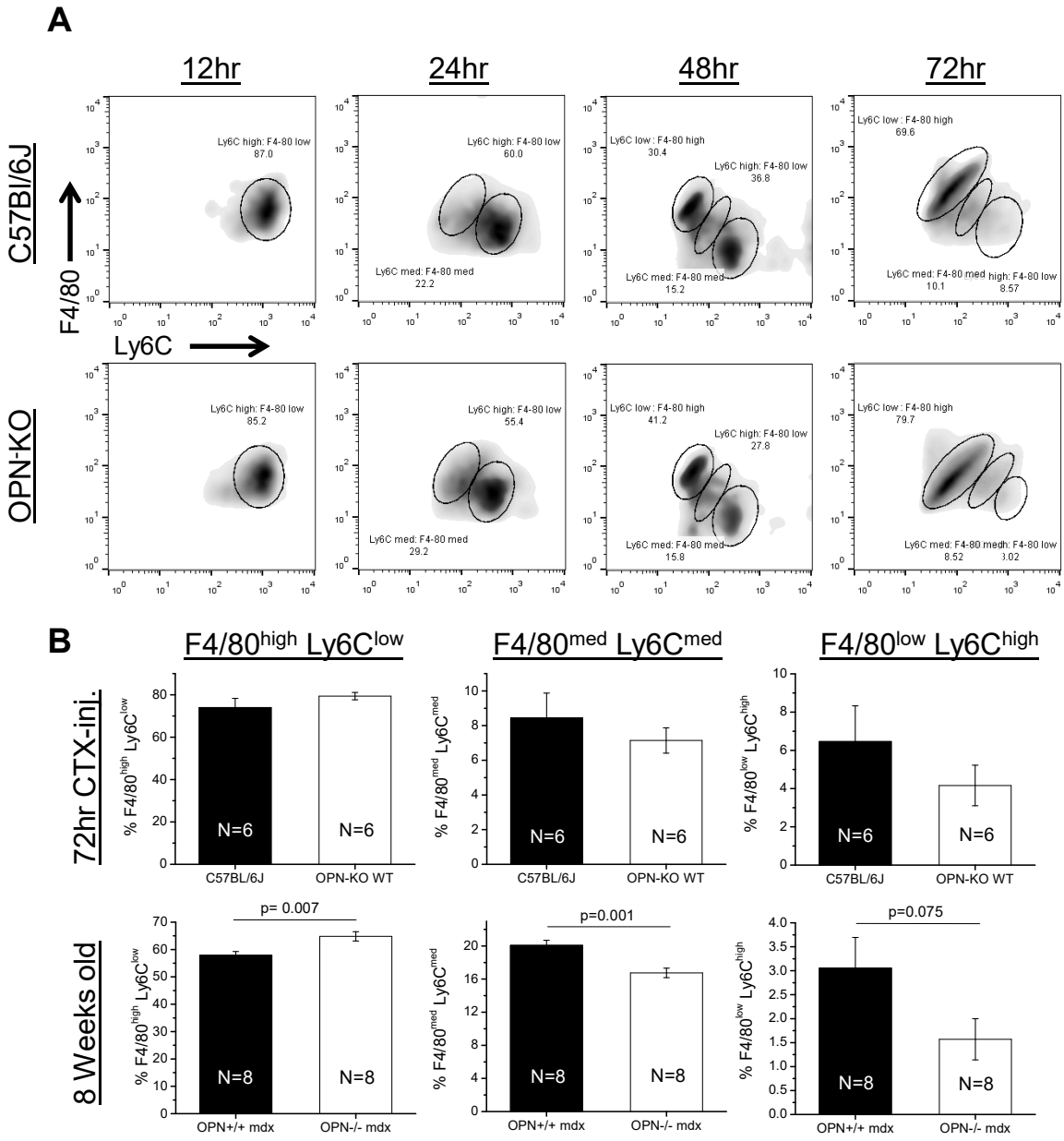

Figure 2.5 Assessment of the effect of OPN on macrophage polarization in acute injury experiments.

A) Representative FACS plots of muscle infiltrating leukocytes isolated from quadriceps muscles of C57BL/6J and OPN-KO mice, at different times after CTX-injection. Cells were labeled with anti-F4/80 and anti-Ly6C antibodies, eosinophils were excluded from the analysis by examination of SSC and FSC distribution. Macrophage populations were plotted in terms of their F4/80 and Ly6C expression. Circled regions represent distinct macrophage subsets. B) Quantification of macrophage subpopulations isolated from muscles of C57BL/6J and OPN-KO mice 72 hours after CTX-injection. Data from Figure 3.4 (8 week old OPN+/+mdx and OPN-/-mdx mice) are shown at the bottom for comparison. Plots depict mean values of pooled data. Vertical lines represent standard errors. Animal numbers are indicated on each bar of the graph. Statistical significance determined by Student's T test. P values are indicated.

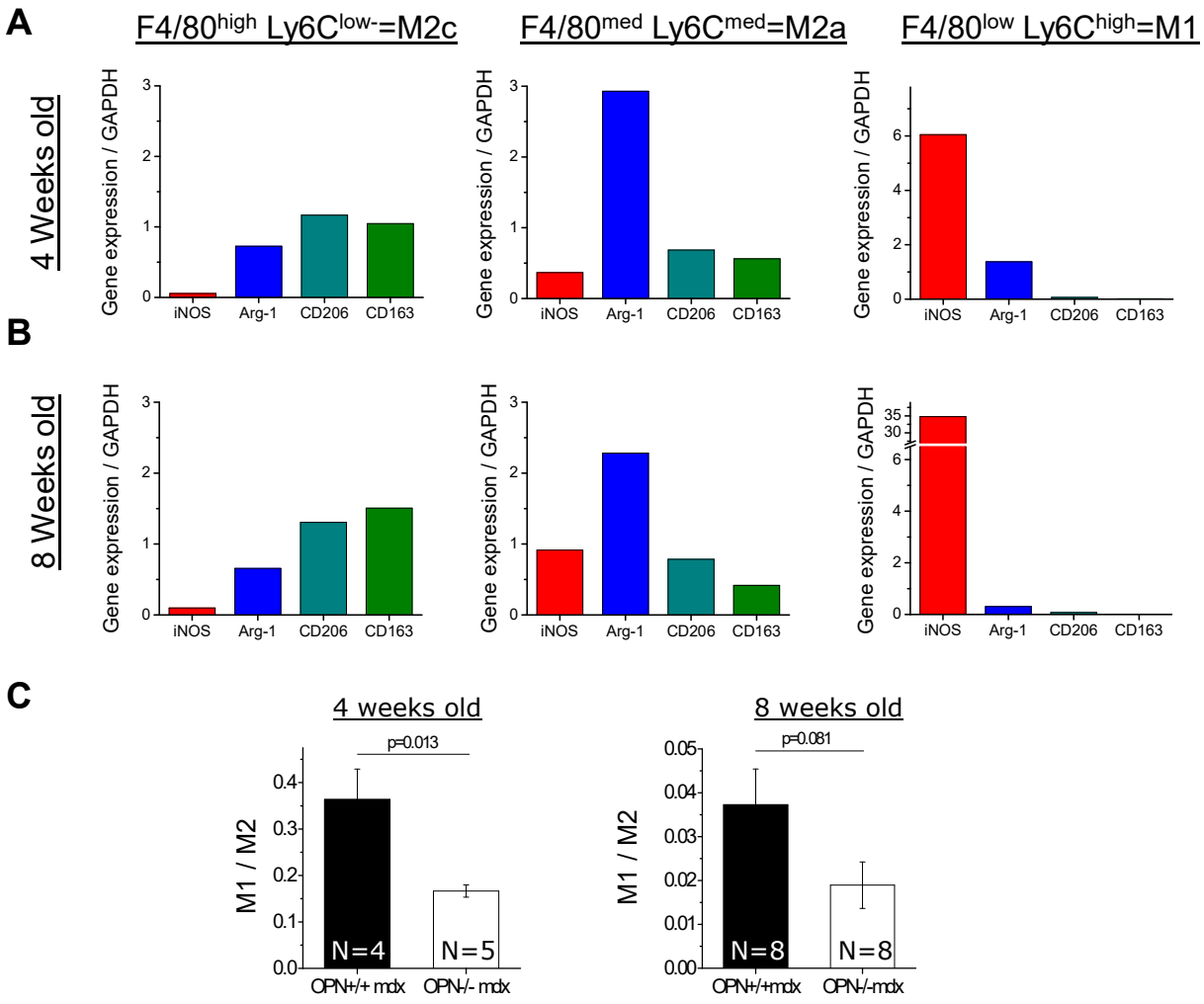

Figure 2.6 Levels of F4/80 and Ly6C correlate with M1, M2a and M2c macrophage sub-types. Quantitative RT PCR was used to evaluate mRNA expression of phenotypic markers from sorted macrophage populations isolated from 4 week (A) or 8 week (B) muscles. All values are expressed relative to GAPDH. (C) Graph of M1 vs M2 ratios at 4 and 8 weeks of age. Vertical bars represent standard error.

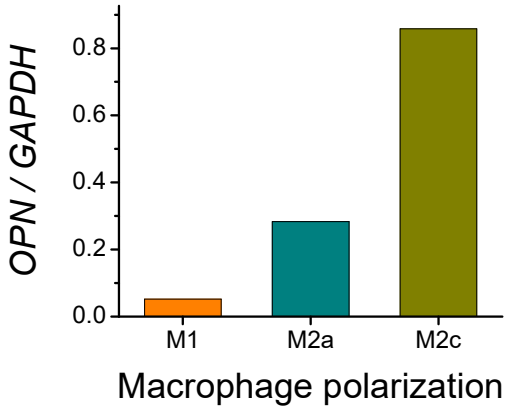

Figure 2.7 Assessment of OPN mRNA levels in FACS sorted macrophage populations
Graph demonstrates data derived from quantitative RT PCR of OPN mRNA from sorted macrophage subtypes. Macrophage populations were defined and sorted according to F4/80 and Ly6C levels and characterized as shown in Figure 3.3. OPN values are expressed relative to GAPDH.

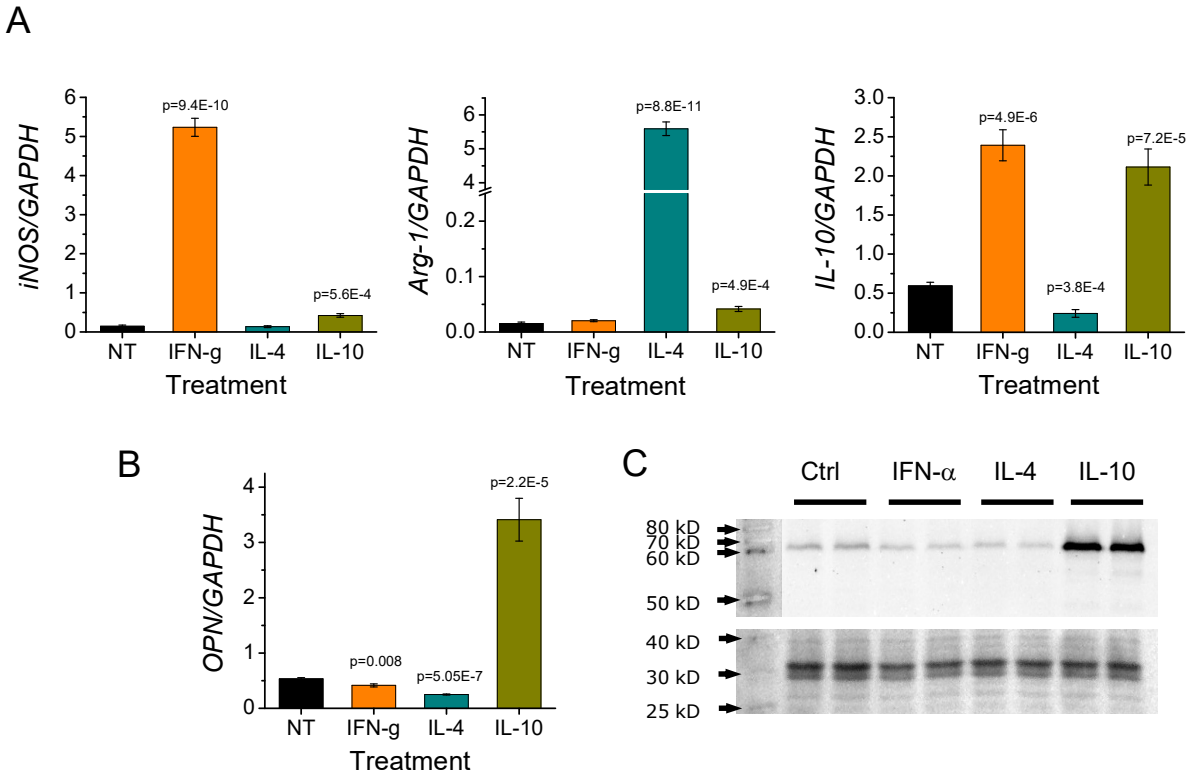

Figure 2.8 In vitro polarization of macrophages reveals high expression of OPN in M2c macrophages

The J774A macrophage cell line was induced to different macrophage subtypes by exposure to polarizing cytokines *in vitro* to model macrophage polarization. Exposure to IFNγ polarizes to M1, exposure to IL4 polarizes to M2a and exposure to IL10 polarizes to M2c, NT=not treated; polarizing treatments are indicated under each bar of the graph. A) Expression of iNOS (M1), Arg-1 (M2a) and IL-10 (M2c) were assessed by qRT-PCR to confirm macrophage phenotype (upper panel). B) qRT-PCR assessment of OPN mRNA expression in polarized macrophages. C) Western blot of polarized macrophage extracts reveals high OPN in M2c macrophages. Polarizing cytokines are indicated above the lanes. All experiments were done in triplicate and repeated three times. Vertical bars represent standard error. P values relative to non-treated cells are indicated, based on Student's T test.

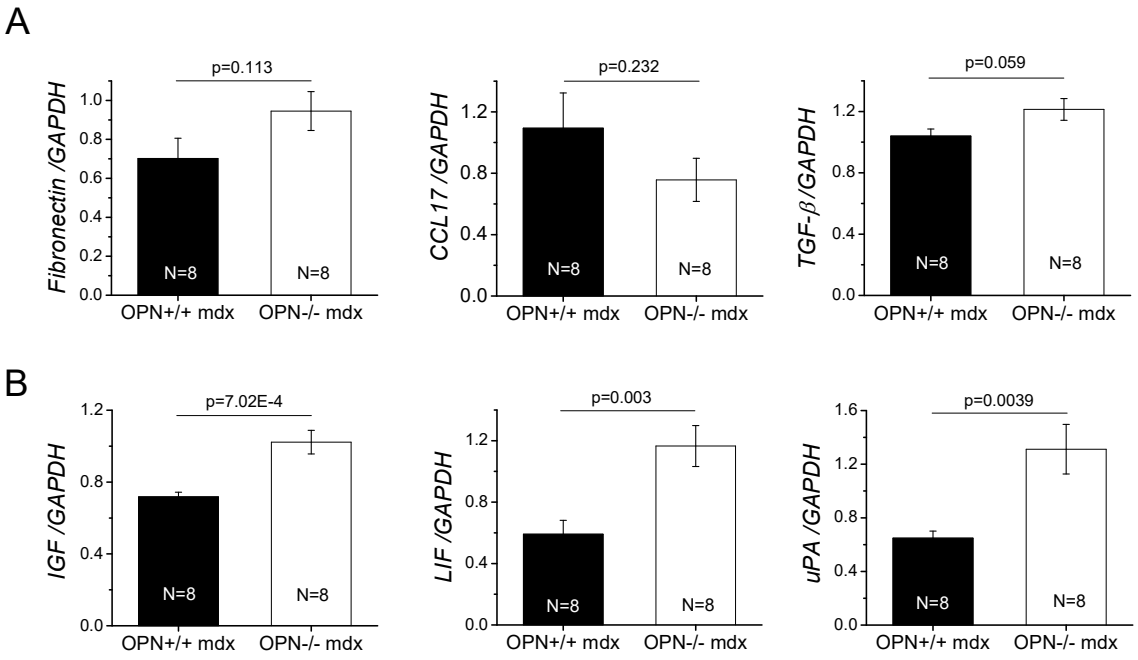

Figure 2.9 OPN-ablation promotes a pro-regenerative macrophage phenotype

F4/80+ sorted macrophages were collected and assessed by qRT PCR for A) pro-fibrotic factors: fibronectin, CCL17 and TGF-b and B) pro-regenerative factors: IGF-1, LIF, uPA. Each sample was collected per single mouse. The number of samples per experiment is indicated on the bars. Vertical lines indicate standard error of the mean. P values are shown based on Student's T test comparison.

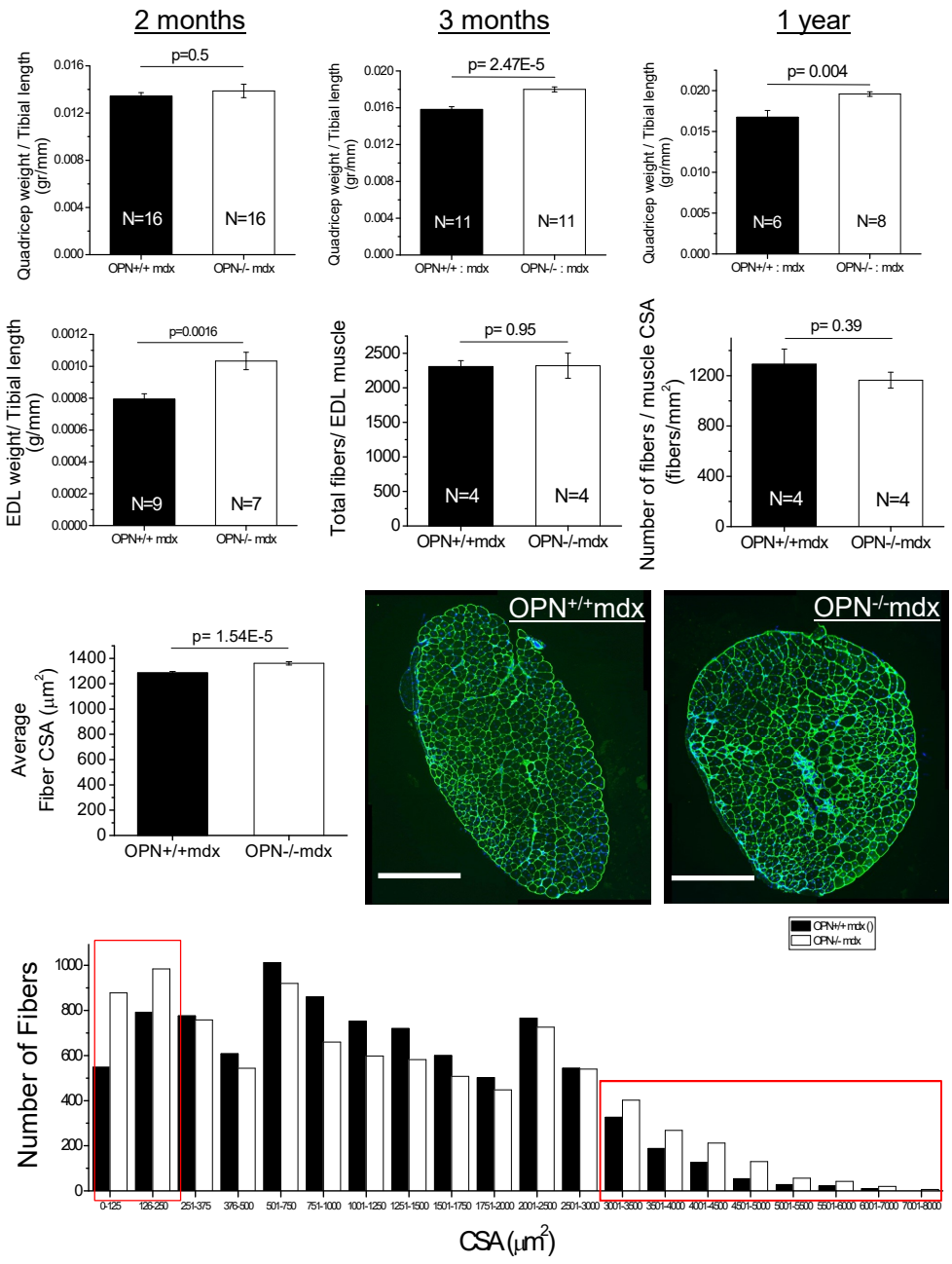

Figure 2.10 OPN ablation leads to increased muscle mass and size

The quadriceps and EDL muscles were evaluated for muscle mass at the ages indicated and data were normalized per tibial length. All cross sectional area and fiber analyses were conducted on the EDL. Vertical lines represent standard error. *, $P < 0.05$; #, $P \leq 0.02$, determined by Student's t test. Bars, 500 µm. CSA, cross-sectional area. Average fiber cross-sectional area was calculated from n = >9,000 fibers per genotype per age.

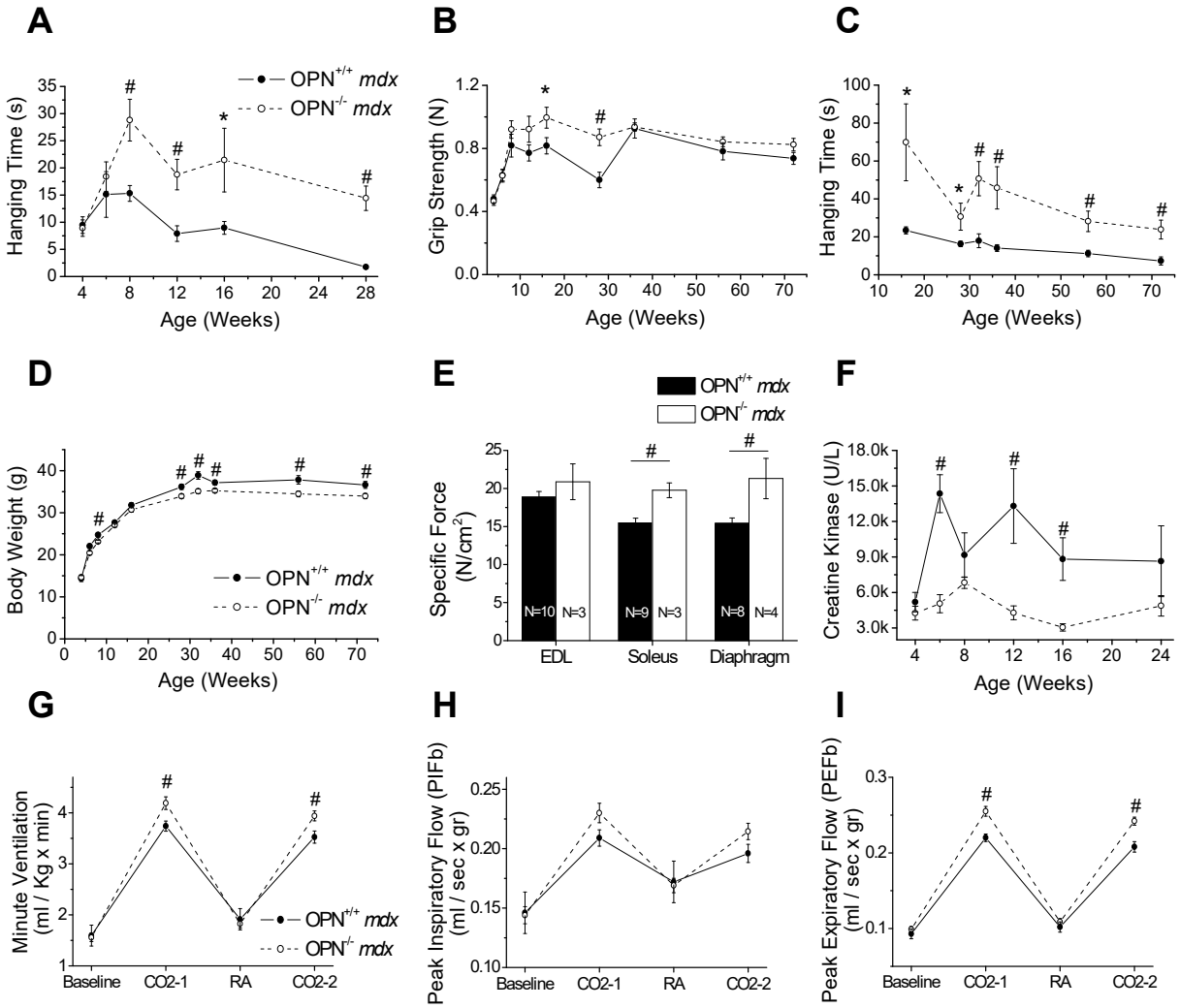

Figure 2.11 Long-term improvements in muscle strength observed by functional and physiological testing of OPN-/-mdx mice

A) Hanging wire test (n= ≥ 9 per genotype and age); B) Grip strength test (n= ≥ 9 per genotype and age); C) Wire mesh test (n= ≥ 10 per genotype and age); D) Body Weight (n= ≥ 9 per genotype and age); E) Specific force (n's are indicated on bars of the graph); F) serum creatine kinase (n= ≥ 6 per genotype and age); G) Minute ventilation (n= ≥ 10 per genotype and age); H) Peak inspiratory flow (n= ≥ 10 per genotype and age); I) Peak expiratory flow (n= ≥ 10 per genotype and age); Vertical lines represent standard error. P values *p<0.05, # P≤0.02 determined by determined by analysis of variance model.

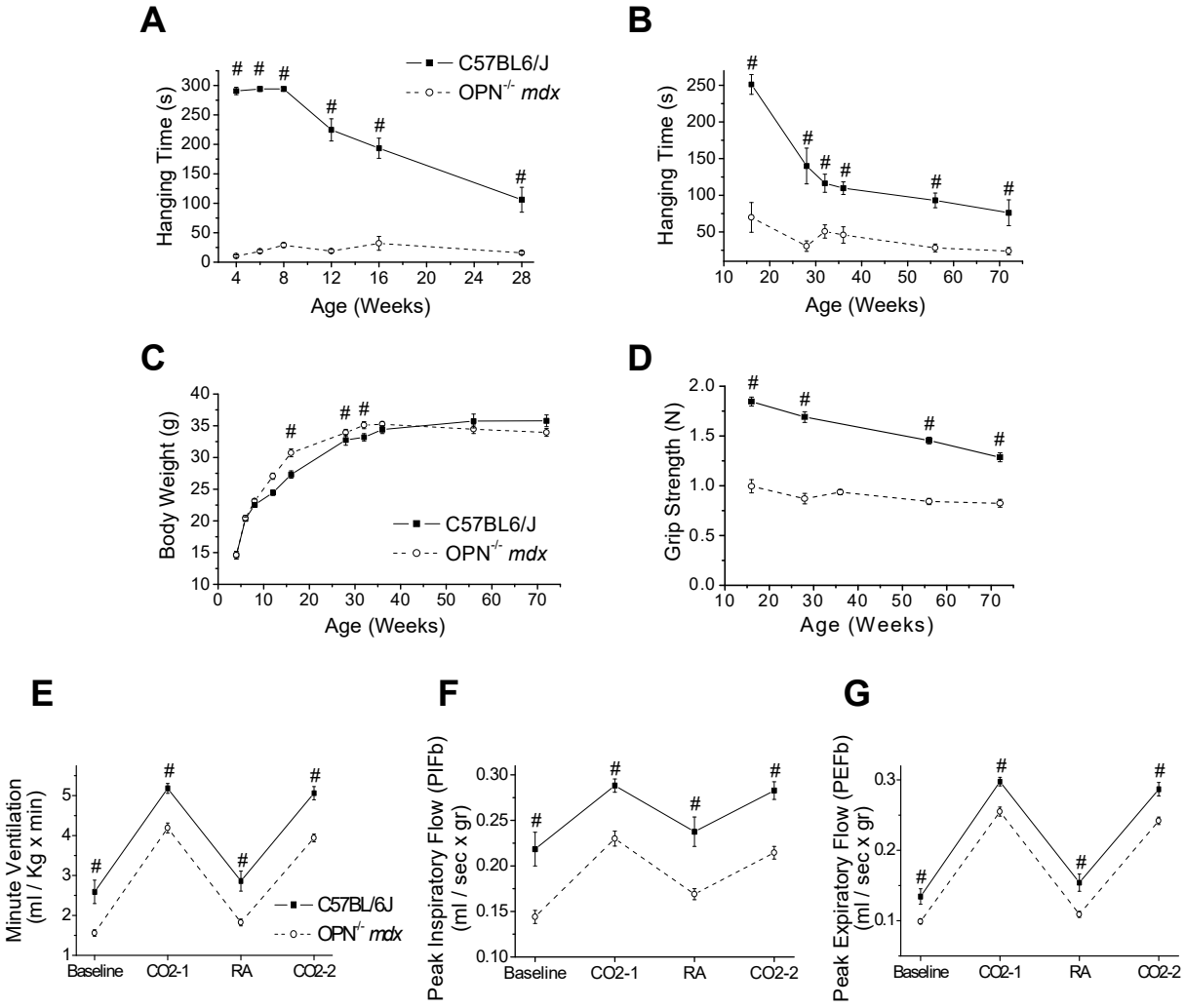

Figure 2.12 Muscle strength testing of C57BL/6 and OPN-/-mdx mice.

The data on OPN-/-mdx are the same data as that shown in Fig. 2.11. Here, the data are plotted against those from C57BL6. A) Hanging wire test (n= ≥ 10 per genotype and age); B) Wire mesh test (n= ≥ 5 per genotype and age); C) Body Weight (n= ≥ 5 per genotype and age); D) Grip strength test (n= ≥ 5 per genotype and age); E) Minute ventilation (n= ≥ 10 per genotype and age); F) Peak inspiratory flow (n= ≥ 10 per genotype and age); G) Peak expiratory flow (n= ≥ 10 per genotype and age); Vertical lines represent standard error. P values # P≤0.02 determined by determined by analysis of variance model.

Chapter 3

OPN's role in the regulation of fibrosis and regeneration in dystrophic muscle

3.1 Abstract

Muscles from Duchenne Muscular Dystrophy (DMD) patients and animal models of DMD are characterized by a high degree of muscle fibrosis and a progressive loss of muscle mass. We have previously demonstrated that osteopontin (OPN, encoded by *Spp1*) promotes dystrophic pathology. OPN ablation in mdx mice causes a significant decrease in skeletal muscle fibrosis, and increases muscle mass and regeneration. These effects are at least partially explained by a change in macrophage polarization away from M1 and towards M2c. This skewed polarization is also associated with an increase in macrophage expression of pro-regenerative factors, without alteration of their pro-fibrotic factor expression and commensurate with increases in muscle growth and regeneration. Thus, OPN has an indirect effect on muscle growth and regeneration via its effects on macrophage polarization.

While it is clear that OPN has an indirect effect on muscle growth and regeneration, it is not clear whether it has direct effects on these processes. Furthermore, our prior research showed that OPN-/- mdx muscles have reduced fibrosis and TGFb, but the reason for these changes has not been clear. One hypothesis is that OPN might directly impact skeletal muscle fibroblasts and promote extracellular matrix

secretion. In this study, we used primary fibroblasts and myoblasts cultures isolated from OPN+/+mdx and OPN-/-mdx mice, to investigate the direct effect of OPN in the regulation of collagen expression and the myogenic program. Conditioned media harvested from these cell sources was also used to examine how OPN derived from fibroblasts and myoblasts impact disease features of fibrosis and regeneration. Our data show that multiple cell types present in mdx muscles can express OPN including leukocytes, fibroblasts, myoblasts and myofibers. Moreover, we show that commercially purchased recombinant OPN does not impact the activity of mdx fibroblasts, but fibroblast-derived OPN exerts a pro-fibrotic effect on primary OPN-/-mdx fibroblasts. In contrast, myoblast-derived OPN has little to no effect on fibroblast expression of collagen. Furthermore, examination of the effect of different sources of OPN, rOPN and fibroblast and myoblast derived OPN, on myogenic differentiation revealed that there was a tendency towards inhibition of myoblast differentiation in dystrophic myoblasts. This study demonstrated that OPN can act directly on fibroblasts and myoblasts to affect the processes of fibrosis and myogenesis in dystrophic muscles. Moreover, the data generated here provide insights into the sources and functions of OPN in the pathogenesis of DMD.

3.2 Introduction

Mutations in the *DMD* gene cause Duchenne muscular dystrophy (DMD) leading to progressive muscle deterioration and early death of the patients [58]. In DMD, muscle membrane integrity is compromised due to the lack of dystrophin expression and the secondary loss of the dystrophin-glycoprotein complex, which leads to membrane tears with regular muscle activity and degeneration [3, 4, 6]. Repeated bouts of muscle fiber degeneration, accompanied by inflammatory cell infiltration, create an intramuscular milieu with elevated cytokines capable of modulating both fibrosis and regeneration [1, 66, 114, 115].

Despite the fact that mutations in the DMD gene are the cause of this muscle disorder, additional genetic changes can act as “modifiers” of the disease affecting the degree of severity of the dystrophic pathology [116-118]. Several modifiers of DMD have been described: Osteopontin (OPN, encoded by *Spp1*) [1, 53], latent transforming growth factor β binding protein 4 (*LTBP4*) [59, 119], annexin A6 (*Anxa6*) [120], CD40 [121] and α-actinin-3 (*ACTN3*) [117]. Two of these modifiers, OPN and LTBP4, are linked to the TGF-β signaling pathway, which highlights the significant role of TGF-β in the modulation of DMD pathology [57, 118]. Multiple members of the TGF-β family have been shown to influence DMD onset and progression, as they drive the development of fibrosis and negatively affect muscle growth and differentiation [122-125].

OPN is small protein (~33 kDa polypeptide backbone) expressed in a wide variety of cell types, that have been shown to be highly up-regulated in dystrophic muscles [1, 14, 51]. This protein can be highly post-translationally modified by phosphorylation, glycosylation, sulfation, transglutamination and proteolytic cleavage [20, 22, 27, 31],

leading to a large assortment of possible OPN forms. OPN has the ability to bind to trans-membrane receptors such as integrins [44, 46, 51, 75, 76] or CD44 (i.e. hyaluronic acid receptor or vitronectin receptor) [126] as well as to the extracellular matrix molecules fibronectin and collagen [127]. These observations of different post translationally modified forms of OPN combined with a large number of potential receptors support the notion that OPN could regulate a diverse number of physiological and pathological processes [23, 39, 43, 128, 129].

OPN expression has been found to be up-regulated in multiple diseases in which tissue fibrosis is present [1, 40, 41, 43, 130-132]. In this regard, a direct role of OPN in the regulation of fibrosis has been previously established, as OPN expression has been shown to be required for TGF-β1 to elicit cardiac and dermal fibroblasts cultures differentiation to myofibroblast [133, 134]. Additionally, OPN has been shown to act as a pro-fibrotic cytokine in the modulation of the expression of different types of collagen, TIMPs and MMPs in experimental models of idiopathic pulmonary fibrosis, heart failure and other diseases [40, 43].

OPN has also been demonstrated to regulate myogenesis in vitro, where rOPN-coated substrata was shown to promote adhesion and fusion of C2C12 cells, while rOPN in solution increased proliferation and decreased fusion and migration of these cells [135]. Moreover, age dependent increases of OPN expression in vivo has been shown to inhibit muscle regeneration in WT mice [39].

In dystrophic muscle, we previously showed that OPN ablation in mdx mice attenuates disease progression. Skeletal muscles from these animals show reductions in fibrosis, increased muscle mass and an increased number of regenerating fibers [1,

136]. Moreover, ablation of OPN in mdx mice skews macrophage polarization towards a pro-regenerative phenotype and increases macrophage expression of the pro-regenerative factors IGF-1, uPA and LIF [136]. On the other hand, macrophage expression of pro-fibrotic factors, such as: fibronectin, CCL17 and TGF-β was not affected with OPN ablation, in spite of the observed reduction in M2a macrophages, suggesting that OPN's role in promotion of fibrosis is likely taking place through its interaction with other cell types present in dystrophic muscle [136].

Here, we explore whether OPN might have direct effects on fibroblasts and myogenic cells in dystrophic muscles to directly modify fibrotic and regenerative processes in the DMD pathology. Because OPN is highly post-translationally modified, it is reasonable to expect that OPN, derived from different cellular sources, could exert diverse effects on its targets. In this investigation we dissect the cell-type specific roles of OPN derived from either fibroblasts or myoblasts on regulation of fibrosis and regeneration. This study shows that OPN secreted from fibroblasts, but not myoblasts, can act as a pro-fibrotic cytokine to promote fibrosis, by directly enhancing fibroblast expression of collagen and TGF-β. Additionally, different forms of OPN including rOPN, fibroblast-derived and myoblast-derived OPN, tend to induce a negative effect on myoblasts differentiation to myotubes. This work supports the notion of OPN acting as a pro-fibrotic cytokine and a negative regulator of myoblast differentiation in the DMD pathology. These studies lend insights to OPN-mediated mechanisms occurring *in vivo* and suggest that OPN has pleiotropic effects on cells in dystrophic muscles.

3.3 Materials and Methods

3.3.1 Animals

All animals used in this project were handled and bred according to the guidelines laid out by the Animal Research Committee at the University of California, Los Angeles. C57BL/6J, *mdx* (C57BL/10ScSn-Dmdmdx/J) and OPN-Knockout mice (OPN-KO, B6.Cg-Spp1tm1Blh/J) were obtained from the Jackson Laboratory. $OPN^{-/-}$ mdx and $OPN^{+/+}$mdx mice are from colonies previously established in the lab. To create these colonies, male OPN-KO mice were bred with homozygous mdx females. The resulting $OPN^{+/-}$mdx mice from this cross were then breed between them to obtain the $OPN^{-/-}$mdx and $OPN^{+/+}$mdx mice [1]. These colonies have been maintained in the UCLA vivarium by homozygous crosses. OPN-/-mdx and OPN+/+mdx mice colonies are maintained in a mixed C57BL10/C57BL6 background with a predominance of the C57BL10 background (~60% as determined by congenic assays). All mice used in these experiments were genotyped using the previously published protocols from Liaw et al. [38] and Amalfitano & Chamberlain [81] for the OPN and dystrophin mutations respectively.

3.3.2 Preparation of primary myoblasts and fibroblasts from skeletal muscle

An adaptation of Dr. Springer's lab protocol [137] was used to isolate primary myoblasts and fibroblasts from mouse muscles. Briefly, 13-15 days old mice were sacrificed and all muscles collected in semi-sterile conditions. Muscles were pooled together and washed twice in PBS (Ca^{2+}, Mg^{2+}-free), then transferred to a dish containing a 1:1 mixture of neutral protease (1.5 U/ml)/ collagenase type 2 (500 U/ml)

(Worthington Biochemical corporation) and minced in this solution using sterile razor blades. The muscle slurry was then transferred to a conical tube and incubated at 37 ^{o}C with slow agitation (~70 rpm) for ~30 min. A borosilicate pipette was used to help break the pieces of tissue still present. Once the tissue was digested, the sample was raised to a final volume of 50ml with sterile PBS (Ca^{2+}, Mg^{2+}-free) and passed through a 70µm cell strainer. The filtrate was then pelleted by centrifugation at 700g for 4 min. The cell's pellet was resuspended in growth medium (nutrient mixture F-10 HAM, 1% penicillin/streptomycin (P/S), 20% Fetal Bovine Serum (FBS), 5 ng/ml FGF(Promega)), plated on entactin, collagen IV, laminin (ECL, Millipore) coated culture plates and maintained in the cell incubator at 37 ^{o}C and 5% CO^{2} for 1 to 2 days. After this, cells were washed to get rid of cellular debris and pre-plated 2 or 3 times for 30 min onto uncoated cell culture plates to separate myoblast and fibroblast populations. Fibroblasts attached to the uncoated cell culture plates, while myoblasts stayed in suspension. Finally, the myoblast suspension was plated onto ECL-coated plates. Myoblast and Fibroblast aliquots at low cell' passages were frozen in a storage solution (90% growth medium, 10% DMSO) for subsequent experiments.

3.3.3 Treatment of fibroblasts with rOPN

Fibroblast cultures were grown up to ~80% confluence in fibroblasts growth medium (nutrient mixture F-10 HAM, 1% P/S, 10% FBS) then washed twice with PBS (Ca^{2+}, Mg^{2+}-free) and switched to: a) plain media (nutrient mixture F-10 HAM, 1% P/S, 0.1% Bovine serum albumin (BSA)) or b) plain media supplemented with 1500 ng/ml of mouse recombinant OPN (rOPN, 441-OP, R&D systems). Increasing concentrations of rOPN (0, 500, 1000, 2000, 4000, 6000 and 8000 ng/ml) were used to study OPN's

effect on fibroblast proliferation. Cell cultures were then collected after 24 hours of incubation.

3.3.4 Treatment of myoblasts with rOPN and induction of differentiation

Myoblast cultures were grown up to ~80% confluence in myoblast growth medium (nutrient mixture F-10 HAM, 1% P/S, 20% FBS, 5 ng/ml FGF(Promega)) then washed twice with PBS (Ca^{2+}, Mg^{2+}-free) and switched to: a) plain media (nutrient mixture F-10 HAM, 1% P/S, 0.1% Bovine serum albumin (BSA)) or b) plain media supplemented with 1500 ng/ml of mouse recombinant OPN (rOPN, 441-OP, R&D systems). Cultures were then collected after 24 hours of incubation for the myoblast samples or switched to: a) differentiation media (DMEM, 1% P/S, 0.1% BSA, 1X Insulin-transferrin-selenium (ITS)) or b) differentiation media supplemented with 1500 ng/ml of mouse recombinant OPN, respectively. These cultures were then collected after 1 or 3 days of incubation for the myotube samples at distinct differentiation stages. ITS was used to induce a more synchronized differentiation from myoblasts to myotubes.

3.3.5 Harvesting of conditioned media

To harvest conditioned media, fibroblast and myoblast cell cultures were grown up to ~80% confluence in fibroblast or myoblast growth medium, respectively, then washed twice with PBS (Ca^{2+}, Mg^{2+}-free) and switched to plain media (nutrient mixture F-10 HAM, 1% P/S, 0.1% BSA) or differentiation media (DMEM, 1% P/S, 0.1% BSA, 1X ITS). 24 hours later (for myoblasts and fibroblasts, or 3 days for myotubes), media was collected and centrifuged at 1000g for 5 min to remove the cells in suspension and cell debris. The pellet was discarded and cleared media was stored at -80 ^{o}C for later use.

Conditioned media collected in the absence of BSA was used to identify the different forms of OPN secreted by the different cell types. Samples of conditioned media without BSA were concentrated 15 times using the vivaspin 6 concentrators (10000 MWCO, Sartorius). Concentrated conditioned media samples were then supplemented with protease and phosphatase inhibitors and mixed with 5X reducing sample buffer (RSB, 250 mM Tris-HCl, pH 6.8, 50% Glycerol, 10% SDS, 500 mM β-mercaptoethanol, 0.1% bromophenol blue) to a final concentration of 1X. Samples were boiled at 100 ^{o}C for 5 min for protein denaturation. OPN's forms present in the conditioned media were determined by immunoblotting with an OPN specific antibody (anti-mouse OPN 1:500, AF808 R&D systems).

3.3.6 Fibroblast treatment with conditioned media

Fibroblast cultures were grown up to ~80% confluence in fibroblast growth medium (nutrient mixture F-10 HAM, 1% P/S, 10% FBS) and washed twice with PBS (Ca^{2+}, Mg^{2+}-free) then switched to: a) fibroblast or myoblast conditioned media from $OPN^{-/-}$mdx cells (negative controls) or b) fibroblast or myoblast conditioned media from $OPN^{+/+}$mdx cells. Cell cultures were then collected after 24 hours of incubation to evaluate collagen and TGF-β expression by qPCR.

3.3.7 Myoblast differentiation in conditioned media

Myoblast cultures were grown up to ~80% confluence in myoblast growth medium (nutrient mixture F-10 HAM, 1% P/S, 20% FBS, 5 ng/ml FGF(Promega)), then washed twice with PBS (Ca^{2+}, Mg^{2+}-free) and switched to: a) fibroblast conditioned media or a 1:1 mix of myoblast and myotube conditioned media from $OPN^{-/-}$mdx cells supplemented with 1X ITS (negative controls) or b) fibroblast conditioned media or a 1:1

mix of myoblast and myotubes conditioned media from $OPN^{+/+}$mdx cells (experimental condition), and 1X ITS. Cell cultures were then collected after 3 days of incubation to evaluate dMHC expression.

3.3.8 Quantitative RT-PCR (qRT-PCR)

Total RNA was isolated from the cell cultures using Trizol (Invitrogen) and then treated with DNAse I (Invitrogen) to avoid any possible contamination from genomic DNA. 1µg of the RNA sample was used to synthesize cDNA, using SuperScript III reverse transcriptase (Invitrogen) and random primers (Invitrogen). All qPCR reactions were performed using iTaq™ Universal SYBR® Green Supermix (Bio-Rad) and processed in the CFX Connect™ Real-Time PCR Detection System (Bio-Rad). Manufacturers' protocols were followed for all these reactions. qPCR programs consisted of 40-50 cycles with a melting temperature of 95 ^{o}C for 15 seconds and an annealing/extension temperature of 58-60 ^{o}C (depending on the melting temperature of the primers) for 30 seconds. Sample fluorescence was read at the end of every annealing-extension cycle. A melting curve at the end of each qPCR program was included to ensure that single and specific PCR products were formed. A list of the primers used is included in table 1.

3.3.9 Muscle fiber isolation

Muscle fiber isolation was carried out using the protocol previously described by Capote et al, 2005 [138]. Briefly, *flexor digitorum brevis* (FDB) and *interoseous* (IO) muscles were dissected from the mouse foot pad and incubated in a Tyrode solution (145 mM NaCl, 5 mM KCl, 2 mM $CaCl_2$, 1 mM $MgCl_2$, 10mM Na-MOPS, and 10 mM dextrose; pH 7.2) containing 1710 U/ml of collagenase (CLS2, Worthington) for 35

minutes at 36.5 ºC and 50 rpm. After incubation with collagenase, muscles were carefully washed with Tyrode solution and gently dissociated from the tendons with a fire-polished Pasteur pipette. Tendons and connective tissue were then removed from the preparation and dissociated fibers in solution were placed into a 15 ml conical tube containing Tyrode solution supplemented with 10% FBS and centrifuged at 600 g for 4 minutes. Cell pellets were then resuspended in 1.5 ml of Tyrode solution supplemented with 10% FBS and place in an Eppendorf vial for subsequently centrifugation of the sample at 800 g for 4 minutes. Supernatant was then removed completely and cell pellets were used for protein sample preparation.

3.3.10 Protein sample preparation and western blots

Cell culture samples were lysed in 1X reducing sample buffer (RSB) (50 mM Tris-HCl pH 6.8, 10% Glycerol, 2% SDS, 100 mM β-mercaptoethanol) supplemented with a protease and phosphatase inhibitor cocktail (Thermo scientific). Bromophenol blue (0.02%) was later added and samples boiled at 100 ºC for 5 min for protein denaturation.

Isolated muscle fiber samples, on the other hand, were homogenized in homogenization buffer (75 mM KCl, 5 mM $MgSO_4$, 20 mM MOPS, 20 mM EGTA) supplemented with protease and phosphatase inhibitor cocktail (Thermo scientific). A differential centrifugation protocol was used to discard the undesired fractions of isolated muscle fibers samples (1000g X 10 min, nuclei and cell debris fraction; 10000g X 10 min contractile apparatus containing fraction; 20000g X 20min mitochondrial fraction). These samples were then mixed with 5X RSB to a final concentration of 1X RSB and samples boiled at 100 ºC for 5 min for protein denaturation.

SDS-PAGE and Western blotting were carried out as previously described [85]. BenchMark™ (Invitrogen) protein ladder was used as molecular weight markers in every gel. Proteins were separated by gel electrophoresis and then transferred to a nitrocellulose membrane. Membranes were later blocked with 5% milk in TBS-T (Tris-Buffered saline, 0.1% Tween) and then incubated with the appropriate concentration of primary antibody (anti-mouse OPN 1:500, AF808 R&D systems; anti-developmental myosin heavy chain (dMHC) 1:500, Novocastra; anti-Myogenin 1:500, DSHB; anti-MyoD 1:500, Santa Cruz biotechnologies; anti-PCNA 1:500, DAKO; anti-Pax7 1:500, DSHB; anti-GAPDH 1:400, Santa Cruz biotechnologies) in 5% milk TBS-T overnight at 4 ^{o}C. Membranes were then washed and incubated with a Horse radish peroxidase (HRP) conjugated secondary antibody in 5% milk TBS-T. The chemiluminescence substrate kit, ChemiGlow West (Protein simple), was used to detect the protein bands. Chemilumiscence signals were detected and densitometry analyzed using the FluorChem FC2 system (Alpha Innotech).

3.3.11 Statistical Analysis

Gene expression was measured in triplicates via qPCR. Triplicates from each sample were then averaged and mean values normalized to the average expression of that sample housekeeping gene (either β-actin (ACTB) or GAPDH). Number of samples used in each experiment is detailed in the figures.

Experimental results were expressed as means ± standard error of the mean (SEM). Data sets were compared using Student's t-test. Values were considered significant if $p \leq 0.05$.

3.4 Results

3.4.1 OPN is expressed by numerous cell types in dystrophic muscle

Our prior studies showed that OPN is greatly elevated in dystrophic muscles and that its ablation in dystrophic mice attenuates disease progression [1, 136]. Here, we sought to identify the potential sources of OPN expression in mdx muscle. OPN has been reported to be synthesized by a variety of cells including fibroblasts, osteoblasts, osteocytes, dendritic cells, macrophages, T and B cells, neutrophils, smooth muscle cells, myoblasts, endothelial cells, and others [30, 34, 35]. To identify the sources of OPN expression in skeletal muscle, we isolated pure populations of leukocytes, fibroblasts, myoblasts and single skeletal muscle myofibers from OPN+/+mdx, OPN-/-mdx and C57-WT mice. Representative micrographs from these cell populations are shown in Figure 3.1B. We tested the protein samples prepared from each cell population for OPN expression by using immunoblotting with OPN-specific antibodies. We show in Figure 3.1C that leukocytes, fibroblasts, myoblasts and mdx muscle fibers are all found to express OPN, while only myoblasts and fibroblasts are sources of OPN expression in C57-WT skeletal muscle (Figure 3.1C).

3.4.2 OPN is secreted by fibroblasts, myoblast and myotubes.

Examination of the conditioned media harvested from dystrophic fibroblasts, myoblasts and myotubes cultures showed that these cells secreted OPN (Figure 3.2A). Moreover, conditioned media from OPN+/+mdx myoblasts present a much higher concentration of the protein than conditioned media from OPN+/+mdx fibroblasts and myotubes (Figure 3.2A). OPN concentration in the conditioned media from OPN+/+mdx myotubes is very low (Figure 3.2A). OPN specific bands were identified by comparison

of the conditioned media samples from OPN+/+mdx and OPN-/-mdx (negative control) cells. Further examination of conditioned media harvested from fibroblasts cultures using immunoblots with OPN-specific showed that different forms of the protein are secreted in the culture media (Figure 3.2B). The most abundant form of OPN secreted in the media of all these cell types had a molecular weight of ~60 kDa as shown in Figure 3.2A and B. Other less abundant forms of the protein are found at smaller molecular weights (Figure 3.2B). The different forms present in the conditioned media from fibroblasts likely arise from different post-translational modifications of the protein.

3.4.3 rOPN supplementation does not affect proliferation or expression of collagens and other ECM proteins in fibroblast cultures

To investigate whether OPN affects fibroblast expression of extracellular matrix (ECM) proteins, we first compared collagen 1 expression (via qPCR) in primary OPN+/+ mdx and OPN-/-mdx fibroblast cultured in plain media (supplemented with 0.1% BSA). Figure 3.3A shows that OPN expression in fibroblast does not significantly affect their expression of Collagen, as both OPN+/+mdx and OPN-/-mdx fibroblast display similar levels of collagen 1 expression. Next, we examined whether recombinant OPN (rOPN) supplementation of fibroblast cultures affected their collagen expression. To this end, we evaluated collagen 1 expression, via qPCR, in OPN+/+mdx and OPN-/- mdx fibroblast cultures treated for 24 hours with or without the addition of rOPN (1500 ng/ml). Neither, OPN+/+mdx (Figure 3.3B) or OPN-/-mdx (Figure 3.3C) fibroblast cultures showed significant differences in collagen 1 expression following addition of rOPN. This indicates not only that rOPN does not affect fibroblast expression of collagen, but also that endogenous OPN expression does not affect fibroblast response

to rOPN. Additionally, further examination of the effect of rOPN supplementation in OPN+/+mdx fibroblast cultures showed that other types of collagens (Col3a1 and Col6a1), MMPs, TIMPs and pro-fibrotic factors (TGF-β and CTGF) expression are also not affected by rOPN addition (Figure 3.4). Moreover, to address the role of OPN in fibroblast proliferation, primary C57-WT fibroblast were treated with increasing concentrations of rOPN (0 – 8000 ng/ml) for 16 hours and proliferation assayed by qPCR measurements of PCNA and cyclin D1, which are markers of active cell proliferation. rOPN did not significantly affect PCNA or Cyclin D1 expression at any of the concentrations tested (Figure 3.5), indicating that rOPN does not affect fibroblast proliferation in vitro.

3.4.4 Conditioned media from fibroblasts induces a more potent pro-fibrotic response than conditioned media from myoblasts

OPN is a highly post-translationally modified protein that is differentially modified by different cell types [20, 27, 132, 139]. These cell-specific modifications have been shown to contribute to OPN's regulation of specific cellular functions. The negative results observed with rOPN in promotion of collagen expression may be due to the absence of post-translational modifications necessary to activate fibroblast expression of collagen. Therefore, to test whether cell-specific post-translational modifications of OPN impact its effect in promoting fibrosis, we measured collagen 1 and TGF-b expression from OPN-/-mdx fibroblasts incubated with conditioned media harvested from either OPN-/-mdx or OPN+/+mdx fibroblast and myoblasts cultures. OPN-/-mdx fibroblasts were used to test the effect of the different conditioned medias, since endogenous OPN expression in fibroblasts cultures did not affect their expression of

collagen in response to rOPN and to avoid any other un-control contribution of OPN in the experiment. OPN-/-mdx fibroblasts that were incubated for 24 hours in OPN+/+mdx fibroblast conditioned media have ~84% higher collagen 1 expression than fibroblasts cultured in OPN-/-mdx conditioned media (Figure 3.6A). However, conditioned media from both, OPN-/-mdx and OPN+/+mdx myoblasts elicited similar levels of collagen expression in OPN-/-mdx fibroblasts (Figure 3.6B). TGF-b expression, on the other hand, tends to be increased similarly in OPN-/-mdx fibroblasts by fibroblasts and myoblasts conditioned media containing OPN (Figure 3.6). TGF-b expression in OPN-/-mdx fibroblast treated with fibroblast and myoblast conditioned media from the OPN+/+mdx genotype tends to be between 60% and 40% higher respectively, than the correspondent conditioned media from OPN-/-mdx cells (Figure 3.6). This shows that cell-specific post-translational modifications of OPN are necessary for its pro-fibrotic effects in muscle primary fibroblast. Moreover, these data reveal that OPN secreted from fibroblasts is a more potent regulator of collagen expression in dystrophic muscle than myoblast derived OPN.

3.4.5 OPN expression in dystrophic myoblasts does not affect their myogenic potential

To study the role of OPN in the regulation of myoblast differentiation, we used primary myoblast cultures isolated from OPN+/+mdx, OPN-/-mdx and wild type (C57-WT) mice. We first examined whether myoblast expression of OPN affects their capability to differentiate and form myotubes. A visual inspection of the morphology of OPN+/+mdx and OPN-/-mdx myoblast cultures before and after induction of differentiation showed that these cultures have no apparent differences at diverse stages, myoblast and myotubes 1 and 2 ½ days after differentiation (Figure 3.7A).

Additionally, these cultures are similar to those of C57-WT cells at the distinctive differentiation stages (Figure 3.7A). To Further examine the role of myoblast endogenous OPN expression in myoblast differentiation, we evaluated the expression of various markers of the myogenic program (Pax 7, PCNA, MyoD, myogenin and dMHC) in OPN+/+mdx and OPN-/-mdx myoblast and myotubes (1 and 2 ½ days after differentiation) cultures via immunoblots (Figure 3.7B). Expression of these markers in C57-WT cultures at the same differentiation stages was used as a positive control (Figure 3.7B). Expression of Pax7, PCNA, MyoD, myogenin and dMHC was found to be similar in OPN+/+mdx and OPN-/-mdx myoblasts and myotubes (1 and 2 ½ days after differentiation) cultures, and again, these are no different from those in C57-WT cultures (Figure 3.7B). These results show that myoblasts' capability to differentiate is not impaired in primary dystrophic myoblasts, compared to C57-WT cultures, and more importantly, that endogenous OPN expression in myoblasts does not affect myotube formation or the myogenic program in dystrophic myoblast (Figure 3.7).

3.4.6 Myogenic program is not significantly affected by rOPN supplementation

As rOPN supplementation of C2C12 cultures have been previously shown to affect myotube formation, we decided to investigate here whether OPN acts as a cytokine to regulate the expression of markers of the myogenic program in dystrophic muscles. We evaluated the expression of Pax 7, PCNA, MyoD and myogenin in OPN+/+mdx and OPN-/-mdx myoblast cultures with or without supplementation with rOPN before (24 hours) and during (1 to 3 days) induction of differentiation. We found that expression of Pax 7, PCNA, MyoD and myogenin in either OPN+/+mdx or OPN-/-mdx cells, treated with rOPN supplementation in this way, is not significantly different

from that in the untreated cells at the diverse differentiation stages (Figure 3.8). dMHC expression was also evaluated in OPN+/+mdx and OPN-/-mdx myotubes, 3 days after the induction of differentiation, treated with and without rOPN only during differentiation (Figure 3.9). OPN+/+mdx and OPN-/-mdx myotubes treated with rOPN tend to have a not significant decreased dMHC expression in comparison to the correspondent untreated cells (Figure 3.9).

3.4.7 Conditioned media from both OPN+/+mdx fibroblasts and myoblasts tends to decrease expression of dMHC in dystrophic myotubes.

We showed previously that OPN derived from diverse cells sources have different abilities to enhance collagen expression in dystrophic fibroblast. Therefore, here we used conditioned media from OPN+/+mdx and OPN-/-mdx fibroblasts, and a 1:1 mix of myoblasts:myotubes media to test the effect of cell type-specific OPN post-translational modifications in OPN-/-mdx myoblast differentiation in vitro. Conditioned media (supplemented with 1X ITS) was used only during differentiation. OPN-/-mdx myoblast were used to test the effect of OPN from different cell sources, since OPN+/+mdx and OPN-/-mdx seems to present the same type of response to rOPN and to avoid any other un-control contribution of OPN in the experiment. A mix of myoblasts and myotubes media was used because although myoblasts conditioned media have a much higher concentration of OPN than myotubes conditioned media, conditioned media from myotubes of either genotype elicit the formation of long and robust myotubes. These experiments showed that OPN derived from both of these sources, fibroblast and myoblast:myotube mix, tends to induce a not statistically significant decrease in the expression of embryonic myosin heavy chain (*Myh3*) (measured by

relative mRNA expression of *Myh3* via qPCR) of 29% and 25% respectively (Figure 3.10). These results are comparable to the nearly 18% and 15% relative decrease in dMHC protein expression observed in OPN+/+mdx and OPN-/-mdx myotubes treated with rOPN during differentiation respectively (Figure 3.10). Thus, OPN secreted from fibroblast and myoblast/myotubes tends to induce a negative effect on the regulation of the myogenic program of dystrophic myotubes by impairing the expression of dMHC.

3.5 Discussion

Our work demonstrates that in dystrophic muscle OPN is expressed by leukocytes, fibroblasts, myoblasts and muscle fibers. Moreover, dystrophic fibroblasts and myoblasts not only express the protein, but are also able to secrete OPN. Further, investigation is needed to understand whether and how the secreted forms of OPN from these cell types have different post-translational modifications. The large number of cell specific sources of OPN and the variety of different potential post-translational modifications suggest that a complex interrelationship exists between sources of and responders to OPN in dystrophic muscles. The correlation between OPN levels and dystrophic disease severity has been demonstrated in mice [1, 136], dogs [113] and humans [56, 140], and these studies have lent support for its role as a DMD modifier and potential biomarker.

We have previously shown that OPN ablation in mdx mice mitigates dystrophic pathology by inducing: a) decreased muscle fibrosis, b) increased skeletal muscle mass, c) increased number of dMHC positive fibers and d) increased muscle strength [1, 136]. Some of these features can be attributed to skewed polarization of the

intramuscular macrophage population, away from a pro-inflammatory M1 phenotype and toward a pro-regenerative M2c phenotype. OPN ablation in mdx mice also increases macrophage expression of pro-regenerative factors [136], but did not affect macrophage expression of pro-fibrotic factors. This suggests that OPN ablation is likely acting on other cell types in dystrophic muscles to affect fibrosis.

Our studies here showed that OPN expression in fibroblasts did not affect collagen expression in resting murine skeletal muscle fibroblast. Moreover, while rOPN supplementation of human and bovine primary pulmonary fibroblasts cultures was previously showed to increase fibroblast migration, proliferation and expression of collagen 1 and TIMP-1 [40, 141], our studies show that rOPN supplementation does not affect the expression of collagens, TGF-b and other ECM proteins in fibroblasts from murine dystrophic muscle. Additionally, rOPN supplementation did not have an effect on fibroblast proliferation, as expression of PCNA and cyclin D1 was not significantly different in fibroblast cultures incubated with increasing rOPN concentrations. The inconsistencies between our results and those previously reported in human and bovine fibroblast could be explained by differences in the rOPN used in these studies. Phosphorylation levels have been found to be highly relevant on the regulation of OPN's functionality depending on the cell type [20, 27]. The source of rOPN used in our study was derived from murine myeloma cells (NS0 cells). In this regard, it has been previously shown that even though most tumor cells express high levels of OPN this is most of the time hypo-phosphorylated OPN [20]. On the contrary, in the studies with human and bovine pulmonary fibroblasts, the OPN used was either produced in HEK cells or isolated from bovine milk, respectively. Of these, at least the one isolated from

bovine milk has been shown to be highly phosphorylated (28 phosphorylated residues) [142]. This difference could potentially indicate that, for OPN to have a pro-fibrotic effect in fibroblasts, high levels of phosphorylation of the protein are necessary.

Considering that OPN can be differentially modified by different cell types and that many of these specific post-translational modifications, are important in the regulation of OPN's function in different cell types [20, 27, 132, 139], we decided to test the efficacy of two different cell sources of OPN from dystrophic muscle: fibroblast and myoblast, in promotion of collagen and TGF-B expression in fibroblasts. We showed in this study that conditioned media from OPN+/+mdx fibroblasts significantly enhanced collagen expression in OPN-/-mdx fibroblasts, while conditioned media from OPN+/+mdx myoblasts induced a much smaller increase in collagen expression, which was not statistically signficant. The differential abilities of these two conditioned media to promote collagen expression in OPN-/-mdx fibroblasts, suggests that OPN proteins produced by these two cell sources are functionally different (or differentially modified). On the other hand, both of these conditioned media tend to similarly, though not significantly, increase TGF-b expression in OPN-/-mdx fibroblasts. The fact that collagen expression in fibroblasts is affected differently by the conditioned media from myoblasts and fibroblasts, while TGF-B expression is similarly affected by these, indicates that these effects are likely mediated by different pathways in skeletal muscle fibroblasts. Further experiments need to be carried out to identify the OPN-dependent pathways involved in the regulation of collagen and TGF-b expression in dystrophic skeletal muscle fibroblasts.

Interestingly, even though conditioned media from OPN+/+mdx fibroblast promotes a larger expression of collagen in OPN-/-mdx fibroblasts than OPN-/-mdx conditioned media, which would indicate an autocrine type of regulation of OPN in collagen expression in fibroblasts, we did not observe a difference in collagen expression from OPN+/+mdx and OPN-/-mdx fibroblasts cultured in serum free media. This observation could result from differences in the levels of OPN in the media or could suggest that OPN+/+mdx and OPN-/-mdx fibroblasts display intrinsic differences in the pathways modulating OPN's effect on collagen expression.

In terms of myogenesis, Paliwal et al. previously described a negative role of OPN on myogenicity [39]. This group showed that age dependent increases of OPN expression in vivo correlated with an inhibition of muscle regeneration in WT mice [39]. Moreover, they showed that rOPN supplementation of satellite cell cultures from young mice (lower OPN expression) reduced their regenerative capacity, while neutralization of OPN in satellite cell cultures from old mice (higher OPN expression) enhanced myogenesis [39]. Also, supplementation of C2C12 cultures with soluble OPN has been previously shown to significantly reduce the fusion index and affect the morphology of C2C12 myotubes [135]. In agreement with this, we show here that different sources of OPN tested, rOPN, fibroblast-derived OPN and myoblast/myotube-derived OPN, tend to decrease dMHC expression in dystrophic myotubes. Even thought, the decrease in dMHC expression in the experiments with each of the OPN sources is not statistically significant, OPN supplementation of myotube cultures consistently exerts an inhibitory effect on the expression of dMHC independently of the source of OPN used. The lack of a difference in the dMHC expression of untreated OPN+/+mdx and OPN-/-mdx

myotubes is likely due to the very low OPN expression levels in myotubes cultures. Moreover, the fact that OPN+/+mdx and OPN-/-mdx cells did not display a difference in the myogenic program, neither in untreated nor rOPN treated conditions, negates the possibility of a potential role for an intracellular form of OPN in the regulation of myogenesis.

These studies demonstrate that OPN likely interacts directly with dystrophic fibroblasts and myoblasts to regulate collagen and dMHC expression, respectively. Moreover, we showed that these effects are likely regulated by cell type specific post-translational modifications of the protein and that in dystrophic muscle, OPN secreted from fibroblasts seems to be more biologically active than OPN secreted from myoblasts.

Table 3.1 qPCR primers used.

	Forward	Reverse
GAPDH	TCCACCACCCTGTTGCTGTA	GACTTCAACAGCAACTCCCAC
Col1a	GTCGCTTCACCTACAGCAC	CAATGTCCAAGGGAGCCAC
Col3a	TGGTTCTGGCTTCCAGACAT	CACCCTTCTTCATCCCACTC
Col6a1	AGTGTCCGGATTATACCTGTCCAA	CGCTCAGCTAGGCGCTTG
Decorin	GTCTGGCCAATGTTCCTCAT	AAGTCATTTTGCCCAACTGC
Fibronectin	TTGGTGATGTGTGAAGGCTC	ACCTCTGCAGACCTACCCAG
OPN	GATGATGATGACGATGGAGACC	CGACTGTAGGGACGATTGGAG
TGF-β	TTTTCACAGGGGAGAAATCG	TGCGCTTGCAGAGATTAAAA
CTGF	GCTTGGCGATTTTAGGTGTC	CAGACTGGAGAAGCAGAGCC
MMP2	GACGGCATCCAGGTTATCAG	TGCAGGAGACAAGTTCTGGA
TIMP-1	TGGGGAACCCATGAATTTAG	ATCTGGCATCCTCTTGTTGC
TIMP-2	TCCTTCTCGCTCACTGCTTT	CTCCTGCTGCTAGCCACG
Myh3	CTTCACCTCTAGCCGGATGGT	AATTGTCAGGAGCCACGAAAAT
Myh8	CAGGAGCAGGAATGATGCTCTGAG	AGTTCCTCAAACTTTCAGCAGCCAA
Cyclin D1	GGGTGGGTTGGAAATGAAC	TCCTCTCCAAAATGCCAGAG
PCNA	TCAGGTACCTCAGAGCAAACG	AAGTGGAGAGCTTGGCAATG

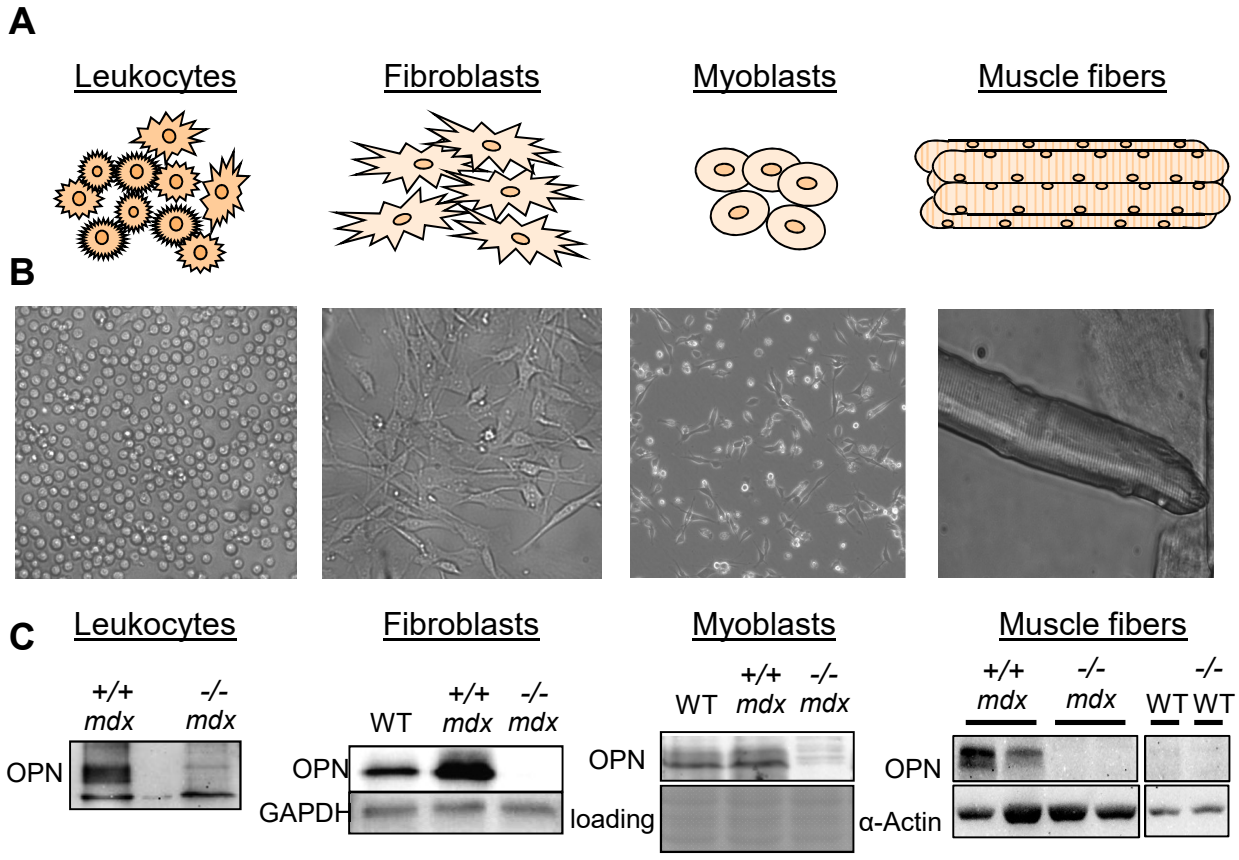

Figure 3.1 OPN is expressed in leukocytes, fibroblasts, myoblasts and dystrophic muscle fibers in mdx muscles.

This figure shows schematic representations of cell types isolated from dystrophic and WT skeletal muscles (Panel A) and DIC images of these isolated cells in culture conditions (Panel B). Western blot assays were used to assess the expression of OPN in protein samples from isolated fibroblasts, myoblasts, leukocytes and muscle fibers (Panel C). OPN-/- muscles were included as a negative control.

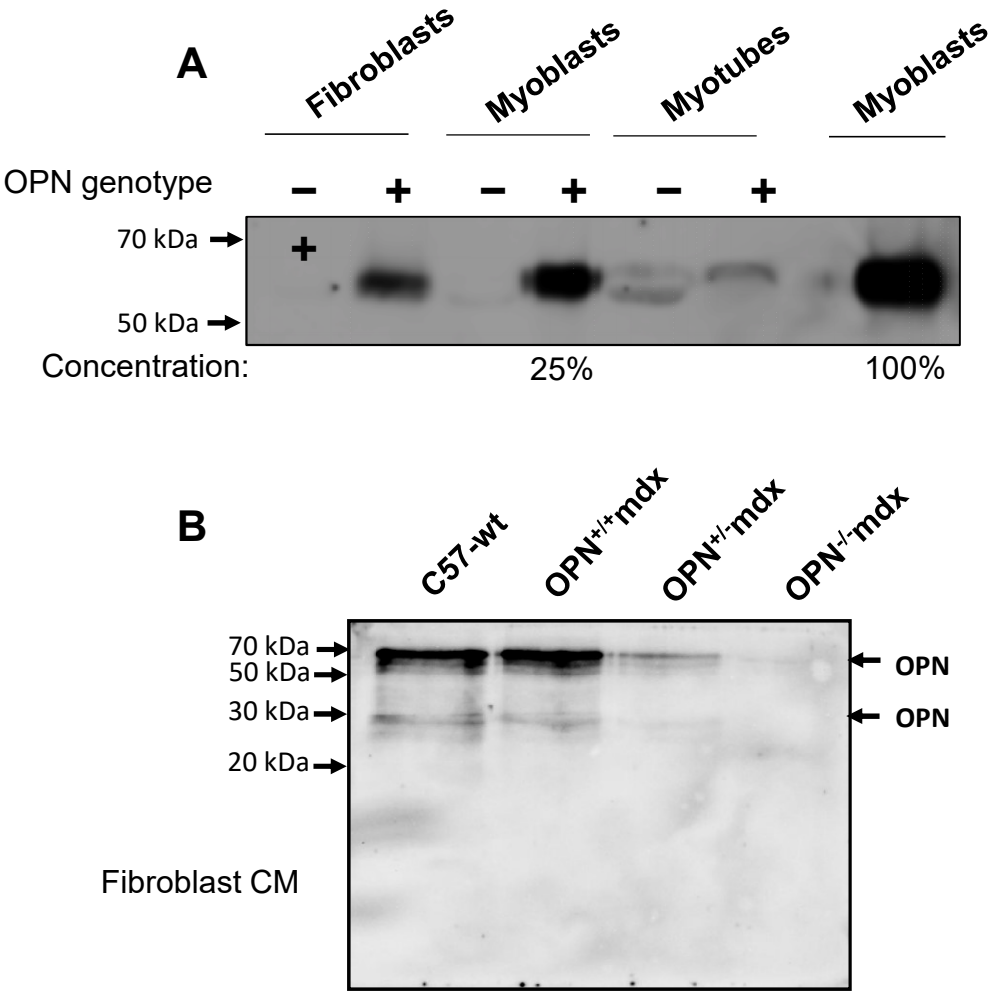

Figure 3.2 OPN is secreted by primary fibroblasts, myoblasts and myotubes.

Western blots were used to assay for the presence of OPN in conditioned media from primary fibroblasts, myoblasts and myotubes cultures. Panel A shows an OPN immunoblot of conditioned media harvested from OPN+/+mdx (+) and OPN-/-mdx (-) primary fibroblasts, myoblasts and myotubes cultures. Panel B shows a western blot revealing the presence of at least two distinguishable bands of OPN in the conditioned media from fibroblasts isolated from C57BL/6J, OPN+/+mdx, OPN+/-mdx, OPN-/-mdx.

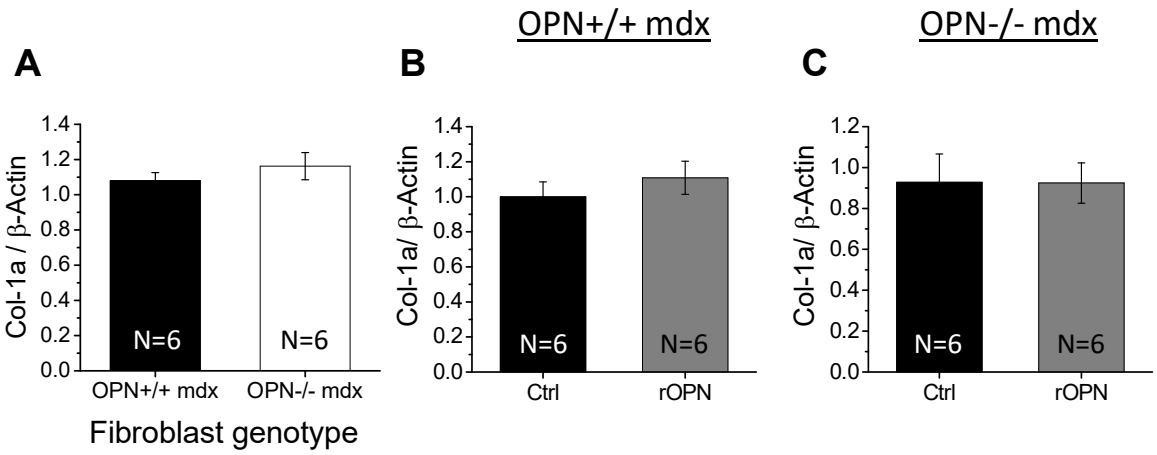

Figure 3.3 Collagen 1 expression in dystrophic fibroblast cultures is not affected by rOPN supplementation

Evaluation of the expression of collagen1 from OPN+/+mdx and OPN-/-mdx fibroblast cultures treated with or without rOPN. Panel A illustrate the average collagen expression in untreated OPN+/+mdx and OPN-/-mdx fibroblasts. Panel B and Panel C show plots of the relative collagen 1 expression in rOPN treated and untreated (Control, Ctrl) OPN+/+mdx and OPN-/-mdx fibroblasts respectively. Gene expression was measured via qPCR and it is plotted normalized to their b-actin expression. The number of samples per experiment is indicated on the bars. Vertical lines indicate standard error of the mean. Statistical significance was established by Student's T test.

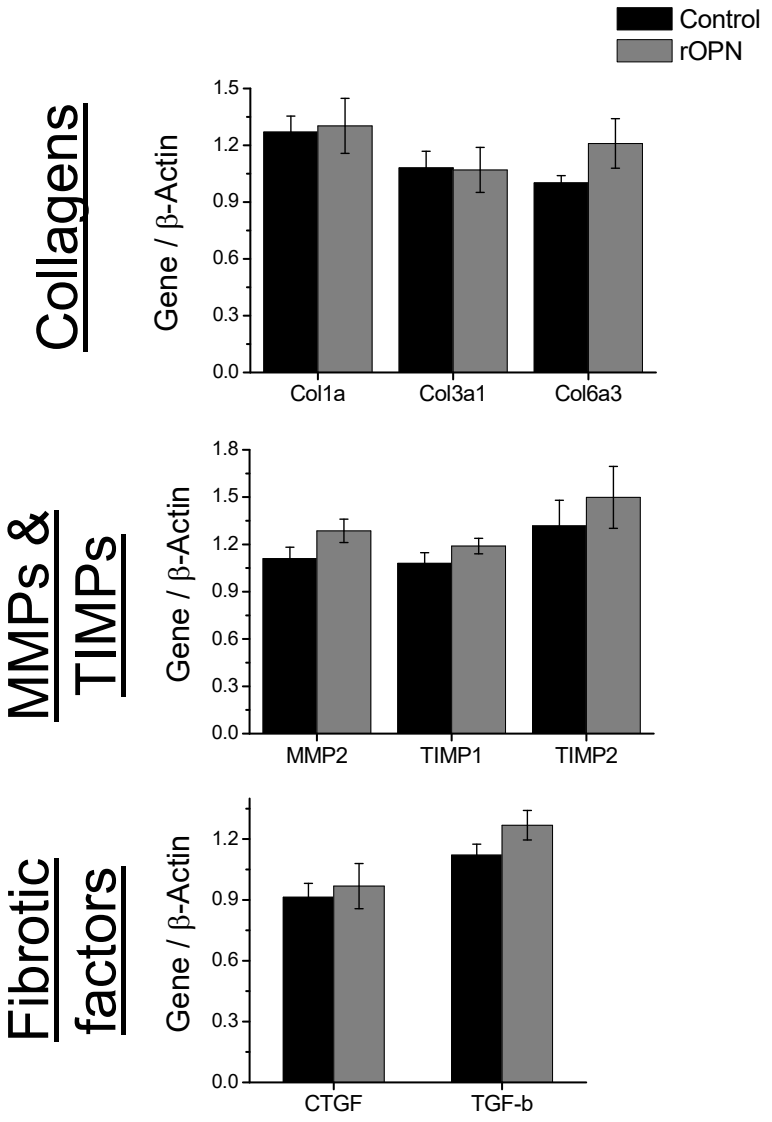

Figure 3.4 rOPN supplementation of dystrophic fibroblast cultures, does not affect their expression of collagens, MMPS, TIMPS and fibrotic factors

Expression of different types of collagens, TIMPs, MMPs, and profibrotic factors, was evaluated in OPN+/+mdx fibroblast cultures treated with or without rOPN. Gene expression was measured via qPCR and is shown normalized by b-actin expression. Sample size is N= 6 from 3 different experiments. Vertical lines indicate standard error of the mean. Statistical significance was established based on Student's T test.

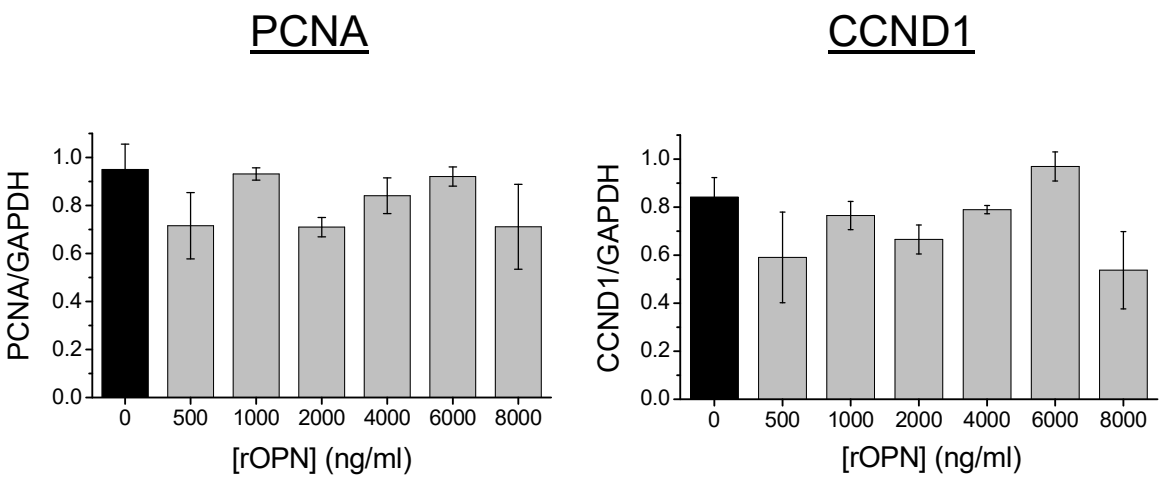

Figure 3.5 rOPN supplementation does not affect proliferation of fibroblasts cultures

The effect of rOPN on fibroblast proliferation was evaluated by measuring the expression of PCNA and cyclin D1 (CCND1) in fibroblast cultures treated with increasing rOPN concentrations. Gene expression was measured via qPCR and values are shown normalized by b-actin expression. Sample size is N=3. Black bars depict the values from cultures without rOPN. Vertical lines indicate standard error of the mean. Statistical significance was established based on Student's T test

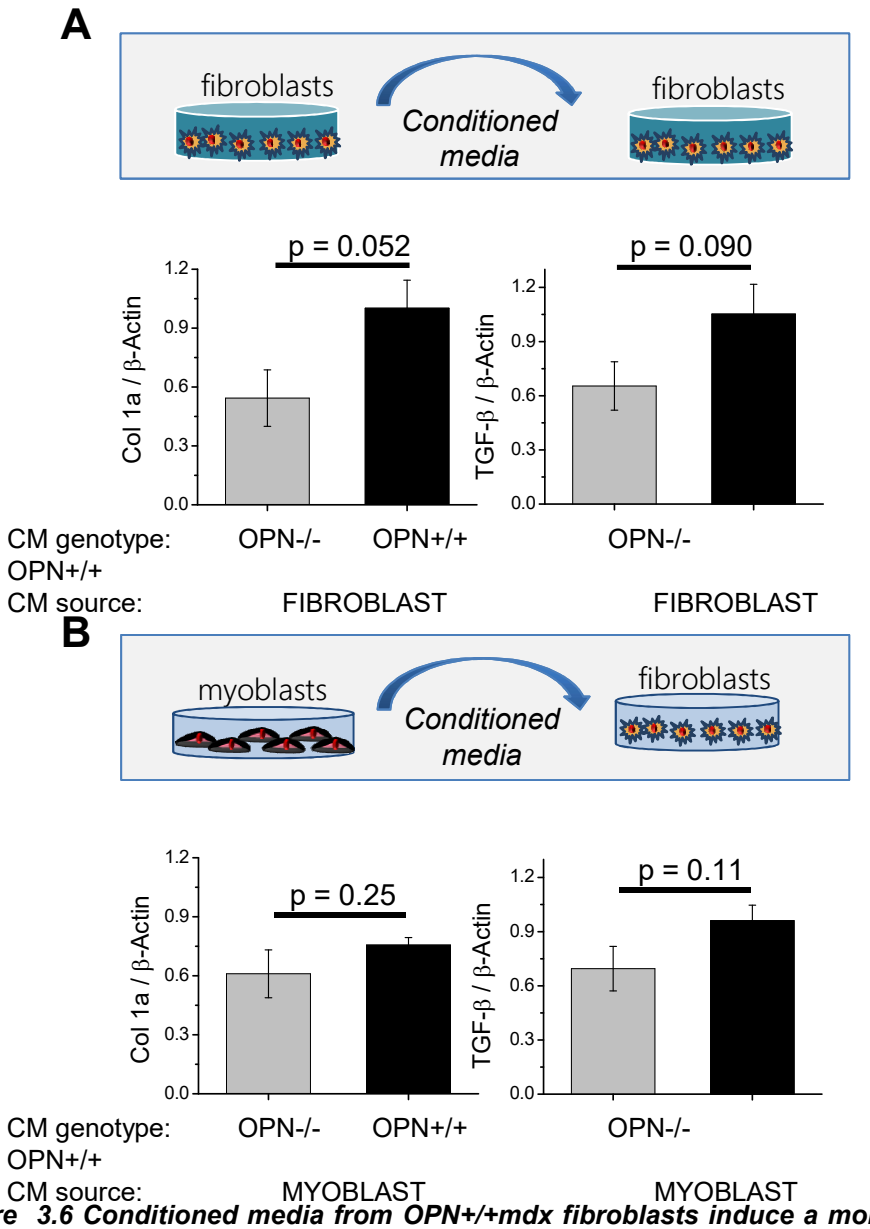

Figure 3.6 Conditioned media from OPN+/+mdx fibroblasts induce a more potent pro-fibrotic response than conditioned media from OPN+/+mdx myoblasts

To test the role of cell type-specific post-translational modifications of OPN in the regulation of fibrosis, collagen 1 and TGF-b expression were measured in OPN-/-mdx fibroblast cultures treated with OPN+/+mdx and OPN-/-mdx conditioned media harvested from fibroblast and myoblast cultures. Panel A shows the results obtained from experiments carried out using fibroblast conditioned media, and panel B from myoblast conditioned media. A scheme of each experimental design is displayed on the top part of each panel. Mean values of the expression of collagen 1 and TGF-b from the fibroblasts treated with fibroblast conditioned media are presented in the plots at the bottom of Panel A. Collagen 1 and TGF-b expression from the fibroblasts treated with myoblast conditioned media are presented in the plots at the bottom of Panel B. Gene expression was measured via qPCR and values are plotted normalized by b-actin expression. Sample size is N=6 from 2 different experiments. Vertical lines indicate standard error of the mean. Statistical significance was established based on Student's T test.

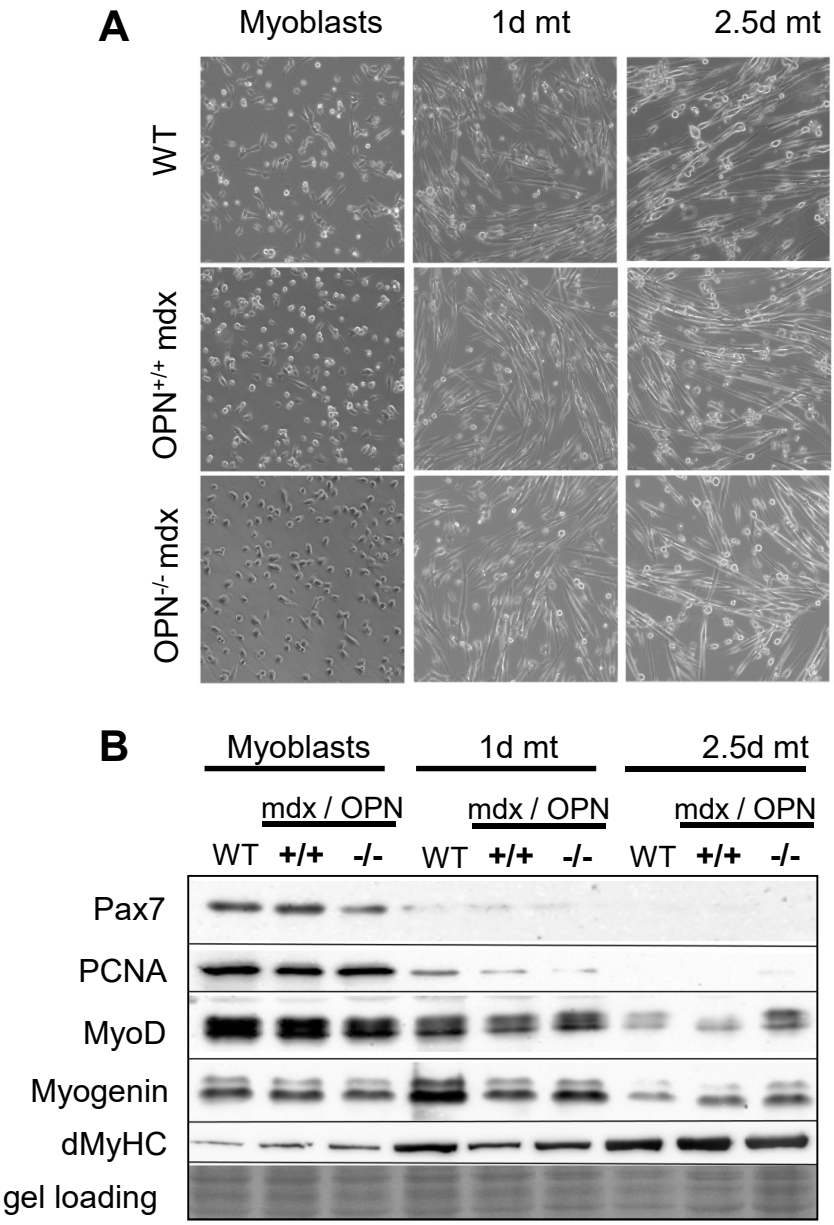

Figure 3.7 Evaluation of myogenesis in OPN+/+ and OPN-/- cultures

Panel A shows representative micrographs from C57-WT, OPN+/+mdx and OPN-/- primary myoblast cultures at various differentiation stages (myoblasts and myotubes 1 and 2 ½ days after induction of differentiation). Panel B shows representative western blots, evaluating the expression of various markers of different stages of the myogenic program (PCNA, Pax7, MyoD, myogenin and developmental myosin heavy chain (dMHC)) from C57-WT, OPN+/+mdx and OPN-/-mdx myoblast and myotube cultures at 1 and 2 ½ days after differentiation . Mt=myotube.

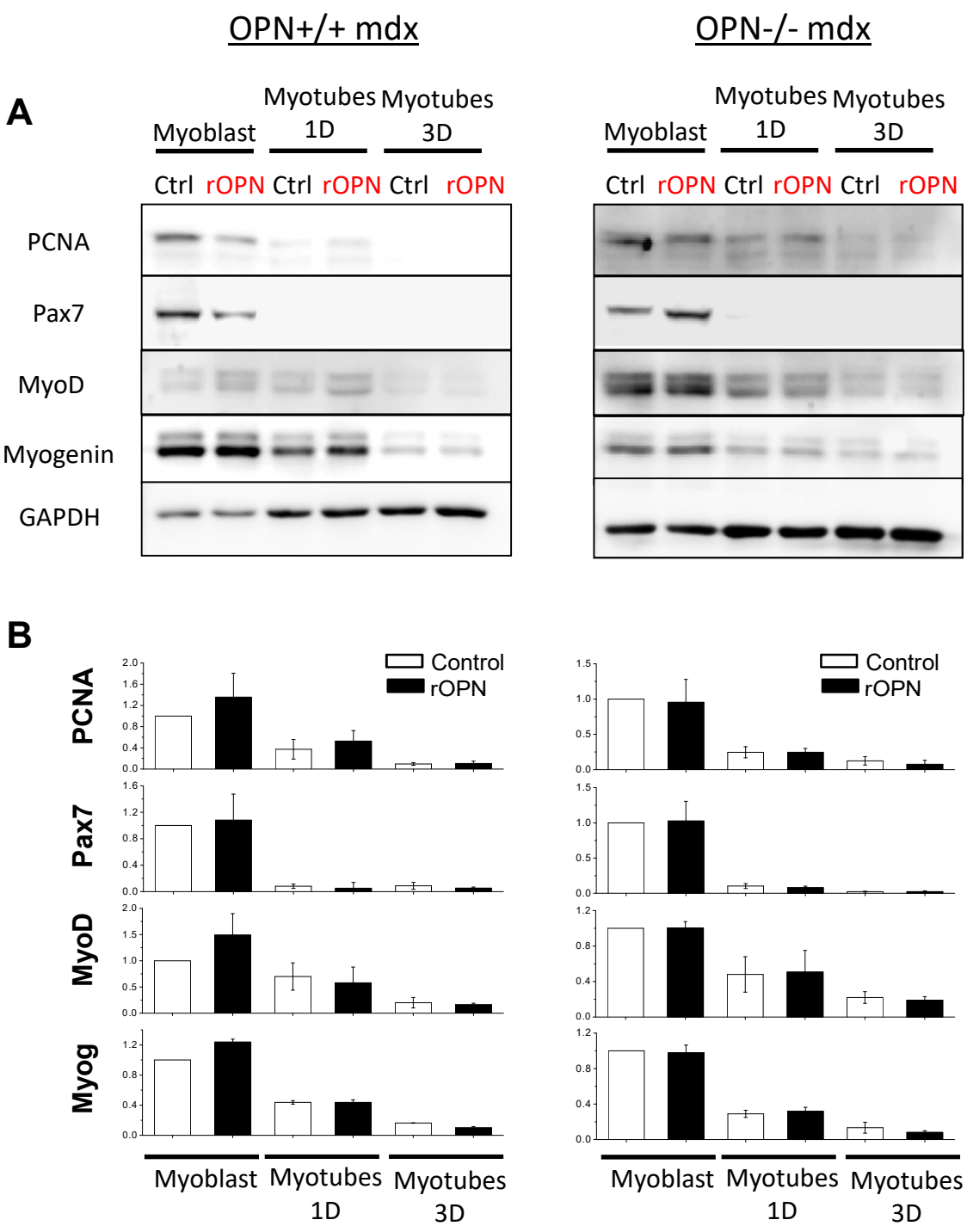
OPN+/+ mdx
OPN-/- mdx
A
Myoblast
Myotubes 1D
Myotubes 3D
Ctrl rOPN Ctrl rOPN Ctrl rOPN
PCNA
Pax7
MyoD
Myogenin
GAPDH
B
Control
rOPN
PCNA
Pax7
MyoD
Myog
Myoblast
Myotubes 1D
Myotubes 3D

Figure 3.8 Commercially produced rOPN supplementation does not affect the expression of myogenic markers during differentiation of dystrophic myoblasts.

Panel A shows a series of representative western blots evaluating the expression of various markers of the myogenic program (PCNA, Pax7, MyoD and myogenin) from OPN+/+mdx (left, N=3) and OPN-/-mdx (right, N=3) myoblast and myotube cultures at 1 and 3 days after differentiation incubated with or without commercially purchased rOPN (1500 ng/ml) before and during induction of differentiation. Relative values of each myogenic marker was calculated as the expression of the marker relative to the expression of GAPDH in the same sample. These values, were then normalized to the relative value of the expression of each gene in control myoblasts for each set of western blots. Panel B shows plots displaying the mean values of the relative expression of the myogenic markers, relative to GAPDH, from three different sets of western blots, similar to those shown in Panel A. Vertical lines indicate standard error of the mean. Statistical significance was established based on Student's T test comparison.

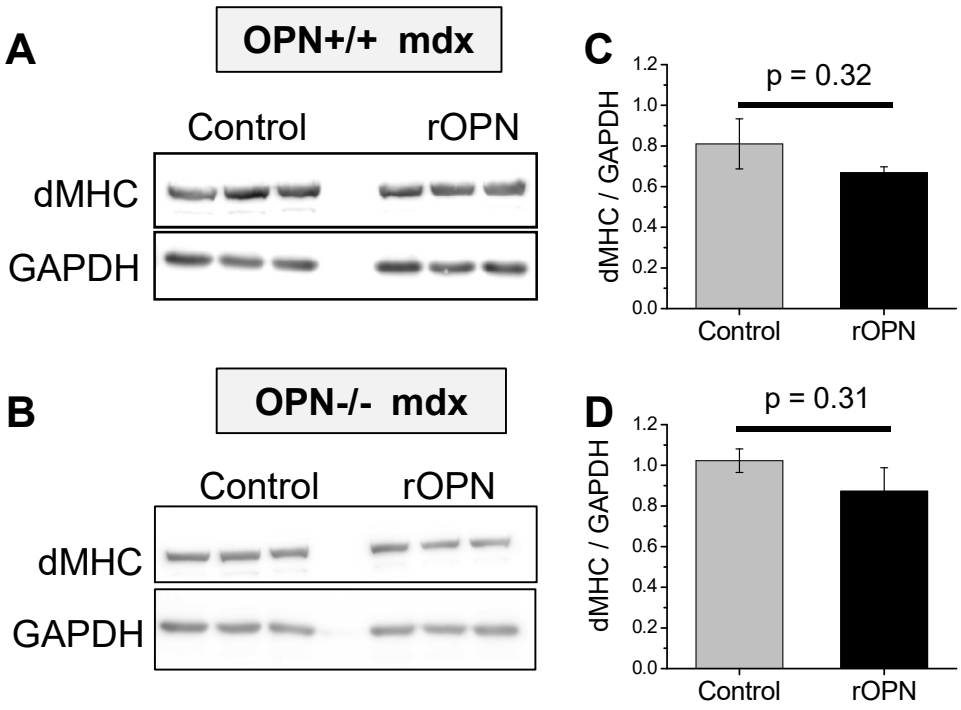

Figure 3.9 rOPN supplementation at the initiation of fusion does not significantly affect dMHC expression in dystrophic myotubes.

Panels A and B show western blots depicting the expression of dMHC and GAPDH in OPN+/+mdx and OPN-/-mdx myotube cultures treated with or without rOPN, only during differentiation, and collected 3 days after the induction of differentiation. Panel C and D show the quantification of the western blots shown in Panels A and B. Relative values of dMHC expression were calculated as the expression of dMHC relative to the expression of GAPDH in each sample. Vertical lines indicate standard error of the mean. Sample size N=3. Statistical significance was established based on Student's T test comparison.

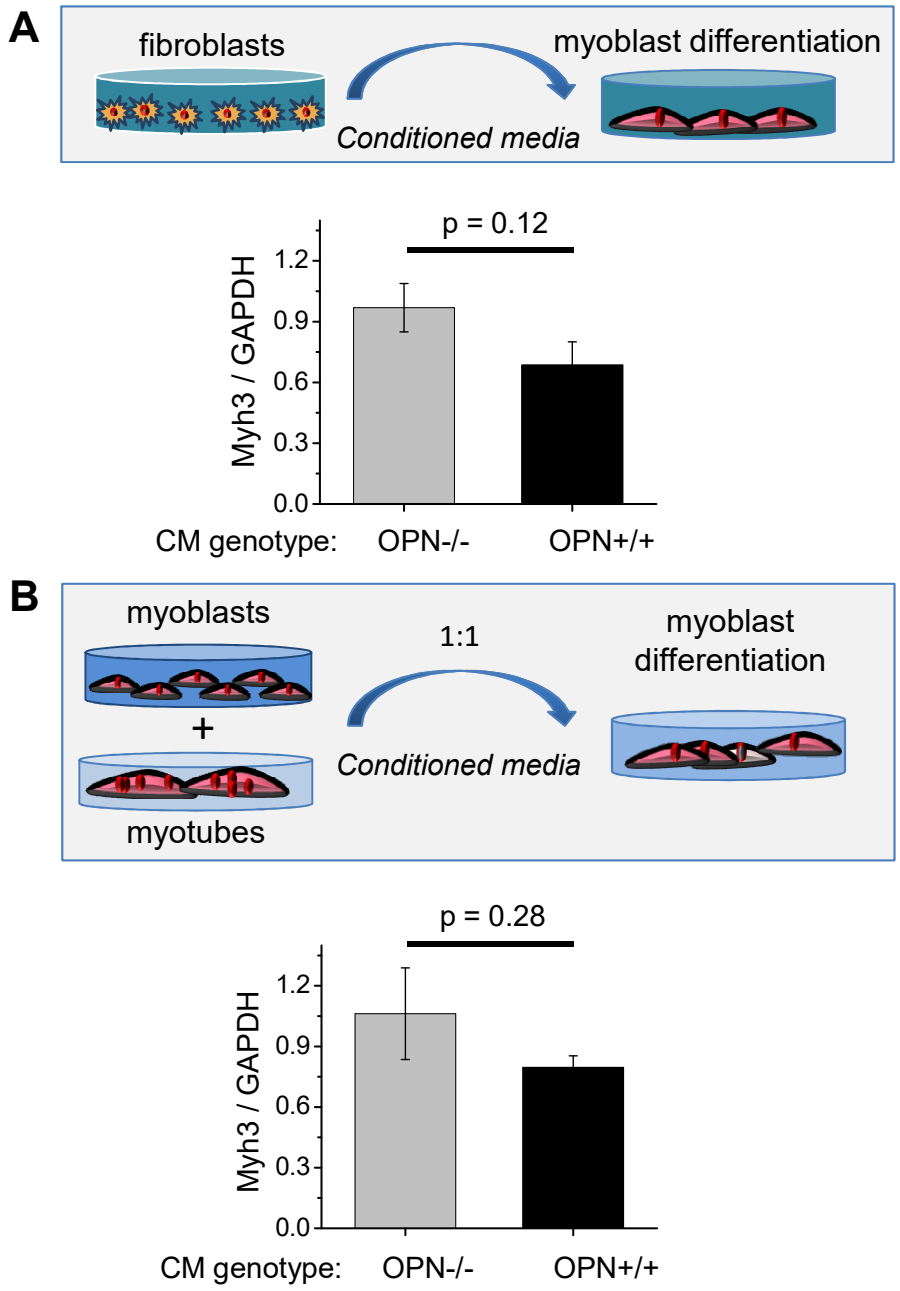

Figure 3.10 Conditioned media from both OPN+/+mdx fibroblasts and myoblasts tend to decrease the expression of dMHC in dystrophic myotubes.

Evaluation of the expression of embryonic myosin heavy chain (Myh3) in OPN-/-mdx 3 day myotubes treated with conditioned media from OPN-/-mdx and OPN+/+mdx fibroblasts (Panel A) or a mix 1:1 of myoblast and myotube cultures (Panel B). A scheme Illustrating each experimental design is displayed on the top part of each panel. The expression of embryonic myosin (Myh3) was normalized to GAPDH expression in each sample. Gene expression was measured via qPCR. Sample size N=6 from 2 different experiments. Vertical lines indicate standard error of the mean. Statistical significance was established based on Student's T test comparison.

Chapter 4

Overall conclusions

OPN has been shown to act as a modifier of the pathology in DMD patients where different single nucleotide polymorphisms in the promoter of the SSP1 gene have been shown to affect muscle strength and the age of loss of ambulation in DMD patients [52, 53, 56]. This role of OPN in the regulation of the DMD pathology has also been observed in different animal models of the disease [1, 113, 136, 143]. Previous work in the lab has shown that ablation of OPN in mdx mice significantly ameliorates their dystrophic pathology by decreasing muscle fibrosis and increasing muscle regeneration and strength in young mice [1]. These changes in the pathology of mdx mice were associated with OPN ablation-induced changes in the immune response, particularly a decrease in the NKT and Gr-1+ cells populations, and decreased intramuscular TGF-β expression [1]. In this project, we expand our previous observations and further explore the ways in which OPN exerts its regulatory role in the dystrophic pathology.

In agreement with our prior studies, we showed that OPN ablation in mdx mice induces an improvement in muscle strength and function, but we additionally show that this improvement is maintained in mdx mice for a long term. OPN-/-mdx mice, up to about one and a half years old, had better performance than their OPN+/+mdx counterparts in the wire and mesh tests and also demonstrated improved respiratory function. They also had less muscle damage, as shown by a significant decrease in serum creatine kinase levels, improved muscle-specific force and increased muscle mass and muscle fiber size.

The data presented in this project demonstrate that the previously observed decrease in the NKT population of mdx mice with OPN ablation is not involved in the mitigation of their dystrophic pathology. Elicited depletion of the NK and NKT populations in mdx mice did not cause any of the improvements observed in mdx mice with OPN ablation. In agreement with this finding, it has been previously reported that a mouse model of DMD lacking T, B and NK cells (*Rag2*$^{-}$, *IL2rd*$^{-}$, *DMD*$^{-}$ mouse) displays a phenotype very similar to that observed in the mdx mouse, indicating that these cells are likely not instrumental in the regulation of the muscle pathology [144].

More importantly, we show that the reduction in the Gr-1 signal (which labels Ly6G+ and Ly6C+ cells) previously observed in mdx with OPN ablation was caused by a specific decrease in Ly6C signal reflecting a switch in macrophage polarization from M1 (F4/80-low Ly6C-high cells) toward a M2C (F4/80-high Ly6C-low cells) phenotype. These kind of changes in the polarization of the intramuscular macrophage population have been previously shown to ameliorate the dystrophic pathology in mdx mice [67, 99, 101]. Moreover, we showed that OPN-ablation in mdx mice enhanced macrophage expression of the pro-regenerative factors IGF-1, LIF and uPA, while it does not affect their expression of the pro-fibrotic factors fibronectin, CCL17 and TGF-b. IGF-1, LIF and uPA have all been previously shown to promote muscle growth and regeneration and also to mitigate the dystrophic phenotype [96-98, 102]. Thus, OPN ablation-induced changes in the macrophage population supports and could at least partially explain the increase in regeneration, muscle size and muscle strength observed in mdx mice with OPN ablation.

Having established an indirect role of OPN in the regulation of the dystrophic pathology via modulation of macrophage polarization, we next decided to explore whether OPN could directly act on myoblasts and fibroblasts to affect fibrosis and regeneration in dystrophic muscle. In this regard, our data show that OPN is capable of promoting collagen expression in fibroblasts. However, we show that this effect of OPN on fibroblasts is likely dependent on cell type-specific post-translational modifications of the protein, as only fibroblast derived OPN, but not rOPN or myoblast derived OPN, was able to significantly increase collagen expression in fibroblasts cultures. Post-translational modifications of OPN have been previously shown to affect the activity of the protein in the regulation of particular cell functions [22, 27, 132, 145]. Moreover, OPN post-translational modifications are often cell type-specific and in some cases, OPN produce in different cell types from the same tissue have been shown to act in distinct ways [146, 147] . Therefore, further investigation is needed to identify the types of variations between OPN secreted from fibroblast and myoblast cultures, leading to functionally different responses.

In addition, OPN seems to also act as a cytokine to negatively affect terminal myoblast differentiation, since multiple sources of OPN, rOPN, fibroblast-derived OPN and myoblast-derived OPN, tend to decrease the expression of embryonic myosin heavy chain in late myotubes cultures. Although more experiments need to be done to confirm these results, our observations agree with previous reports establishing OPN as a negative regulator of muscle regeneration [39, 135].

In summary, we show in this project that OPN expression in dystrophic muscle impairs muscle regeneration both indirectly, by skewing the macrophage population

toward a less pro-regenerative phenotype, and directly, by impairing terminal differentiation of myoblasts (Figure 6.1). Moreover, OPN also promotes muscle fibrosis in dystrophic muscle by directly eliciting an increase in collagen expression in fibroblasts (Figure 6.1). Our project confirms OPN as a viable and valuable therapeutic target in DMD, as it is involved in the regulation of several pathological features that worsen dystrophic pathology. Moreover, we showed that OPN ablation causes long term amelioration of the pathology with no evident side effects in dystrophic mice.

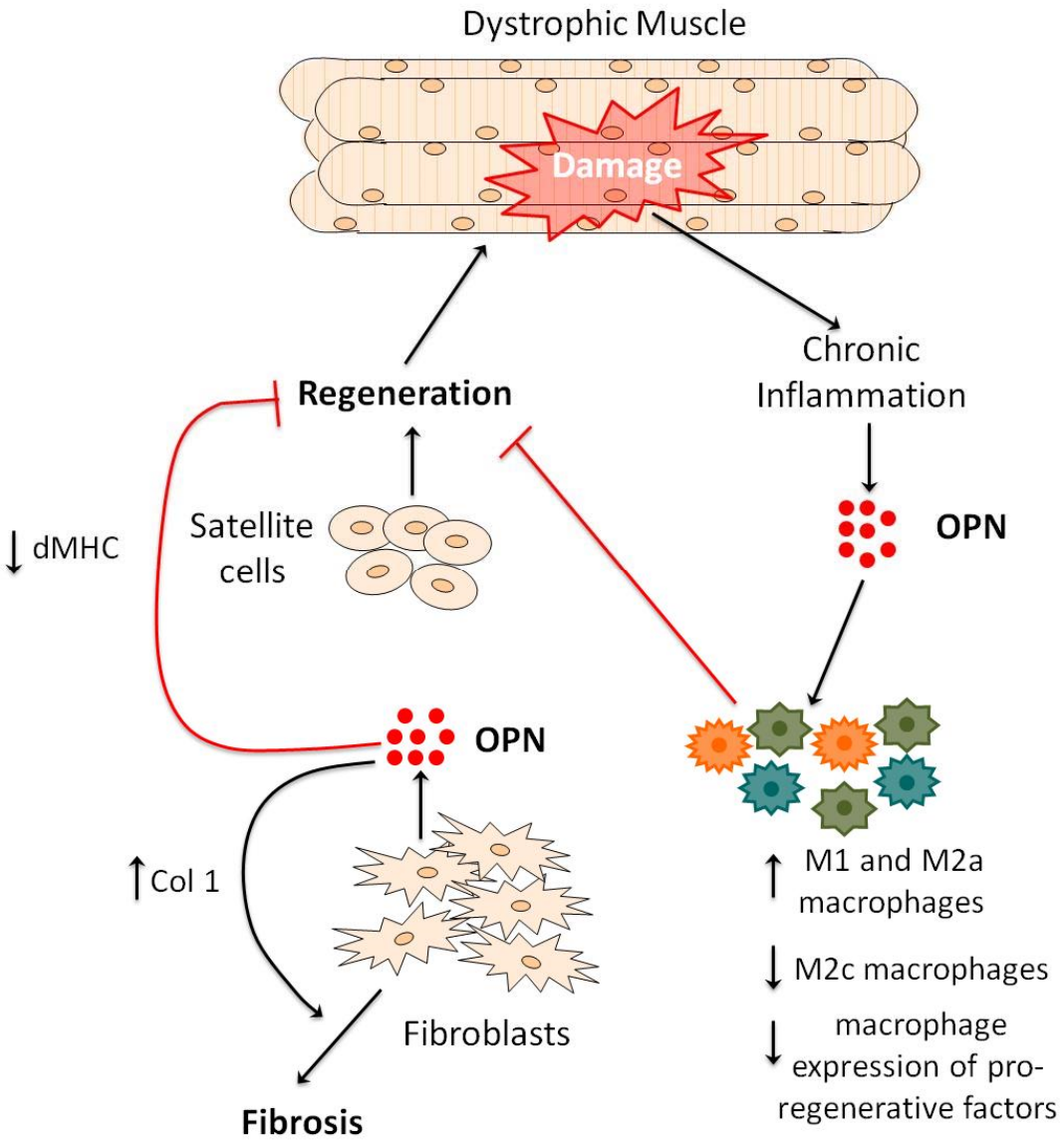

Figure 4.1 OPN regulation of the dystrophic pathology

Diagram illustrates the different ways in which OPN promotes the dystrophic pathology in mdx muscle. OPN expression in dystrophic muscle skews macrophage polarization by increasing M1 and M2a phenotypes and decreasing M2c macrophages. OPN expression also decreases macrophage expression of pro-regenerative factors. Therefore, impairing regeneration. Fibroblast secreted OPN promotes muscle fibrosis in dystrophic muscle by directly eliciting an increase in collagen expression in fibroblasts and tends to impair terminal myoblast differentiation by decreasing dMHC expression in myotubes. Red arrows depict negative interactions.

References

1. Vetrone, S.A., et al., *Osteopontin promotes fibrosis in dystrophic mouse muscle by modulating immune cell subsets and intramuscular TGF-beta.* J Clin Invest, 2009. **119**(6): p. 1583-94.
2. Nowak, K.J. and K.E. Davies, *Duchenne muscular dystrophy and dystrophin: pathogenesis and opportunities for treatment.* EMBO Rep, 2004. **5**(9): p. 872-6.
3. Pasternak, C., S. Wong, and E.L. Elson, *Mechanical function of dystrophin in muscle cells.* J Cell Biol, 1995. **128**(3): p. 355-61.
4. Blake, D.J., et al., *Function and genetics of dystrophin and dystrophin-related proteins in muscle.* Physiol Rev, 2002. **82**(2): p. 291-329.
5. Gumerson, J.D. and D.E. Michele, *The Dystrophin-Glycoprotein Complex in the Prevention of Muscle Damage.* Journal of Biomedicine and Biotechnology, 2011. **2011**: p. 13.
6. KUMAR, A., et al., *Loss of dystrophin causes aberrant mechanotransduction in skeletal muscle fibers.* The FASEB Journal, 2004. **18**(1): p. 102-113.
7. Spencer, M.J. and J.G. Tidball, *Do immune cells promote the pathology of dystrophin-deficient myopathies?* Neuromuscul Disord, 2001. **11**(6-7): p. 556-64.
8. Manning, J. and D. O'Malley, *What has the mdx mouse model of Duchenne muscular dystrophy contributed to our understanding of this disease?* J Muscle Res Cell Motil, 2015. **36**(2): p. 155-67.
9. Rodrigues, M., et al., *Current Translational Research and Murine Models For Duchenne Muscular Dystrophy.* J Neuromuscul Dis, 2016. **3**(1): p. 29-48.

10. Evans, N.P., et al., *Dysregulated intracellular signaling and inflammatory gene expression during initial disease onset in Duchenne muscular dystrophy.* Am J Phys Med Rehabil, 2009. **88**(6): p. 502-22.

11. Madaro, L. and M. Bouche, *From innate to adaptive immune response in muscular dystrophies and skeletal muscle regeneration: the role of lymphocytes.* Biomed Res Int, 2014. **2014**: p. 438675.

12. Pescatori, M., et al., *Gene expression profiling in the early phases of DMD: a constant molecular signature characterizes DMD muscle from early postnatal life throughout disease progression.* FASEB J, 2007. **21**(4): p. 1210-26.

13. Porter, J.D., et al., *Dissection of temporal gene expression signatures of affected and spared muscle groups in dystrophin-deficient (mdx) mice.* Hum Mol Genet, 2003. **12**(15): p. 1813-21.

14. Porter, J.D., et al., *A chronic inflammatory response dominates the skeletal muscle molecular signature in dystrophin-deficient mdx mice.* Hum Mol Genet, 2002. **11**(3): p. 263-72.

15. Acharyya, S., et al., *Interplay of IKK/NF-kappaB signaling in macrophages and myofibers promotes muscle degeneration in Duchenne muscular dystrophy.* J Clin Invest, 2007. **117**(4): p. 889-901.

16. Ermolova, N.V., et al., *Long-term administration of the TNF blocking drug Remicade (cV1q) to mdx mice reduces skeletal and cardiac muscle fibrosis, but negatively impacts cardiac function.* Neuromuscul Disord, 2014. **24**(7): p. 583-95.

17. Messina, S., et al., *Nuclear factor kappa-B blockade reduces skeletal muscle degeneration and enhances muscle function in Mdx mice.* Exp Neurol, 2006. **198**(1): p. 234-41.

18. Radley, H.G., M.J. Davies, and M.D. Grounds, *Reduced muscle necrosis and long-term benefits in dystrophic mdx mice after cV1q (blockade of TNF) treatment.* Neuromuscul Disord, 2008. **18**(3): p. 227-38.

19. Villalta, S., et al., *Shifts in macrophage phenotypes and macrophage competition for arginine metabolism affect the severity of muscle pathology in muscular dystrophy.* Hum Mol Genet, 2009. **18**: p. 482 - 96.

20. Anborgh, P.H., et al., *Pre- and post-translational regulation of osteopontin in cancer.* J Cell Commun Signal, 2011. **5**(2): p. 111-22.

21. Inoue, M. and M.L. Shinohara, *Intracellular osteopontin (iOPN) and immunity.* Immunol Res. **49**(1-3): p. 160-72.

22. Sodek, J., B. Ganss, and M.D. McKee, *Osteopontin.* Crit Rev Oral Biol Med, 2000. **11**(3): p. 279-303.

23. Uede, T., *Osteopontin, intrinsic tissue regulator of intractable inflammatory diseases.* Pathol Int. **61**(5): p. 265-80.

24. Giachelli, C.M., et al., *Osteopontin is elevated during neointima formation in rat arteries and is a novel component of human atherosclerotic plaques.* J Clin Invest, 1993. **92**(4): p. 1686-96.

25. Young, M.F., et al., *cDNA cloning, mRNA distribution and heterogeneity, chromosomal location, and RFLP analysis of human osteopontin (OPN).* Genomics, 1990. **7**(4): p. 491-502.

26. Agnihotri, R., et al., *Osteopontin, a novel substrate for matrix metalloproteinase-3 (stromelysin-1) and matrix metalloproteinase-7 (matrilysin).* J Biol Chem, 2001. **276**(30): p. 28261-7.

27. Christensen, B., et al., *Cell type-specific post-translational modifications of mouse osteopontin are associated with different adhesive properties.* J Biol Chem, 2007. **282**(27): p. 19463-72.

28. Senger, D.R., et al., *Adhesive properties of osteopontin: regulation by a naturally occurring thrombin-cleavage in close proximity to the GRGDS cell-binding domain.* Mol Biol Cell, 1994. **5**(5): p. 565-74.

29. Yokosaki, Y., et al., *The integrin alpha(9)beta(1) binds to a novel recognition sequence (SVVYGLR) in the thrombin-cleaved amino-terminal fragment of osteopontin.* J Biol Chem, 1999. **274**(51): p. 36328-34.

30. Mazzali, M., et al., *Osteopontin--a molecule for all seasons.* Qjm, 2002. **95**(1): p. 3-13.

31. Wang, K.X. and D.T. Denhardt, *Osteopontin: role in immune regulation and stress responses.* Cytokine Growth Factor Rev, 2008. **19**(5-6): p. 333-45.

32. Saitoh, Y., et al., *Expression of osteopontin in human glioma. Its correlation with the malignancy.* Lab Invest, 1995. **72**(1): p. 55-63.

33. Yan, W., et al., *Expression pattern of osteopontin splice variants and its functions on cell apoptosis and invasion in glioma cells.* Neuro Oncol. **12**(8): p. 765-75.

34. Bellahcene, A., et al., *Small integrin-binding ligand N-linked glycoproteins (SIBLINGs): multifunctional proteins in cancer.* Nat Rev Cancer, 2008. **8**(3): p. 212-26.

35. Giachelli, C.M. and S. Steitz, *Osteopontin: a versatile regulator of inflammation and biomineralization.* Matrix Biol, 2000. **19**(7): p. 615-22.

36. Barbosa-Souza, V., et al., *Osteopontin, a chemotactic protein with cytokine-like properties, is up-regulated in muscle injury caused by Bothrops lanceolatus (fer-de-lance) snake venom.* Toxicon. **58**(5): p. 398-409.

37. Dai, J., et al., *Osteopontin induces angiogenesis through activation of PI3K/AKT and ERK1/2 in endothelial cells.* Oncogene, 2009. **28**(38): p. 3412-22.

38. Liaw, L., et al., *Altered wound healing in mice lacking a functional osteopontin gene (spp1).* J Clin Invest, 1998. **101**(7): p. 1468-78.

39. Paliwal, P., et al., *Age dependent increase in the levels of osteopontin inhibits skeletal muscle regeneration.* Aging (Albany NY), 2012. **4**(8): p. 553-66.

40. Pardo, A., et al., *Up-regulation and profibrotic role of osteopontin in human idiopathic pulmonary fibrosis.* PLoS Med, 2005. **2**(9): p. e251.

41. Patouraux, S., et al., *The osteopontin level in liver, adipose tissue and serum is correlated with fibrosis in patients with alcoholic liver disease.* PLoS One. **7**(4): p. e35612.

42. Rittling, S.R. and A.F. Chambers, *Role of osteopontin in tumour progression.* Br J Cancer, 2004. **90**(10): p. 1877-81.

43. Szalay, G., et al., *Osteopontin: a fibrosis-related marker molecule in cardiac remodeling of enterovirus myocarditis in the susceptible host.* Circ Res, 2009. **104**(7): p. 851-9.

44. Barry, S.T., et al., *A regulated interaction between alpha5beta1 integrin and osteopontin.* Biochem Biophys Res Commun, 2000. **267**(3): p. 764-9.

45. Denhardt, D.T. and M. Noda, *Osteopontin expression and function: role in bone remodeling.* J Cell Biochem Suppl, 1998. **30-31**: p. 92-102.

46. Barry, S.T., et al., *Analysis of the alpha4beta1 integrin-osteopontin interaction.* Exp Cell Res, 2000. **258**(2): p. 342-51.

47. Schack, L., et al., *Osteopontin enhances phagocytosis through a novel osteopontin receptor, the alphaXbeta2 integrin.* J Immunol, 2009. **182**(11): p. 6943-50.

48. Kang, J.A., et al., *Osteopontin regulates actin cytoskeleton and contributes to cell proliferation in primary erythroblasts.* J Biol Chem, 2008. **283**(11): p. 6997-7006.

49. Zohar, R., et al., *Intracellular osteopontin is an integral component of the CD44-ERM complex involved in cell migration.* J Cell Physiol, 2000. **184**(1): p. 118-30.

50. Junaid, A., et al., *Osteopontin localizes to the nucleus of 293 cells and associates with polo-like kinase-1.* Am J Physiol Cell Physiol, 2007. **292**(2): p. C919-26.

51. Zanotti, S., et al., *Osteopontin is highly expressed in severely dystrophic muscle and seems to play a role in muscle regeneration and fibrosis.* Histopathology, 2011. **59**(6): p. 1215-28.

52. Bello, L., et al., *Importance of SPP1 genotype as a covariate in clinical trials in Duchenne muscular dystrophy.* Neurology. **79**(2): p. 159-62.

53. Pegoraro, E., et al., *SPP1 genotype is a determinant of disease severity in Duchenne muscular dystrophy.* Neurology. **76**(3): p. 219-26.

54. Giacopelli, F., et al., *Polymorphisms in the osteopontin promoter affect its transcriptional activity.* Physiol Genomics, 2004. **20**(1): p. 87-96.

55. Piva, L., et al., *TGFBR2 but not SPP1 genotype modulates osteopontin expression in Duchenne muscular dystrophy muscle.* J Pathol, 2012. **228**(2): p. 251-9.

56. Bello, L., et al., *Genetic modifiers of ambulation in the CINRG duchenne natural history study.* Ann Neurol, 2015.

57. van den Bergen, J.C., et al., *Validation of genetic modifiers for Duchenne muscular dystrophy: a multicentre study assessing SPP1 and LTBP4 variants.* J Neurol Neurosurg Psychiatry, 2014.

58. Bushby, K., et al., *Diagnosis and management of Duchenne muscular dystrophy, part 1: diagnosis, and pharmacological and psychosocial management.* Lancet Neurol, 2010. **9**(1): p. 77-93.

59. Heydemann, A., et al., *Latent TGF-beta-binding protein 4 modifies muscular dystrophy in mice.* J Clin Invest, 2009. **119**(12): p. 3703-12.

60. Borthwick, L.A., T.A. Wynn, and A.J. Fisher, *Cytokine mediated tissue fibrosis.* Biochim Biophys Acta, 2013. **1832**(7): p. 1049-60.

61. Cantini, M., et al., *Macrophage-secreted myogenic factors: a promising tool for greatly enhancing the proliferative capacity of myoblasts in vitro and in vivo.* Neurol Sci, 2002. **23**(4): p. 189-94.

62. Dumont, N. and J. Frenette, *Macrophages protect against muscle atrophy and promote muscle recovery in vivo and in vitro: a mechanism partly dependent on the insulin-like growth factor-1 signaling molecule.* Am J Pathol, 2010. **176**(5): p. 2228-35.

63. Saclier, M., et al., *Differentially activated macrophages orchestrate myogenic precursor cell fate during human skeletal muscle regeneration.* Stem Cells, 2013. **31**(2): p. 384-96.

64. Wehling, M., M.J. Spencer, and J.G. Tidball, *A nitric oxide synthase transgene ameliorates muscular dystrophy in mdx mice.* J Cell Biol, 2001. **155**(1): p. 123-31.

65. McDouall, R.M., M.J. Dunn, and V. Dubowitz, *Nature of the mononuclear infiltrate and the mechanism of muscle damage in juvenile dermatomyositis and Duchenne muscular dystrophy.* J Neurol Sci, 1990. **99**(2-3): p. 199-217.

66. Mann, C.J., et al., *Aberrant repair and fibrosis development in skeletal muscle.* Skelet Muscle. **1**(1): p. 21.

67. Villalta, S.A., et al., *Shifts in macrophage phenotypes and macrophage competition for arginine metabolism affect the severity of muscle pathology in muscular dystrophy.* Hum Mol Genet, 2009. **18**(3): p. 482-96.

68. Liu, Y.C., et al., *Macrophage polarization in inflammatory diseases.* Int J Biol Sci, 2014. **10**(5): p. 520-9.

69. Mantovani, A., A. Sica, and M. Locati, *New vistas on macrophage differentiation and activation.* Eur J Immunol, 2007. **37**(1): p. 14-6.

70. Novak, M.L. and T.J. Koh, *Macrophage phenotypes during tissue repair.* J Leukoc Biol, 2013. **93**(6): p. 875-81.

71. Novak, M.L. and T.J. Koh, *Phenotypic transitions of macrophages orchestrate tissue repair.* Am J Pathol, 2013. **183**(5): p. 1352-63.

72. Rigamonti, E., et al., *Macrophage plasticity in skeletal muscle repair.* Biomed Res Int, 2014. **2014**: p. 560629.

73. Song, E., et al., *Influence of alternatively and classically activated macrophages on fibrogenic activities of human fibroblasts.* Cell Immunol, 2000. **204**(1): p. 19-28.

74. Haslett, J.N., et al., *Gene expression comparison of biopsies from Duchenne muscular dystrophy (DMD) and normal skeletal muscle.* Proc Natl Acad Sci U S A, 2002. **99**(23): p. 15000-5.

75. Bayless, K.J., et al., *Osteopontin is a ligand for the alpha4beta1 integrin.* J Cell Sci, 1998. **111 (Pt 9)**: p. 1165-74.

76. Casals, G., et al., *Osteopontin and alphavbeta3 integrin expression in the endometrium of infertile and fertile women.* Reprod Biomed Online, 2008. **16**(6): p. 808-16.

77. Das, R., et al., *Osteopontin: it's role in regulation of cell motility and nuclear factor kappa B-mediated urokinase type plasminogen activator expression.* IUBMB Life, 2005. **57**(6): p. 441-7.

78. Kahles, F., H.M. Findeisen, and D. Bruemmer, *Osteopontin: A novel regulator at the cross roads of inflammation, obesity and diabetes.* Mol Metab, 2014. **3**(4): p. 384-93.

79. Nystrom, T., P. Duner, and A. Hultgardh-Nilsson, *A constitutive endogenous osteopontin production is important for macrophage function and differentiation.* Exp Cell Res, 2007. **313**(6): p. 1149-60.

80. Sicinski, P., et al., *The molecular basis of muscular dystrophy in the mdx mouse: a point mutation.* Science, 1989. **244**(4912): p. 1578-80.

81. Amalfitano, A. and J.S. Chamberlain, *The mdx-amplification-resistant mutation system assay, a simple and rapid polymerase chain reaction-based detection of the mdx allele.* Muscle Nerve, 1996. **19**(12): p. 1549-53.

82. Barton, E.R., et al., *Diaphragm displays early and progressive functional deficits in dysferlin-deficient mice.* Muscle Nerve, 2010. **42**(1): p. 22-9.

83. Moorwood, C., et al., *Isometric and eccentric force generation assessment of skeletal muscles isolated from murine models of muscular dystrophies.* J Vis Exp, 2013(71): p. e50036.

84. Barton, E.R., et al., *Systemic administration of L-arginine benefits mdx skeletal muscle function.* Muscle Nerve, 2005. **32**(6): p. 751-60.

85. Kramerova, I., et al., *Null mutation of calpain 3 (p94) in mice causes abnormal sarcomere formation in vivo and in vitro.* Hum Mol Genet, 2004. **13**(13): p. 1373-88.

86. Godfrey, D.I. and M. Kronenberg, *Going both ways: immune regulation via CD1d-dependent NKT cells.* J Clin Invest, 2004. **114**(10): p. 1379-88.

87. Byrne, P., et al., *Depletion of NK cells results in disseminating lethal infection with Bordetella pertussis associated with a reduction of antigen-specific Th1 and enhancement of Th2, but not Tr1 cells.* Eur J Immunol, 2004. **34**(9): p. 2579-88.

88. Nakagawa, R., et al., *Mechanisms of the antimetastatic effect in the liver and of the hepatocyte injury induced by alpha-galactosylceramide in mice.* J Immunol, 2001. **166**(11): p. 6578-84.

89. Nakano, Y., et al., *Roles of NKT cells in resistance against infection with Toxoplasma gondii and in expression of heat shock protein 65 in the host macrophages.* Microbes Infect, 2002. **4**(1): p. 1-11.

90. Slifka, M.K., R.R. Pagarigan, and J.L. Whitton, *NK markers are expressed on a high percentage of virus-specific CD8+ and CD4+ T cells.* J Immunol, 2000. **164**(4): p. 2009-15.

91. Arnold, L., et al., *Inflammatory monocytes recruited after skeletal muscle injury switch into antiinflammatory macrophages to support myogenesis.* J Exp Med, 2007. **204**(5): p. 1057-69.

92. Crane, M.J., et al., *The monocyte to macrophage transition in the murine sterile wound.* PLoS One, 2014. **9**(1): p. e86660.

93. Varga, T., et al., *Tissue LyC6- macrophages are generated in the absence of circulating LyC6- monocytes and Nur77 in a model of muscle regeneration.* J Immunol, 2013. **191**(11): p. 5695-701.

94. Vidal, B., et al., *Fibrinogen drives dystrophic muscle fibrosis via a TGFbeta/alternative macrophage activation pathway.* Genes Dev, 2008. **22**(13): p. 1747-52.

95. Belperio, J.A., et al., *The role of the Th2 CC chemokine ligand CCL17 in pulmonary fibrosis.* J Immunol, 2004. **173**(7): p. 4692-8.

96. Barton, E.R., et al., *Muscle-specific expression of insulin-like growth factor I counters muscle decline in mdx mice.* J Cell Biol, 2002. **157**(1): p. 137-48.

97. Hunt, L.C., et al., *An anti-inflammatory role for leukemia inhibitory factor receptor signaling in regenerating skeletal muscle.* Histochem Cell Biol, 2013. **139**(1): p. 13-34.

98. Suelves, M., et al., *uPA deficiency exacerbates muscular dystrophy in MDX mice.* J Cell Biol, 2007. **178**(6): p. 1039-51.

99. Villalta, S.A., et al., *IFN-gamma promotes muscle damage in the mdx mouse model of Duchenne muscular dystrophy by suppressing M2 macrophage activation and inhibiting muscle cell proliferation.* J Immunol, 2011. **187**(10): p. 5419-28.

100. Villalta, S.A., et al., *Interleukin-10 reduces the pathology of mdx muscular dystrophy by deactivating M1 macrophages and modulating macrophage phenotype.* Hum Mol Genet, 2011. **20**(4): p. 790-805.

101. Mojumdar, K., et al., *Inflammatory monocytes promote progression of Duchenne muscular dystrophy and can be therapeutically targeted via CCR2.* EMBO Mol Med, 2014. **6**(11): p. 1476-92.

102. Bryer, S.C., et al., *Urokinase-type plasminogen activator plays essential roles in macrophage chemotaxis and skeletal muscle regeneration.* J Immunol, 2008. **180**(2): p. 1179-88.

103. To, W.S. and K.S. Midwood, *Plasma and cellular fibronectin: distinct and independent functions during tissue repair.* Fibrogenesis Tissue Repair, 2011. **4**: p. 21.

104. Yogo, Y., et al., *Macrophage derived chemokine (CCL22), thymus and activation-regulated chemokine (CCL17), and CCR4 in idiopathic pulmonary fibrosis.* Respir Res, 2009. **10**: p. 80.

105. Rollo, E.E. and D.T. Denhardt, *Differential effects of osteopontin on the cytotoxic activity of macrophages from young and old mice.* Immunology, 1996. **88**(4): p. 642-7.

106. Rollo, E.E., D.L. Laskin, and D.T. Denhardt, *Osteopontin inhibits nitric oxide production and cytotoxicity by activated RAW264.7 macrophages.* J Leukoc Biol, 1996. **60**(3): p. 397-404.

107. Weber, G.F., et al., *Phosphorylation-dependent interaction of osteopontin with its receptors regulates macrophage migration and activation.* J Leukoc Biol, 2002. **72**(4): p. 752-61.

108. Naldini, A., et al., *Cutting edge: IL-1beta mediates the proangiogenic activity of osteopontin-activated human monocytes.* J Immunol, 2006. **177**(7): p. 4267-70.

109. Koguchi, Y., et al., *Penicillium marneffei causes osteopontin-mediated production of interleukin-12 by peripheral blood mononuclear cells.* Infect Immun, 2002. **70**(3): p. 1042-8.

110. Gao, C., et al., *Osteopontin induces ubiquitin-dependent degradation of STAT1 in RAW264.7 murine macrophages.* J Immunol, 2007. **178**(3): p. 1870-81.

111. Ashkar, S., et al., *Eta-1 (osteopontin): an early component of type-1 (cell-mediated) immunity.* Science, 2000. **287**(5454): p. 860-4.

112. Goodison, S., V. Urquidi, and D. Tarin, *CD44 cell adhesion molecules.* Mol Pathol, 1999. **52**(4): p. 189-96.

113. Galindo, C.L., et al., *Translating golden retriever muscular dystrophy microarray findings to novel biomarkers for cardiac/skeletal muscle function in Duchenne muscular dystrophy.* Pediatr Res, 2015.

114. De Paepe, B. and J.L. De Bleecker, *Cytokines and chemokines as regulators of skeletal muscle inflammation: presenting the case of Duchenne muscular dystrophy.* Mediators Inflamm, 2013. **2013**: p. 540370.

115. Kharraz, Y., et al., *Understanding the process of fibrosis in Duchenne muscular dystrophy.* Biomed Res Int, 2014. **2014**: p. 965631.

116. Heydemann, A., K.R. Doherty, and E.M. McNally, *Genetic modifiers of muscular dystrophy: implications for therapy.* Biochim Biophys Acta, 2007. **1772**(2): p. 216-28.

117. Hogarth, M.W., et al., *Evidence for ACTN3 as a genetic modifier of Duchenne muscular dystrophy.* Nat Commun, 2017. **8**: p. 14143.

118. Vo, A.H. and E.M. McNally, *Modifier genes and their effect on Duchenne muscular dystrophy.* Curr Opin Neurol, 2015. **28**(5): p. 528-34.

119. Flanigan, K.M., et al., *LTBP4 genotype predicts age of ambulatory loss in Duchenne muscular dystrophy.* Ann Neurol, 2013. **73**(4): p. 481-8.

120. Swaggart, K.A., et al., *Annexin A6 modifies muscular dystrophy by mediating sarcolemmal repair.* Proc Natl Acad Sci U S A, 2014. **111**(16): p. 6004-9.

121. Bello, L., et al., *Association Study of Exon Variants in the NF-kappaB and TGFbeta Pathways Identifies CD40 as a Modifier of Duchenne Muscular Dystrophy.* Am J Hum Genet, 2016. **99**(5): p. 1163-1171.

122. Li, Y., et al., *Transforming growth factor-beta1 induces the differentiation of myogenic cells into fibrotic cells in injured skeletal muscle: a key event in muscle fibrogenesis.* Am J Pathol, 2004. **164**(3): p. 1007-19.

123. Li, Z.B., H.D. Kollias, and K.R. Wagner, *Myostatin directly regulates skeletal muscle fibrosis.* J Biol Chem, 2008. **283**(28): p. 19371-8.

124. Liu, D., B.L. Black, and R. Derynck, *TGF-β inhibits muscle differentiation through functional repression of myogenic transcription factors by Smad3.* Genes & Development, 2001. **15**(22): p. 2950-2966.

125. Schabort, E.J., et al., *TGF-beta's delay skeletal muscle progenitor cell differentiation in an isoform-independent manner.* Exp Cell Res, 2009. **315**(3): p. 373-84.

126. Katagiri, Y.U., et al., *CD44 variants but not CD44s cooperate with beta1-containing integrins to permit cells to bind to osteopontin independently of arginine-glycine-aspartic acid, thereby stimulating cell motility and chemotaxis.* Cancer Res, 1999. **59**(1): p. 219-26.

127. Mukherjee, B.B., et al., *Interaction of osteopontin with fibronectin and other extracellular matrix molecules.* Ann N Y Acad Sci, 1995. **760**: p. 201-12.

128. Rittling, S.R., *Osteopontin in macrophage function.* Expert Rev Mol Med. **13**: p. e15.

129. Song, G., et al., *Osteopontin promotes ovarian cancer progression and cell survival and increases HIF-1alpha expression through the PI3-K/Akt pathway.* Cancer Sci, 2008. **99**(10): p. 1901-7.

130. Chen, G., et al., *Role of osteopontin in synovial Th17 differentiation in rheumatoid arthritis.* Arthritis Rheum. **62**(10): p. 2900-8.

131. Petrow, P.K., et al., *Expression of osteopontin messenger RNA and protein in rheumatoid arthritis: effects of osteopontin on the release of collagenase 1 from articular chondrocytes and synovial fibroblasts.* Arthritis Rheum, 2000. **43**(7): p. 1597-605.

132. Take, Y., et al., *Specifically modified osteopontin in rheumatoid arthritis fibroblast-like synoviocytes supports interaction with B cells and enhances production of interleukin-6.* Arthritis Rheum, 2009. **60**(12): p. 3591-601.

133. Lenga, Y., et al., *Osteopontin expression is required for myofibroblast differentiation.* Circ Res, 2008. **102**(3): p. 319-27.

134. Pereira, R.O., et al., *Osteopontin expression in coculture of differentiating rat fetal skeletal fibroblasts and myoblasts.* In Vitro Cell Dev Biol Anim, 2006. **42**(1-2): p. 4-7.

135. Uaesoontrachoon, K., et al., *Osteopontin and skeletal muscle myoblasts: association with muscle regeneration and regulation of myoblast function in vitro.* Int J Biochem Cell Biol, 2008. **40**(10): p. 2303-14.

136. Capote, J., et al., *Osteopontin ablation ameliorates muscular dystrophy by shifting macrophages to a pro-regenerative phenotype.* J Cell Biol, 2016. **213**(2): p. 275-88.

137. Springer, M.L., T.A. Rando, and H.M. Blau, *Gene delivery to muscle.* Curr Protoc Hum Genet, 2002. **Chapter 13**: p. Unit13 4.

138. Capote, J., et al., *Calcium transients in developing mouse skeletal muscle fibres.* J Physiol, 2005. **564**(Pt 2): p. 451-64.

139. Uchinaka, A., et al., *SVVYGLR motif of the thrombin-cleaved N-terminal osteopontin fragment enhances the synthesis of collagen type III in myocardial fibrosis.* Mol Cell Biochem, 2015. **408**(1-2): p. 191-203.

140. Kyriakides, T., et al., *SPP1 genotype is a determinant of disease severity in Duchenne muscular dystrophy: predicting the severity of Duchenne muscular dystrophy: implications for treatment.* Neurology, 2011. **77**(20): p. 1858; author reply 1858-9.

141. Anwar, A., et al., *Osteopontin is an endogenous modulator of the constitutively activated phenotype of pulmonary adventitial fibroblasts in hypoxic pulmonary hypertension.* Am J Physiol Lung Cell Mol Physiol, 2012. **303**(1): p. L1-L11.

142. Sorensen, E.S., P. Hojrup, and T.E. Petersen, *Posttranslational modifications of bovine osteopontin: identification of twenty-eight phosphorylation and three O-glycosylation sites.* Protein Sci, 1995. **4**(10): p. 2040-9.

143. Burks, T.N. and R.D. Cohn, *Role of TGF-beta signaling in inherited and acquired myopathies.* Skelet Muscle, 2011. **1**(1): p. 19.

144. Vallese, D., et al., *The Rag2-Il2rb-Dmd- Mouse: a Novel Dystrophic and Immunodeficient Model to Assess Innovating Therapeutic Strategies for Muscular Dystrophies.* Mol Ther, 2013. **21**(10): p. 1950-1957.

145. Kubota, T., et al., *Multiple forms of Spp1 (secreted phosphoprotein, osteopontin) synthesized by normal and transformed rat bone cell populations: regulation by TGF-beta.* Biochem Biophys Res Commun, 1989. **162**(3): p. 1453-9.

146. Jono, S., C. Peinado, and C.M. Giachelli, *Phosphorylation of osteopontin is required for inhibition of vascular smooth muscle cell calcification.* J Biol Chem, 2000. **275**(26): p. 20197-203.

147. Maeda, K., et al., *Distinct roles of osteopontin fragments in the development of the pulmonary involvement in sarcoidosis.* Lung, 2001. **179**(5): p. 279-91.